Fondo Sociale Europeo - FSE
Programma Operativo Nazionale 2000/06
"Ricerca, Sviluppo tecnologico ed Alta Formazione nelle regioni dell'Obiettivo 1" - Misura 1.1 (F.S.E)

University of Calabria

PhD Course in Chemical and Materials Engineering

Thesis

TOTAL AND PARTIAL OXIDATION REACTIONS IN PHOTOCATALYTIC MEMBRANE REACTORS

Settore Scientifico Disciplinare CHIM07 – Fondamenti Chimici delle Tecnologie

Supervisor

Ch.mo Prof. Raffaele MOLINARI

PhD Student

Angela CARUSO
Ciclo XXI

PhD Coordinator

Ch.mo Prof. Raffaele MOLINARI

A.A. 2007-2008

To
my Family

ABSTRACT

Photocatalytic Membrane Reactors (PMRs) for degradation or conversion reactions have shown to be very powerful and promising hybrid processes, especially because a synergistic effect has been often observed.

In this PhD thesis different configurations of PMRs for total or partial oxidation reactions of organic compounds in water have been studied.

In particular, the performance of two configurations of PMR, pressurized and de-pressurized (submerged) membrane systems (PPMR and SPMR), for the degradation of two pharmaceuticals (Gemfibrozil and Tamoxifen), using suspended TiO_2 as catalyst, have been investigated. The results showed a good operating stability in the continuous systems, reaching a complete abatement of the drug and a constant retentate mineralization of 60 %, although the TOC rejection values evidenced the need to identify a membrane selective to intermediate products. In both systems common benefits were the retention of the suspended catalyst in the reaction ambient and the possibility to run continuous operations, although the higher permeate flux (65.1 L h^{-1} m^{-2}) in the SPMR showed it more interesting for application purposes.

The one-step conversion of benzene to phenol in a photocatalytic membrane contactor (PMC) coupling simultaneous reaction and product separation was studied in the second part of this work. The effects of parameters such as pH of aqueous TiO_2 suspensions, initial amount of benzene and catalyst concentration were investigated in the batch tests. L-L extraction experiments and transport tests, using benzene as organic extractant, showed a phenol distribution coefficient of 2.1 and an extraction percentage of 24 ± 2 %, assuring, also, a constant feed of substrate. In the PMC phenol production and separation was tested, investigating the influence of pH and catalyst concentration on the performance of the realized system. Despite a negligible difference on the phenol flux in the benzene phase (1.16 ± 0.11 mmol $h^{-1}m^{-2}$), a better control on formation and extraction of oxidation intermediates at pH 3.1 was obtained. The influence of dissolved ions (Fe^{3+}, Cu^{2+} and V^{3+}) was also investigated, evidencing a positive effect in presence of iron(III) ion with a phenol flux in the organic phase almost two times greater than those measured without salts.

RIASSUNTO

I Reattori Fotocatalitici a Membrana (PMRs), applicati in reazioni di degradazione o conversione, risultano essere promettenti processi ibridi, grazie all'effetto sinergico spesso osservato accoppiando la fotocatalitisi a processi di separazione a membrana.
In questa tesi di dottorato sono state studiate differenti configurazioni di PMRs da applicare a reazioni di ossidazione totale e parziale di composti organici in acqua.
In particolare, è stata investigata l'efficienza di due configurazioni di PMR, a membrana pressurizzata e depressurizzata (PPMR e SPMR), per la degradazione di due farmaci (Gemfibrozil e Tamoxifene), usando TiO_2 come catalizzatore. I risultati ottenuti hanno evidenziato una buona stabilità operativa dei sistemi in continuo, raggiungendo un completo abbattimento del farmaco e una mineralizzazione del 60% nel retentato, anche se i valori di reiezione al TOC hanno mostrato la necessità di identificare una membrana più selettiva verso gli intermedi di reazione. Benefici comuni in entrambi i sistemi sono stati la ritenzione del catalizzatore nell'ambiente reattivo e la possibilità di operare in continuo, sebbene il SPMR è risultato essere più interessante per scopi applicativi per il più alto flusso misurato (65.1 L h^{-1} m^{-2}).
Nella seconda parte di questo lavoro è stata studiata la conversione del benzene a fenolo in un contattore a membrana fotocatalitico (PMC), accoppiando simultaneamente la reazione e la separazione del prodotto. Gli effetti di parametri come pH delle sospensioni acquose di TiO_2, quantità iniziale di benzene e concentrazione del catalizzatore, sono stati investigati in prove in batch. Estrazioni L-L e test di trasporto, usando il benzene come estraente, hanno mostrato un coefficiente di distribuzione del fenolo pari a 2.1, con un'estrazione del 24 ± 2 %, e un continuo rifornimento di substrato. La produzione e separazione del fenolo è stata effettuata nel PMC, investigando l'influenza che pH e concentrazione del catalizzatore avevano sull'efficienza del sistema realizzato. Nonostante le differenze trascurabili sul flusso di fenolo nella fase benzene (1.16 ± 0.11 mmol $h^{-1}m^{-2}$), è stato, tuttavia, ottenuto a pH 3.1 un miglior controllo sulla formazione ed estrazione degli intermedi di reazione. Inoltre, studiando l'influenza di ioni disciolti (Fe^{3+}, Cu^{2+} and V^{3+}), è stato evidenziato un effetto positivo in presenza di ferro(III) con un flusso doppio di fenolo in fase organica rispetto a quello misurato senza sali.

INDEX

INTRODUCTION

Photocatalytic Membrane Reactors (PMRs) represent an interesting alternative technology useful both in the field of water and air purification and as synthetic pathway.

The necessity to develop chemical products and industrial processes that reduce or eliminate the use and the generation of toxic substances along with the risk for human health and for environment constitutes the aim of the research efforts based on principles of Green Chemistry.

Heterogeneous photocatalysis is a technology extensively studied for about three decades, since Fujishima and Honda (1972) discovered the photocatalytic splitting of water on TiO_2 electrodes in 1972.

Photocatalysis, included in a special class of oxidation techniques, defined as advanced oxidation processes (AOPs), comprises a large variety of reactions such us partial or total oxidations, hydrogen transfer, functionalization, rearrangements, dehydrogenation, mineralization, etc. (Herrmann, 2005).

When a separation membrane methods is coupled with a photocatalytic process it is possible to obtain a synergic effect minimizing environmental and economic impacts. In this hybrid system, in fact, the radicals produced by irradiation of the catalyst were exploited to perform partial or total redox reactions leading to selective products or clarified solutions which can be separated by the membrane.

Several characteristics make a PMR a "green" technology, as the safety of the photocatalyst used, the mild operative conditions, the possibility to operate in continuous mode, in which the recovery of the catalyst, the reactions and the products separation occur in one step, with remarkable times and costs saving.

The choice of an appropriate membrane and the knowledge of the parameters influencing the photocatalytic process represent, therefore, an important step in the design of a PMR.

Besides, the possibility to perform the photocatalytic reactions using the solar light, makes this process very interesting for future industrial applications.

Aim of this PhD thesis was the development of Photocatalytic Membrane Reactors for total and partial oxidation reactions of organic compounds in water and simultaneous separation of the product(s) of interest.

In Section I the basic fundamentals and the main application fields of photocatalysis are examined, with a wide overview on the current progresses and drawbacks present in literature. Then, a detailed presentation of membrane reactors is reported, summarizing the possible membrane materials, configuration and driving force of membrane processes. Finally, a review on the application and modelling of photocatalytic membrane reactors (PMRs) is treated.

Section II reports the experimental results obtained in this study on the total oxidation of organic compounds in PMRs. In particular, the photodegradation of two drugs, Gemfibrozil and Tamoxifen, in water and the separation of the clarified solution is studied using two different configuration of PMRs: Pressurized and De-pressurized (Submerged) Photocatalytic Membrane Reactors (PPMR and SPMR).

In Section III, the one-step photosynthesis of phenol and its simultaneous separation is reported as model of partial oxidation reaction in a PMR. The photoconversion of benzene to phenol is studied using a membrane contactor module in which benzene acts not only as substrate, but also as organic extractant. The performance of the system is evaluated in terms of productivity and membrane selectivity towards phenol and its oxidation by-product, investigating also the effects of some dissolved ions on the system efficiency.

SECTION I

PHOTOCATALYSIS AND PHOTOCATALYTIC MEMBRANE REACTORS*

I.1 PHOTOCATALYSIS AS A GREEN PROCESS

Traditional processes for making chemical products are unsustainable in terms of resources and environmental impact. In particular, although in the last decades the chemical industries have made great improvements in the efficiency of their processes, the need to identify renewable feedstocks, the use of toxic or scarce catalysts and the generation of hazardous waste effluents remain some of the unsolved problems which attract the scientific community (Poliakoff and Licence, 2007). The application of innovative scientific solutions to solve these problems is the main aim of the Green Chemistry, also know as Sustainable Chemistry. This new approach, based on the "12 Principles of Green Chemistry" originally published by Paul Anastas and John Warner (1998), promotes innovative and sustainable chemical technologies which allow to reduce or eliminate the use or generation of hazardous substances in the environmentally conscious design, manufacture, and use of chemical products and engineering processes (www.epa.gov/greenchemistry). Several organizations in the world are involved in the development and promotion of these "green" concepts.

In this context, the Photocatalytic Membrane Reactors, used both as purification methods and synthetic pathway, represent a promising green technology.

---

* This part of work is a textbook processing as:

- R. Molinari, A. Caruso, L. Palmisano, "Photocatalytic Membrane Reactors in the Conversion or Degradation of Organic Compounds" in *Membrane operations. Innovative Separation and Transformations*, E. Drioli, L. Giorno (Ed.s), Wiley-VCH.
- R. Molinari, A. Caruso, L. Palmisano, "Photocatalytic processes in membrane reactors" in *Comprehensive Membranes Science and Engineering*, E. Drioli (Ed.), Elsevier Publisher.

As reported by several authors (Ollis, 2000; Anpo, 2000, Palmisano et al., 2007a; Herrmann et al., 2007), "green" characteristics make photocatalysis an attractive process:

- the use of greener safer photocatalyst, as TiO_2 which is a component of pharmaceuticals and toothpastes;
- the use of mild oxidants, such as molecular oxygen;
- the possibility to work with mild reactions conditions running closer to room temperature and pressure;
- very few auxiliary additives are request;
- no production of harmful chemicals.

These potentialities are further improved when a membrane separation technique is coupled to a photocatalytic route. Photocatalytic Membrane Reactors, in fact, allow to realize a continuous one-step process in which the reduction of the catalyst and solvent amounts, the minimization of the purification steps and a better control of the equilibrium reactions can be achieved, avoiding the large amounts of waste products generally formed during a multistep process. Besides, a continuous reactor can be much smaller than the corresponding batch reactor and the use of an appropriate membrane can allow to remove continuously higher purity products.

I.1.1 Basics of Heterogeneous Photocatalysis

Photocatalysis is an important technology widely studied in the last decades. In particular, the scientific research has been addressed to the understanding of mechanisms, variables and kinetic parameters which influence the whole process.

Heterogeneous photocatalysis is a term which describes a process in which the photocatalyst is in a different phase with respect to the substrate. In this condition, the reaction scheme implies the previous formation of an interface between the (solid) photocatalyst and a liquid or a gas phase containing the reactants. The comprehension of these phenomena is important in order to enhance the performance of photocatalytic systems.

I.1.1.1 Mechanism

A semiconductor presents an electronic structure characterized by a conduction band and a valence band separated by a band-gap of energy (E_G).

The irradiation of the catalyst, with photons whose energy ($h\upsilon$) is equal to or greater than its band gap, promotes an electron from the valence band to the conduction band with the creation of electron-hole pair ($e^-_{cb} - h^+_{vb}$) (Figure I.1).

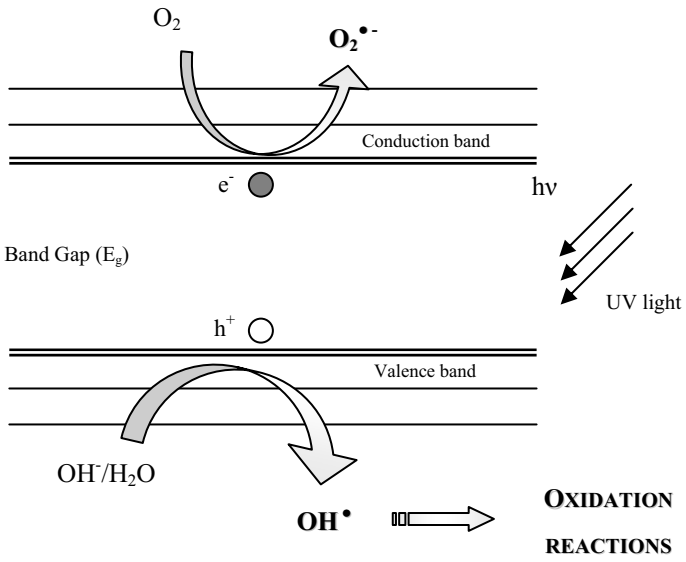

Figure I.1: Energy band-gap of a semiconductor.

The lowest energy level of the conduction band defines the reduction potential of the photoelectrons while the highest one of the valence band determines the oxiding power of the photoholes, respectively.

In the absence of suitable electron and holes scavengers, the input energy is dissipated as heat within a few nanoseconds by recombination.

The initial step of the activation of the photocatalytic process is the photonic excitation of the catalyst and the main steps, representing the photocatalytic mechanisms, are proposed by several authors (Kavita et al., 2004; Hoffmann et al., 1995):

1) Excitation of the catalyst

$TiO_2 + h\upsilon \rightarrow e^- + h^+$

2) Adsorption on the catalyst surface

$Ti^{IV} + H_2O \rightarrow Ti^{IV}\text{-}H_2O$

$Ti^{IV} + OH^- \rightarrow Ti^{IV}\text{-}OH^-$

catalyst site + $S_1 \rightarrow S_{1ads}$

3) Electron and hole trapping

$Ti^{IV} + e^- \rightarrow Ti^{III}$

$Ti^{IV}\text{-}H_2O + h^+ \rightarrow Ti^{IV}\text{-}OH^{\bullet} + H^+$

$Ti^{IV}\text{-}OH^- + h^+ \rightarrow Ti^{IV}\text{-}OH^{\bullet}$

$S_{1ads} + h^+ \rightarrow S_{1ads}^+$

$Ti^{III} + O_2 \rightarrow Ti^{IV}\text{-}O_2^{\bullet -}$

4) Recombination of electron-hole pairs

$e^- + h^+ \rightarrow$ heat

As widely accepted, the primary oxidants in these systems are the hydroxyl radicals generated by the oxidation of electron donor molecules (water or hydroxyl ions) in the valence band. The attack of hydroxyl radicals to the substrate (S) can occur under different conditions:

- $Ti^{IV}\text{-}OH^{\bullet} + S_{1ads} \rightarrow Ti^{IV} + S_{2ads}$
- $OH^{\bullet} + S_{1ads} \rightarrow S_{2ads}$
- $Ti^{IV}\text{-}OH^{\bullet} + S_1 \rightarrow Ti^{IV} + S_2$
- $OH^{\bullet} + S_1 \rightarrow S_2$

Whereas, in the conduction band acceptor molecules can be reduced if their reduction potential is higher than that of the photoelectrons, such as O_2 to yield a superoxide ions or metal ions reduced to their lower valence states:

- $O_2 + e^- \rightarrow O_2^{\bullet -}$
- $M^n + e^- \rightarrow M^{(n-1)}$

I.1.1.2 Photocatalytic reaction parameters

In this section the main factors influencing a photocatalytic process are summarized:

- *Catalyst amount*

A catalyst works accelerating the rate of a reaction without being consumed. Nevertheless, the UV light only (reported as photolysis) can allow the degradation of some organic substrates, but it is unable to mineralize the organic intermediates as reported in a study on the photodegradation of pharmaceuticals in water (Molinari et al., 2008).

In a true heterogeneous catalytic regime, in which the photonic excitation of the catalyst surface represents the initial step of the process activation, the initial rate of the reaction is proportional to the amount of photocatalyst (Herrmann et al., 2005). However, above a certain level of mass catalyst (m), the rate of reaction reaches a plateau condition that corresponds to the maximum amount of catalyst in which all the surface active sites are illuminated and occupied by the substrate.

Besides, it was observed that agglomeration of catalyst particles occurs for high catalyst amount and consequently light penetration into suspension decreases, which leads to a decrease of photocatalyst activity (Kavita et al., 2004; Konstantinou et al., 2004).

To avoid excess of catalyst and to ensure a satisfactory reaction efficiency, the optimum amount of catalyst must be used as function of substrate concentration.

- *Substrate concentration*

The dependence of photocatalytic rate on substrate concentration is an aspect broadly studied in literature.

As reported by Konstantinou and Albanis (2004) in a review on the photocatalytic degradation of azodyes, it is generally accepted that degradation rate increases increasing substrate concentration to certain values; over these ones the rate decreases. This aspect can be explained by considering the mechanisms of photocatalytic reactions which involve the creation of OH radicals and substrate adsorption on catalyst surface.

Initially, the enhanced substrate concentration increases the probability of reaction between molecules and oxidizing species. A further increase, nevertheless, leads to a reduction in OH radicals generation due to light scattering and to a decrease in the active catalyst sites available for OH radicals production.

- pH of the aqueous solutions

The photocatalytic process is strongly affected by the pH of the reactive environment. In particular, pH changes can influence the acid-base properties of the catalyst surface and, therefore, the adsorption phenomena.

Several studies (Konstantinou et al., 2004; Bekkouche et al., 2004) reported that under acidic condition the TiO_2 surface is positively charged, whereas in alkaline media it is negatively charged according to the following equilibrium:

$$TiOH + H^+ \leftrightarrows TiOH_2^+$$
$$TiOH + OH^- \leftrightarrows TiO^- + H_2O$$

On this basis, although at alkaline pH the hydroxyl radicals are easier to be generate because of the higher number of hydroxide ions available on the catalyst surface, nevertheless a decrease in the photocatalytic activity was observed probably due to repulsion phenomena between the negative charged surface of TiO_2 and the hydroxyl anions.

Coulomb interaction can be hypothesized also between the catalyst and the substrate molecules. This aspect explains the different reaction products observed (Kavita et al., 2004; Robert et al., 2002) changing the pH value. Depending on the substrates, in fact, an increase of pH can determine a positive or negative effect on reaction rate. Anionic molecules are lesser or more adsorbed at alkaline or acidic pH, respectively, due to a different ionization state of the catalyst surface, as reported by Bekkouche et al. (2004) in a study of adsorption of phenol on titanium oxide.

An increase in the reduction rate of BrO_3^- lowering the pH from 7 to 5 was observed also by Noguchi et al. (2003), due to an enhancement of the electrical interaction between the anionic substrates and the positively charged surfaces of the TiO_2 photocatalyst which increases the amount of adsorbed BrO_3^-.

Besides, at acidic condition an aggregation of catalyst particles is observed which reduces the available catalytic active sites for photon absorption and substrates adsorption leading to a decrease in the catalytic activity.

- *Presence of oxygen*

Oxygen plays an important role in the photocatalytic oxidation of many substrates both as electron scavengers and as strong oxidant. Its reaction with the photoelectron in the valence band allows to prevent the electron-hole recombination prolonging the lifetime of the holes. Moreover, the superoxide ions formed ($O_2^{\bullet-}$) initiate a chain of reactions leading to the creation of additional hydroxyl radicals, also via the formation of hydrogen peroxide.

$O_2 + e^- \rightarrow O_2^{\bullet-}$

$O_2^{\bullet-} + H^+ \rightarrow HO_2^{\bullet}$

$HO_2^{\bullet} + e^- \rightarrow HO_2^-$

$HO_2^- + H^+ \rightarrow H_2O_2$

$H_2O_2 + e^- \rightarrow OH^{\bullet} + OH^-$

Therefore, the reactive radical species formed enhance the photocatalytic efficiency of the whole process.

- *Presence of others species*

Presence of others species in the reaction environment can give positive or negative effects on the rate of the photocatalytic process depending on the reaction mechanism.

In particular, the addition of oxyanion oxidants, such as $S_2O_8^{2-}$, BrO_3^-, IO_4^-, ClO_2^- and ClO_3^- increases the photoreactivity by scavenging the conduction-band electrons and reducing charge-carrier recombination (Konstantinou et al., 2004; Kavita et al., 2004):

$S_2O_8^{2-} + e^- \rightarrow SO_4^{2-} + SO_4^{\bullet-}$

$SO_4^{\bullet-} + H_2O \rightarrow SO_4^{2-} + {}^{\bullet}OH + H^+$

Another oxidant species which influences positively the photocatalytic reaction is H_2O_2 due to the formation of hydroxyl radicals. However, as reported by Augugliaro et al. (2006), an excess of H_2O_2 can have a detrimental effect because it acts as scavenger of valence band holes and $^{\bullet}OH$, producing hydroperoxyl radicals which has a less oxidizing power than $^{\bullet}OH$:

$$H_2O_2 + 2h^+ \rightarrow O_2 + 2H^+$$
$$H_2O_2 + {}^{\bullet}OH \rightarrow H_2O + HO_2^{\bullet}$$

Other studies (Sykora et al., 1997; Brezova et al., 1995) reported the influence of dissolved metal ions on the photocatalytic reactions. Metal cations, used in their higher oxidation state, act as photoelectron acceptors preventing the charge-carrier recombination:

$$M^{n+} + e^- \rightarrow M^{(n-1)+}$$

Moreover, the reduced species can react with H_2O_2 to give additional $^{\bullet}OH$ by photo-Fenton reaction by the following general expression:

$$M^{(n-1)+} + H_2O_2 \rightarrow M^{n+} + {}^{\bullet}OH + OH^-$$

This aspect was broadly investigated by Brezova et al. (1995) in a study on the photodegradation of phenol in titanium dioxide suspensions in the presence of dissolved metals. They observed an increase in the photodegradation rate adding ferric ions but inhibition effects with dissolved Mn^{2+}, Co^{2+}, $Cr^{3+}$and Cu^{2+} ions. In particular, it was demonstrated the reduction of cupric ions into the unreactive form Cu^0 and its deposition on the catalyst surface and a competitive adsorption of Cr^{3+} ions on the TiO_2 surface, which probably causes the decrease of photocatalytic phenol degradation. Instead, no effects are observed in the presence of Ca^{2+}, Mg^{2+}, Zn^{2+} and Ni^{2+}.

Because of a different role of these metal ions on the photocatalytic efficiency was reported in other studies (Kavita et al., 2004; Konstantinou et al., 2004; Sykora et al.,

1997), it can be supposed a controversial behaviour depending on the physico-chemical properties of the substrates.

On the other hand, it was reported that co-dissolved anions like Cl^-, NO_3^-, PO_4^{3-} can affect the rate of reaction because of their possible adsorption onto TiO_2 surface, competing with the substrate and hamper the formation of OH• radicals (Robert et al., 2002; Konstantinou et al., 2004).

Finally, negative effects can be expected in the presence of other organic molecules which can compete for the active sites of the catalyst surface, deactivate the photocatalyst or act as light screens.

- *Wavelength and light intensity*

As previously described, the first step in a photocatalytic process is irradiation of the catalyst surface. Several studies (Emeline et al., 2000; Herrmann, 2005; Brosillon et al., 2008a) reported that the rate of reaction depends on wavelength and intensity of the light source and on the absorption spectrum of the catalyst used. In particular, effective activation of the photocatalyst takes place only with photons which have a λ smaller than or equal to the absorbtion edge of the catalyst and this phenomenon is predominant at low light intensity (Konstantinou et al., 2004), whereas a recombination of electron-hole pairs was supposed occurs for higher light intensity (these aspects will broadly be discussed in the following sections).

I.1.2 Photocatalytic activity of semiconductor materials

I.1.2.1 Photocatalysts

A photocatalyst is a semiconductor material that must be able to convert the light energy of the irradiation in the chemical energy of the electron-hole pairs. Therefore, a suitable band-gap energy together with chemical and physical stability, non-toxic nature, availability and low cost are important requirements that allow it to operate in the photocatalytic reactions.

A lot of semiconductor materials are used in literature as photocatalysts, the most common are oxides (TiO_2, Fe_2O_3, SnO_2, ZnO, ZrO_2, CeO_2, WO_3, V_2O_5, etc.) or sulfides (CdS, ZnS, WS_2, etc). Their redox potentials range between +4.0 and -1.5

volts vs Normal Hydrogen Electrode (NHE) for the valence and the conduction bands, respectively, allowing, therefore, their use to convert a wide range of molecules via photocatalytic reactions.

The most common semiconductor materials used in literature with their band gap energy and wavelength required for the activation, are reported in Table I.1.

Table I.1: Band positions of some common semiconductors used for photocatalytic processes (Choi, 2006; Robertson, 1996; Robert, 2007; Kavita et al., 2004; Liu X. et al., 2006).

Semiconductor	**Valence band (V vs NHE)**	**Conductance band (V vs NHE)**	**Band gap (eV)**	**Band gap wavelength (nm)**
TiO_2 anatase	+3.1	-0.1	3.2	387
TiO_2 rutile	+3.1	+0.1	3.0	380
SnO_2	+4.1	+0.3	3.8	318
ZnO	+3.0	-0.2	3.2	387-390
ZnS	+1.4	-2.3	3.7	335-336
Fe_2O_3	+2.6	-0.4	2.2	560
ZrO_2	+4.2	-0.8	5.0	460
WO_3	+3.0	+0.2	2.8	443
CdS	+2.1	-0.4	2.5	496-497
CdSe	+1.6	-0.1	1.7	729-730
V_2O_5			2.0	600
GaAs	+1.0	-0.4	1.4	886-887
GaP	+1.3	-1.0	2.3	539-540

I.1.2.2 Titanium Dioxide

The most widely used photocatalyst is the polycrystalline Titanium dioxide, TiO_2, due to its strong catalytic activity, long lifetime of electron hole-pairs, high chemical stability in aqueous media and in a large range of pH (0-14), low cost (due to the abundance of Ti in the earth's crust, 0.44%) and harmlessness. It exists in nature in three different polymorphs: rutile and anatase (tetragonal minerals) and brookite (a rare orthorhombic mineral). All three crystalline structures consist of deformed TiO_6 octahedra connected differently by corners and edges. The more stable form is rutile, whereas anatase and brookite are metastable and are readily transformed to rutile when heated (Di Paola et al., 2008). These three types exhibit different photoactivity due to a difference in their energy structure. In particular, in anatase and rutile forms,

the position of the valence band is deep, and the resulting positive holes show sufficient oxidative power. Nevertheless, the conduction band in the anatase type is closer to the negative position than in the rutile type; therefore, the reducing power of anatase type is stronger than that of rutile type. Moreover the recombination rate of the photoproduced electron-hole pairs is usually higher for rutile with respect to anatase.

It is worth noting, however, that not only the intrinsic electronic factors but also the surface physico-chemical and morphological/textural properties of the photocatalysts can influence the photoactivity. Nanosized TiO_2 has been described to possess special characteristics and high photoactivity, due to quantum size effect and to high surface area.

Thanks to its high photocatalytic activity, TiO_2 is employed in a wide range of industrial applications: as a thickener in cosmetic and skin care products; to prevent white tiles, aluminium panels, glass, tents, paints and coating materials; to protect tunnel lightings, mirrors, window blinds; as antibacterial in textile fibres, medical instruments and supplies (Anpo, 2000).

I.1.2.3 New generation of photocatalysts

The efficiency of the classical photocatalysts is often reduced by some drawbacks, such as:

- quickly recombination of the photogenerated electron-hole pairs (within 10-100 ns) which releases thermal energy or unproductive photons;
- high reactivity that leads to fast backward or secondary reactions with the formation of undesirable by-products;
- a low absorption in the visible region which determines their inability to use solar light (less than 5% is used in the case of TiO_2 anatase).

In the last years, therefore, the development of new efficient photocatalysts able to overcome these problems represents one of the main topic in the photocatalytic research.

Photocatalysts with a more stable charge separation, able to absorb visible light and more selective in the reactions pathway, are reported in literature both as modified common catalyst and new synthesized semiconductor materials.

As reported by Ni et al. (2007), the photocatalytic efficiency of the semiconductor materials can be improved by different techniques divided in two broad groups: photocatalyst modification, including noble metal loading, ion doping, catalyst sensitisation, and addition of chemical additives, such as electron acceptors or donors.

Some of the most recent photocatalysts and their applications are reported in Table I.2.

Transitional metal ion doping and noble metal loading have been extensively studied in order to enhance the photocatalytic activity of various photocatalysts (Taylor, 2005; Colmenares et al., 2006; Mizukoshi et al., 2007; Wang C., 2007; Arana et al., 2008; Chen C. et al., 2008; Wu G. et al.,2008). The metal acts as electrons traps, while the photo-generated VB holes remain on the catalyst, provoking a decrease in the electron-hole recombination and increasing, therefore, the catalyst efficiency. Moreover, the metal could reduce the band gap energy of the photocatalyst, thus shifting the photo-response to the visible region (Kudo et al., 2000; Egerton et al., 2008; Ge, 2008). This last effect was also obtained when the catalyst was doped with anions, such as N, F, C, S, etc. (Ling et al., 2008; Peng et al., 2008; Sun H. et al., 2008; Wong et al., 2008; Xu J. et al., 2008).

To increase the efficiency of solar photocatalytic process, another approach is reported in literature (Kobasa et al., 2002; Chen F. et al., 2008; Li S. et al., 2008; Su et al., 2008; Xia H. et al., 2008; Xiao G. et al., 2008; Zang Y. et al., 2008) consisting of composite systems in which a large band gap semiconductor was coupled with a small band gap semiconductor having a more negative CB level. In these systems, after irradiation with visible light, the electrons formed in the CB level of the small band gap photocatalyst can be injected in that of the large band gap semiconductor achieving also a wide electron-hole separation.

Table I.2: Some recent photocatalysts and their applications.

Photocatalyst	**Reaction**	**Author**	**Year**
Arg-TiO_2	Selective reduction	Ahn et al.	2007
Acridine yellow G (AYG)	Total oxidation	Amat et al.	2007
Cu-doped TiO_2	Total oxidation	Arana et al.	2008
Membrane-W10	Oxidation	Bonchio et al.	2006
V_2O_5/MgF_2 composite systems	Total oxidation	Chen F. et al.	2008
Doped-TiO_2	Selective oxidation	Colmenares et al.	2006
Pt-loaded $BiVO_4$	Total oxidation	Ge	2008
$ZnWO_4$	Photodegradation	Huang G et al.	2007
TaON	Total oxidation	Ito et al.	2005
$AgGaS_2$	Hydrogen production	Jang et al.	2007
TiO_2 nanowires	Hydrogen evolution	Jitputti et al.	2008
Fe-ZSM-5	Reduction	Kanthasamy et al.	2007
Bi_2S_3/CdS	Partial reduction	Kobasa et al.	2002
Ni-doped ZnS	Hydrogen production	Kudo et al.	2000
Dye sensitizer/photocatalyst systems	Solar photocatalysis	Kuo et al.	2008
Ag_2ZnGeO_4	Photodegradation	Li X. et al.	2008
Bi_3SbO_7	Total oxidation	Lin et al.	2008
Fe(III)-OH complexes	RedOx	Liu Y. et al.	2007
POM	Functionalization	Maldotti et al.	2003
Zn phthalocyanine complexes	Photodegradation	Marais et al.	2007
Pt, Au, Pd –doped TiO_2	Hydrogen production	Mizukoshi et al.	2007
Hydrous alumina-doped TiO_2	Reduction	Noguchi et al.	2003
Bi^{3+}–doped TiO2	Reduction	Rengaraj et al.	2007
Activated carbon - ZnO	Photodegradation	Sobana et al.	2008
N-doped TiO_2	Photodegradation	Sun H et al.	2008
La-, Cu-, Pt- doped WO_3	Selective oxidation	Taylor	2005
POM	Reduction	Troupis et al.	2004
Au/Fe_2O_3	Degradation (ox)	Wang C. et al.	2007
F-doped TiO_2 film	Photodegradation	Xu J. et al.	2008

A similar result can be obtained with another modification technique reported as dye sensitization (Jana et al., 2000; Gurunathan, 2000, Kuo, 2008). When the system catalyst/dye is illuminated with visible light, the dye acts as photo sensitizer transferring the electrons to the conduction band of the catalyst.

In order to solve the photocatalytic drawbacks, several studies investigated on the addition of dissolved electron donors, like BiO_3^-, CN^- (Sohrabi et al., 2008), NO_3^-, SO_4^{2-} (Konstantinou et al., 2004), or electron acceptors, such as Fe^{3+} (Ortiz-Gomez et al., 2008), K^+, Mg^{2+}, Ca^{2+}, Zn^{2+}, Co^{2+} (Qourzal et al., 2008). Besides, several preparation techniques have been recently proposed to synthesize more efficient photocatalysts immobilized on mesopourous support (Chen Y. et al., 2008; Huang J. et al., 2008), inert support (Kansal et al., 2008), activate carbon (Sobana et al., 2008; Zhang X. et al., 2008), ceramic membranes (Wang Y. et al., 2008), building materials (Demeestere et al., 2008), ceramic monolith channel (Du P. et al., 2008). Moreover, new synthesized photocatalysts which allow a better control of the whole photocatalytic process thanks to a delay in charge recombination and an enhanced activity under visible light irradiation, are reported in the recent photocatalytic works (Bi J. et al., 2008; Li X. et al., 2008; Lin X. et al., 2008; Wu L. et al., 2008; Amat et al., 2007; Marais E. et al., 2007).

I.1.3 Applications of the Photocatalytic Technologies

Photocatalytic processes can be performed in various media. They include a great variety of reactions, such as partial or total oxidation, degradation of organic compounds, reduction reactions, fuel synthesis (e.g. H_2 production through water splitting), metal corrosion prevention, disinfection, etc.

The application fields of this technology can be divided in two main groups (Figure I.2), purification processes and synthetic pathways, although combined reactions are often exploited to increase the efficiency of the system.

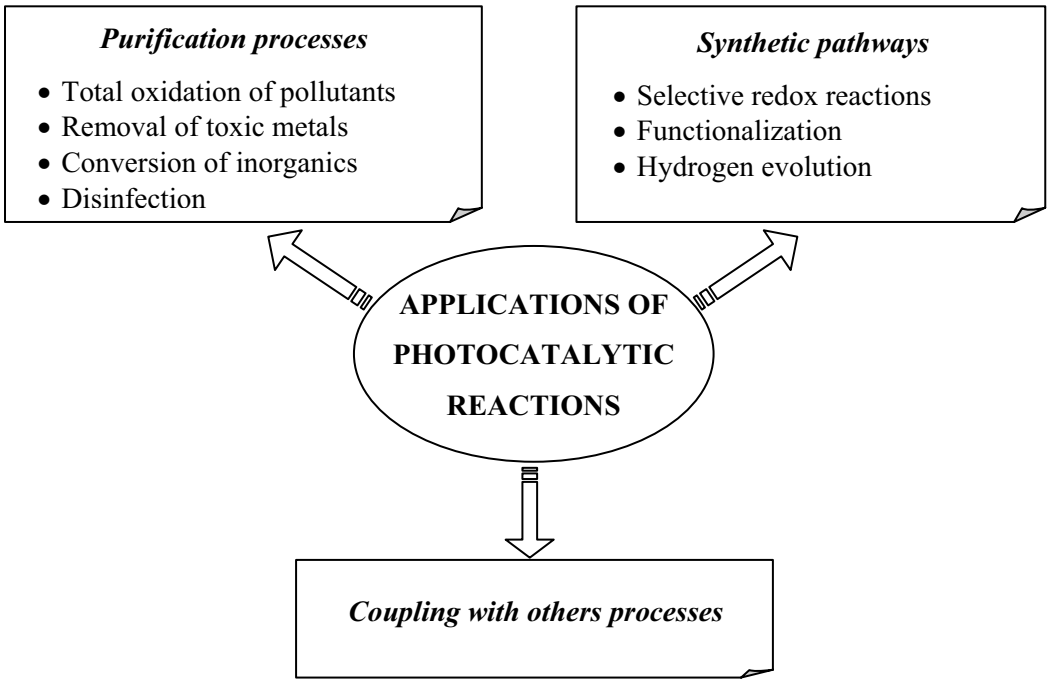

Figure I.2: Main photocatalytic applications reported in literature.

Some of the most recent applications of the photocatalytic processes present in literature are reported in Table I.3.

I.1.3.1 Purification processes

- I.1.3.1.1 Total oxidation of environmental pollutants

Main use of the photocatalytic techniques was the removal of organic pollutants in water and air. This application, that in the last years has found an important relevance in commercial materials, has been widely studied in literature. The growing resistance of various classes of organic compounds to common chemical and biological degradation treatments, has focused the attention of the international scientific community on the development of alternative methods. In this context, photocatalysis represents an useful alternative "green" purification technique, because, as result of a chain of oxidation reactions, a wide range of organic molecules also containing in their structure heteroatoms, can be mineralised to inorganic species: carbon to CO_2, hydrogen to H_2O, nitrogen to nitrate, sulphur to sulphates and phosphorus to phosphate.

Table I.3: Applications of the photocatalytic processes.

Application	Substrate	Product	Author
Total oxidation	Dyes		Chen C.C., 2007; Kansal, 2007; Lou, 2007; Wang C., 2007; Xu, 2007; Sobana, 2007
	Pharmaceuticals		Molinari, 2006a; Augugliaro, 2005
	Toxic organic compounds		Amat, 2007; Huang X, 2007; Ito, 2005; Marais, 2007; Tang, 2005; Waldner, 2007
	Pesticides		Lhomme, 2007; Abu Tariq, 2007.
	Herbicides		Topalov, 2000; Singh, 2007; Sleiman, 2007
	Hormones		Zhang Y., 2007
Partial oxidation	2-propanol	Acetone, CO_2	Colmenares, 2006
	4-methoxybenzyl alcohol	p-anisaldehyde	Palmisano G., 2007b
	Cyclohexane	Cyclohexanol	Du, 2006
	Hydrocarbons	Corresponding oxigenates	Gonzales, 1999
	Aniline	Azobenzene	Karunakaran, 2006
	Carbonate	Methane, methanol	Ku Y., 2004
	Methane	Methanol	Taylor, 2005
	Benzene	Phenol	Park, 2005, Shimizu, 2004
	NH_3	N_2	Yamazoe, 2007
	Herbicide		Zertal, 2004
Reduction	4-nitrophenol	4-aminophenol	Ahn, 2007
	Metal ions	Noble metals	Chen D., 2001; Sharma, 2005; Kanthasamy, 2007; Troupis, 2004; Wang X., 2004
	BrO_3^-	Br^-	Noguchi, 2003
	Nitrite	Ammonia	Ranjit, 1995
	Nitrate	N_2	Rengaraj, 2007
	CO_2	Methane and H_2	Sing Tan, 2007
	Dyes destruction		Troupis, 2007
	p-chloronitrobenzene	p-chloroaniline	Zhang T., 2006
	Dyes		Kobasa, 2002
Redox	Cr(VI), BPA	Cr(III), oxidation products	Liu Y., 2007
	Cr(VI), dyes	Cr(III), oxidation products	Papadam, 2007
Functionalization			
Halogenation	Arenes, Cycloalkenes	Halo-derivates, epoxide	Maldotti, 2000; Molinari A., 2007
Ciclization	Amino acid	cicloderivates	Ohtani, 2003
Thiolation	Propene/H_2S	Propan-1-thiol	Schoumacker, 2002
Hydrogen production	Water		Jang J.S., 2007; Kudo, 2000-2003; Ni, 2007
	Ethanol/H_2O		Mizukoshi, 2007

Contamination of wastewater is a very important environmental problem and many studies have been carried out with the aim to remove by photocatalytic reactions the most common pollutants: dyes (Baran et al., 2008; Ge, 2008; Li X. et al., 2008; Sohrabi et al., 2008; Zang Y. et al., 2008; Yang X. et al., 2008), pesticides and herbicides (Kuo et al., 2008; Lhomme et al, 2007; Sakkas et al., 2004); pharmaceutical compounds (Augugliaro et al., 2005; Molinari et al., 2006a- 2008; Yurdakal et al., 2007); hormones (Zhang Y. et al., 2007), various toxic organic molecules (Huang X. et al., 2008; Lair et al., 2008; Karunakaran et al., 2008; Shon et al., 2008).

In order to resolve the problem of the environmental effects of gaseous emissions from industries and other human activities, photocatalytic air treatments was also reported as a promising field of application of these processes. Several VOCs such as MTBE (Arana et al., 2008), toluene (Augugliaro et al., 1997a; Augugliaro et al., 1999; Marcì et al., 2003; Demeestere et al., 2008), bromomethane (Huang J. et al., 2008), benzene (Xiao G. et al., 2008; Yan T. et al., 2008), formaldehyde (Huang G. et al., 2007), etc., were successfully degraded by photocatalytic processes.

In the last years, the purification property of the TiO_2 was exploited in building materials not only at laboratory levels but also in concrete structures for maintaining their aesthetic characteristics, such as the church "Dives in Misericordia" in Rome (Italy), 'l'Ecole de Musique' in Chambe´ (France), the Marunouchi Building in Tokyo (Japan).

- I.1.3.1.2 Removal of toxic metal ions

Metal ions are generally non-degradable and toxic in specific valence states. The reduction by semiconductor photocatalytic processes is a relatively new technique that can be used to change the hazardous ionic states of dissolved metal ions in wastewater (Chen D., 2001).

The application of the photocatalytic reduction is reported to be effective to remove various toxic metal ions, such as: Cr(VI) (Aarthi et al., 2008; Cappelletti et al., 2008; Wang L. et al., 2008, Kanthasamy et al., 2007), Hg(II) (Wang X. et al., 2004), Pd(II) (Troupis et al., 2004), etc. The reduction of such metals results not only in pollution

prevention but also in recovery and reuse of valuable metal products with environmental and economic concerns, respectively.

Further investigations combined the reduction of metallic ions with the simultaneous degradation of organic contaminants achieving a synergic effect. Redox reactions were used in literature for the purification of aqueous systems containing contaminants such as Cr(VI) and bisphenol A (Liu Y. et al., 2007), Fe(VI) and ammonia (Sharma et al., 2005), Cr(VI) and azodyes (Papadam et al., 2007), Ag(I) and dyes (Wong M. et al., 2008).

- I.1.3.1.3 Conversion of inorganic contaminants

Photocatalytic processes has been exploited also for the conversion of other potentially toxic inorganic ions and molecules in the corresponding harmless forms.

In this context, photocatalytic reactions are reported in literature to reduce bromate ions to Br^- (Noguchi et al., 2003), nitrite and nitrate to ammonia and nitrogen (Rengaraj et al., 2007; Ranjit et al., 1995), or to oxidize sulphite, thiosulphate and sulphide ions into innocuous SO_4^{2-} ions, PO_3^{3-} into PO_4^{3-} or CN^- into NO_3^- (Augugliaro et al., 1997b; Herrmann et al., 2007).

- I.1.3.1.4 Antimicrobial and antitumor activity

Interesting recent researches investigated the possibility to use the photogeneration of active oxygenated radicals to attack the cell membrane of microorganisms and to cause their inactivation. The antimicrobial activity of UV-irradiated photocatalyst has been tested against several types of bacteria, yeasts, algae and viruses (Coronado et al., 2005; Rincon et al., 2003; Guillard et al., 2008, Kim et al., 2003).

Besides, the cytotoxicity of photocatalysis was also tested in the last years for cancer treatment. Cai et al. (1992), in a study on the effects of photo excited TiO_2 particles on HeLa cells cultured *in vitro*, observed a complete cell death in the presence of TiO_2 (50 μg/ml) with 10-min UV irradiation. The antineoplastic photocatalytic effect was widely investigated by Fujishima et al. (2000) by *in vitro* experiments which confirmed the inhibition of the tumour growth. They developed a device, built by modifying an endoscope, in order to access various parts of the human body.

These studies extended therefore the application of photocatalytic processes to the medical field.

I.1.3.2 Synthetic pathways

- I.1.3.2.1 Selective oxidations and reductions

Due to the highly unselective reactions involved in the photocatalytic processes, the application of this technology was addressed mainly to the treatment of hazardous compounds in liquid and gas phases. However, it was widely demonstrated that selecting or modifying some photocatalytic parameters, such as the semiconductor surface or the wavelength, it is possible to control the reaction obtaining a better selectivity towards some products. On this basis, photocatalysis could represent an alternative synthetic route able to satisfy several of the principles of Green Chemistry.

Several studies reported the selective oxidation of hydrocarbons in aqueous and organic phase (Gonzales et al., 1999; Almquist et al., 2001; Du et al., 2006; Palmisano G. et al., 2007b; Shimizu et al., 2004; Taylor et al., 2005)

In a study on the partial photocatalytic oxidation of different benzene derivates, Palmisano et al. (2007b) demonstrated how the substituent groups can affect the selectivity to hydroxylated compounds. In particular, they observed that organic molecules containing an electron withdrawing group (cyanobenzene, nitrobenzene, benzoic acid, etc.) were unselectively converted in a mixture of mono-hydroxy derivates, while in the presence of an electron donor group (phenol, phenylamine, *N*-phenylacetamide) the attack of OH radicals was selective in the *ortho* and *para* positions.

Park and Choi (2005), studying the photocatalytic conversion of benzene to phenol, showed the possibility to enhance the phenol production yield and selectivity adding Fe^{3+} or/and H_2O_2 to the TiO_2 suspension or modifying the catalyst surface by deposition of Pt nanoparticles (Pt/TiO_2).

Gondal et al. (2004) studied the photocatalytic activity of different semiconductor catalysts for the conversion of methane into methanol at room temperature in the aqueous solution. They observed a percentage conversions of 29%, 21% and 20% using WO_3, TiO_2 and NiO, respectively. This selective oxidation reaction was also

investigated by Taylor et al. (2005) using a lanthanum-doped tungsten oxide. They observed an increase in the methanol production when an electron transfer reagent (hydrogen peroxide) was added to the solution.

Moreover, selective photo oxidation reactions were also reported to convert alcohols to carbonyls (Pillai et al., 2002; Mohamed et al., 2002; Palmisano et al., 2007c).

Palmisano G. et al (2007c) studied the selective oxidation of 4-methoxybenzyl alcohol to p-anisaldehyde in organic-free aqueous TiO_2 suspensions, obtaining a considerable yield of 41.5% mol. The homemade photocatalysts were obtained under mild conditions and showed to be more selective than two common commercial samples, i.e. TiO_2 Degussa P25 and Merck. Nevertheless, although the reported findings are very intriguing in the light of the possibility to potentially synthesize fine chemicals in green conditions, it should be highlighted that the initial alcohol concentration used in this work (ca. 1.1 mM) is quite low in comparison with that used for typical organic syntheses.

Colmenares et al. (2006) reported the use of different metal doped TiO_2 systems for the gas phase selective photo-oxidation of 2-propanol to acetone. They observed that doping the catalyst with Pd, Pt or Ag caused an increase in molar conversion as compared to bare-TiO_2, whereas the presence of Fe and Zr had a detrimental effect.

Although the reduction ability of the conduction band is lower than the oxidizing power of the valence band hole, several studies on the photocatalytic reduction of chemicals are reported in literature to convert nitrobenzene compounds to the corresponding amino-derivates (Ahn et al., 2007; Zhang T. et al., 2006; Maldotti et al., 2000; Brezova et al., 1997), carbonate to methane and methanol (Ku Y. et al., 2004; Dey et al., 2004; Yahaya et al., 2004; Sasirekha et al., 2006).

- I.1.3.2.2 Functionalization

In last years many efforts have been addressed on the use of photocatalytic synthesis for the functionalization of organic compounds in various solvents and several interesting results are reported in literature. Photocatalyzed reactions were used to obtain dihydropyrazine by cyclization of propylene glycol with ethylenediamine (Subba Rao et al., 2000), carbamate by carbonylation of *p*-nitrotoluene with EtOH (Maldotti et al., 2005), the monooxygenation and/or chlorination of cycloalkenes

(Maldotti et al., 2003), mono-brominated derivates from phenol and anisole (Molinari A. et al., 2007), the addition of tertiary amines to alkenes (Marinkovic et al., 2001), unsaturated amines adding cyclopentene and cyclohexene to imines (Schindler et al., 1997), heterocyclic aldehydes by the reaction between heterocyclic bases and ethers (Caronna et al., 2005), propan-1-thiol by addition of H_2S on propene.

Moreover, the wide potentiality of photocatalysis was also applied for the transformation of functional groups such as selective cyclization of amino acids in aqueous suspensions (Ohtani et al., 2003, Takei et al., 2005) or to produce a coumarin compound from phenanthrene in an acetonitrile solution containing 8 wt% water (Higashida et al., 2006).

- I.1.3.2.3 Hydrogen evolution

Hydrogen is considered as an attractive alternative energy source because it is a clean, storable and renewable fuel that does not produce pollutants or greenhouse gases upon combustion. About 95% of the commercial hydrogen is produced from fossil fuels, such as natural gas, petroleum and coal, although it may be also extracted from water via biological production or using electricity or heat. Therefore, the development of less expensive methods of bulk production of hydrogen represents an interesting field of scientific research.

Photocatalytic systems can offer a cleanest way to produce hydrogen and, starting from 1972 when Fujishima and Honda (1972) reported the photo electrochemical hydrogen production using TiO_2 as catalyst, many studies have been performed in order to improve this reaction. Photocatalytic water splitting is a reaction in which water molecules are reduced by the electrons to form H_2 and oxidized by the holes to form O_2, using semiconductor materials. TiO_2 represent the main photocatalyst used in literature for hydrogen evolution (Ni et al., 2007), although Kudo (2003) demonstrated that other semiconductor materials, such as $Pt/SrTiO_3$ codoped with Cr and Sb or Ta, $Pt/NaInS_2$, $Pt/AgInZn_7S_9$ and Cu- or Ni-doped ZnS photocatalysts, showed high activities for H_2 production from aqueous solutions under visible light irradiation.

Besides, other photocatalytic approaches were reported to produce hydrogen by reduction of ethanol aqueous solutions (Mizukoshi et al., 2007) or methanol solutions (Jitputti et al., 2008).

Moreover, Tan et al. (2007-2008) reported an interesting work on the conversion of carbon dioxide with water into hydrogen and methane. This system could contribute to the control of CO_2 emission from industrial processes allowing, contemporarily, to obtain interesting industrial products.

I.1.3.3 Photocatalysis coupled to others technologies

An interesting application of photocatalysis, especially in the field of wastewater treatment, results from its coupling with other technologies, which exploited the synergic effects to reduce the reaction time and to increase the efficiency of the overall process.

In literature several hybrid systems were obtained combining photocatalysis with chemical or physical operations (Augugliaro et al., 2006). A positive influence on the photocatalytic mechanism was achieved coupling photocatalysis with chemical operations such as ozonation (Addamo et al., 2005; Hernandez-Alonso et al., 2002; Sun L. et al., 2008), photo-Fenton reaction, ultrasonic irradiation (Torres et al., 2008) or electrochemical treatment.

When coupling is with methods like biological treatment (Parra et al., 2000; Brosillon et al., 2008b), physical adsorption or membrane systems (Molinari et al., 2008; Azrague et al., 2007; Camera-Roda et al., 2007; Shon et al., 2008), the combination does not affect the mechanisms but increases the efficiency of the whole process.

These hybrid processes offer a good strategy to achieve a better wastewater treatment, particularly when photocatalysis is exploited to transform recalcitrant pollutants in non-recalcitrant molecules which subsequently can be easily degraded by the conventional methods.

I.1.4 Potentials and limits of the photocatalytic processes

On the basis of the considerations reported in the previous sections, several characteristics make photocatalysis an attractive green process not only as purification method, but also as synthetic pathway.

Several advantages can be summarized for the photocatalytic process:

- it can be applied to a wide range of compounds in aqueous, gaseous and solid phase;
- reactions are performed in short times and under mild experimental conditions, usually under ambient temperature and pressure;
- generally no additives are required, only oxygen from air;
- it is applicable also to solutions at low concentrations;
- it is able to destroy a variety of hazardous molecules with the formation of innocuous products, solving the disposal pollutant problem associate to the conventional wastewater treatment methods;
- it can be exploited to convert toxic metal ions in their non-toxic forms which can be recovered and reused;
- a synergistic effect can be obtained when it is coupled with others technologies;
- the possibility to use the solar light makes it an attractive inexpensive process.

Nevertheless, the application of photocatalytic process at industrial level is limited by different drawbacks related to the involved reactions and reactor configuration.

The development of photocatalytic systems needs the knowledge of kinetic models which include all the parameters influencing the process and allows to plan a reactor useful for industrial applications.

As previously described, the radical reactions which occur in a photocatalytic process are highly unselective and very fast. When the purpose is to employ photocatalysis as synthetic pathway, therefore, it is important to control reaction kinetics in order to avoid secondary reactions which lead to undesirable products and reduce the yields of the process. On this respect, in the last years many efforts have been realized with the aim to obtain more selective reactions modifying the classical semiconductor materials or synthesizing new photocatalysts.

On the contrary, regards the reactor configuration, as observed by Choi et al. (2006), few studies have been performed for the design of efficient photoreactors for commercial exploitation. In particular, one of the main drawbacks regards the recovery of the catalyst and/or the separation of the products from the reactive environment.

For what concerns the catalyst, two operative configurations can be identified: catalyst suspended or catalyst immobilized on a support.

In the immobilized system the catalyst can be coated on the walls of the reactor, supported on a solid substrate or deposited around the case of the light source, using as supported materials alumina, zeolite (Shimizu et al., 2004; Zama et. al, 2000), activated carbon (AC) (Sobana et al., 2008; Zhang X. et al., 2008), silica support (Coronado et al., 2005; Herrmann, 2005; Biard et al., 2007), glass beads (Chen Y. et al., 2008; Huang J. et al., 2008), polymeric membranes (Bonchio et al., 2006; Rivas et al., 1998; Rincon et al., 2003; Wang Y. et al., 2008).

Several advantages are reported in literature on the use of immobilized systems. For example, in a study on the photodegradation of 4-acetylphenol, Sobana et al. (2008), observed that activated carbon-zinc oxide catalysts showed a much more higher adsorption and photodegradation rate than bare ZnO due to a higher adsorption of the substrate on the AC. Besides, Xu J. et al. (2008), studying the performance of several F-doped TiO_2 films, demonstrated that the photocatalytic activity of the prepared photocatalyst film almost keeps the same after three times reusing, with a little decline after six cycles.

Another immobilized system was proposed by Tsuru et al. (2003) for the gas-phase photocatalytic degradation of volatile organic pollutants using methanol as target molecule. In this study the TiO_2 catalyst was immobilized in a porous membrane and the permeate stream was oxidized with OH radicals after one-pass permeation through the TiO_2 membranes. Comparing the reaction rate using the photocatalytic membrane reactor with that without membrane permeation at various reaction conditions (residence time, feed concentration), it was observed an enhanced performance of photocatalytic reaction for the first system.

Thus, the possibility to exploit the synergic effects obtained with particular support, to recover the catalyst without additional separation steps and to design continuous

flow photoreactors, makes the immobilized systems interesting for industrial application.

Nevertheless, as widely demonstrated in literature (Kansal et al., 2008; Molinari et al., 2002; Dijkstra et al., 2001; Mascolo et al., 2007; Sakkas et al., 2004), the suspended systems seem to be more efficient than those based on immobilized catalysts.

This evidence can be explained considering that heterogeneous catalysis is a surface phenomenon, therefore the overall kinetic parameters are dependent from the real exposed catalyst surface area. In the supported systems only a part of the photocatalyst is accessible to light and to substrate. Besides, the immobilized catalyst suffers from the surface deactivation since the support could enhance the recombination of photo generated electron/hole pairs and a limitation of oxygen diffusion in the deeper layers is observed.

Another important aspect which limited practical application of photocatalytic process is the selective separation of the products or/and intermediates from the reactive environment. Although separation systems such as distillation or precipitation can be useful to separate the final mixture, however these techniques, involving further treatment steps, do not allow to operate in continuous mode.

On this basis more efforts in photocatalytic engineering and reactor development are required to realize an efficient photocatalytic reactor.

A very promising approach to overcome these photocatalytic drawbacks is the use of hybrid systems in which photocatalysis is coupled with a membrane module (Molinari et al., 2000; Azrague et al., 2007; Tang C. et al., 2004; Chin S.S. et al., 2007; Huang G. et al., 2007).

I.2 MEMBRANE REACTORS

I.2.1 Membrane

I.2.1.1 Definition and classification of membranes

Membrane technology is a rapidly emerging technology used today in a wide range of separation processes. Although it is difficult to give an exact definition of a membrane, it could be defined as a selective semipermeable barrier which, under a certain driving force, permits preferential passage of one or more species or components of a gaseous and/or liquid mixture or solution (Figure I.3).

It is, therefore, a separation system placed between two environments or phases: the first one is defined as feed phase and the primary species rejected is called retentate(s), while the second one is usually termed permeate and contains the species passing through the membrane.

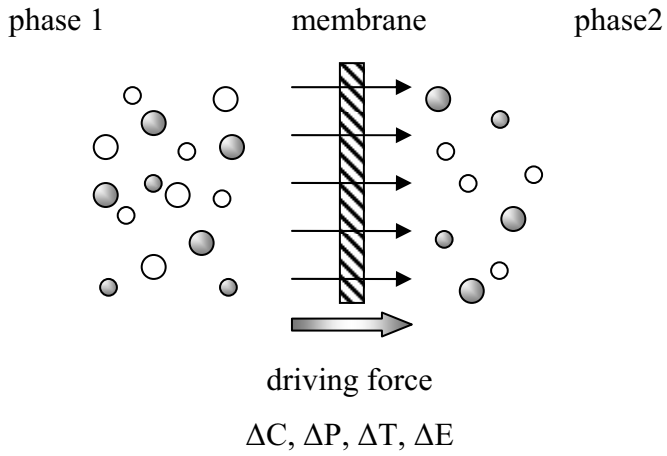

Figure I.3: Schematic representation of a membrane system (Mulder, 1991).

Membranes can be classified according to different view points (Mulder, 1991) . A first main classification divided membranes on the base of their nature in biological or synthetic membranes which differ completely in structure and functionality. The biological membranes can be subdivided into living and non-living membranes. The latter, which include liposomes and vesicles, are important in medical and

biomedical separation processes. On the other hand, synthetic membranes can be classified into organic (polymeric or liquid) and inorganic (ceramic and metal) membranes.

Another classification (for the synthetic types) is based on their structural characteristics, distinguishing them in symmetric and asymmetric membranes (Figure I.4). The symmetric categories, including porous and dense (nonporous) membrane, have an homogeneous structure and composition with thicknesses range from 10 to 200 μm. Since the flow rate through the membrane is inversely proportional to its thickness, it is very desirable to make the homogeneous membrane layer as thin as possible.

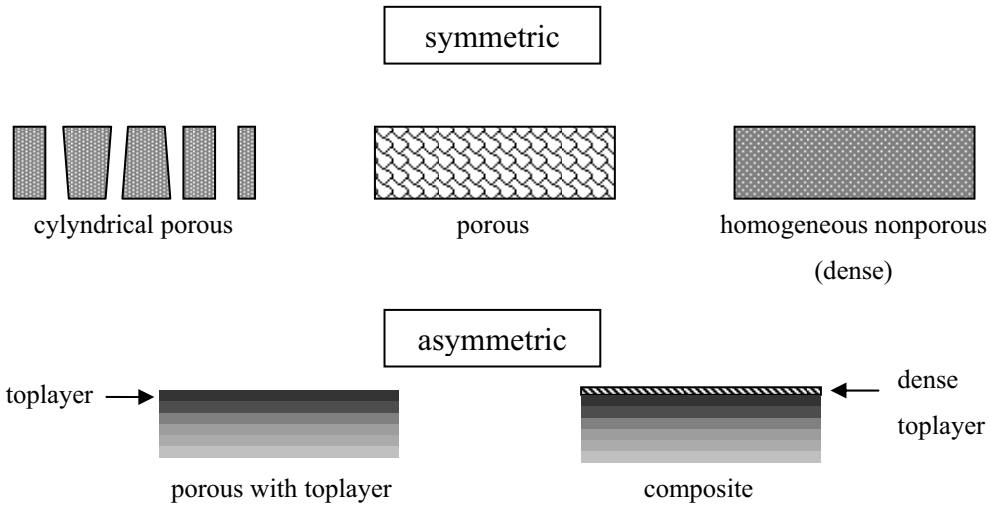

Figure I.4: Schematic representation of various membrane cross-section (Mulder, 1991).

If a membrane has a graded pore structure but is made in one processing step, frequently from the same material across its thickness, it is defined as asymmetric membrane. These consist of a very dense toplayer or skin with a thickness of 0.1 – 0.5 μm supported by a porous sublayer with a thickness of about 50 to 150 μm. In these types of membrane, the resistance to mass transfer is determined largely or completely by the thin toplayer. Therefore, they combine the high selectivity of a dense structure with the high permeation rate of a very thin membrane.

If the membrane has two or more different layers originate from different polymeric materials and made at different step the resulting structure is called a composite membrane. Generally, the necessary mechanical strength is provided by a predominantly thick layer (support layer) on which a thin dense layer is deposited (toplayer). The composite membranes have the advantage that each layer can be optimised independently.

I.2.1.2 Membrane materials

The membrane material is an intrinsic property of the membrane system. On the base of the material, synthetic membranes can be divided in organic (polymeric) and inorganic (ceramic, metal, glass) membranes. The most used (in more than 90% of applications) are polymeric membranes (Franken, 1998).

The choice of a given polymer as a membrane material is based on very specific properties and required a good knowledge of the separation process. Basically, all polymers can be used as barrier or membrane material, but their chemical and physical properties limit their practical use. For the porous membranes, used in microfiltration and ultrafiltration processes, the choice of material takes into account the processing requirements, the fouling tendency and the stability of the membrane. For the dense nonporous membranes, applied in gas separation and pervaporation, the choice determines directly the membrane performance in terms of selectivity and flux.

Hydrophobic materials such as polytetrafluoroethylene (PTFE), poly(vinilydene fluoride) (PVDF and polypropylene (PP) and hydrophilic polymers like cellulose and its derivates, polyacrylonitrile (PAN), poysulfone (PSf), polyethersulfone (PES), polyetherketone (PEK) are used for microfiltration and ultrafiltration membranes. The choice of material for nonporous membrane is determined by the type of application and the polymer can range from elastomer to a glassy material.

Inorganic membranes generally possess superior chemical and thermal stability respect to polymeric membranes. On the basis of the inorganic materials used, the inorganic membranes can be subdivided into: ceramics, formed by the combination of a metal (titanium, silicium, zirconium) with a non-metal in the form of oxide, nitride or carbide; metallic membranes, obtained via sintering of metal powders

(stainless, molybdenum, tungsten); glass membranes, constituted by silicon oxide or silica (SiO_2) and zeolite membranes.

I.2.1.3 Membrane configurations

The choice for a certain kind of membrane system is determined by a great number of aspects, such as costs, risks of plugging of the membranes, packing density and cleaning opportunities. Membranes are never applied as one flat plate, due to the necessity to realize a system in which a large membrane surface is put in the smallest possible volume.

The smallest unit into which the membrane area is packed is called a module and several type of membrane modules are available for separation processes.

Not all membrane modules are suited for every type of separation process; configuration with a high packing density (defined as the surface per module volume) are not suited for the treatment of feed streams having a high potential fouling (like in microfiltration), on the other hand, for processes with low fluxes through the membrane and feed streams which have a low fouling potential, such as reverse osmosis and gas separation, the need for high packing density is evident.

Membranes are implemented in several types of modules classified in two main configuration: flat (plate-and-frame and spiral-wound modules) and tubular (tubular, capillary and hollow fiber modules) (Mulder, 1991; Franken, 1998; www.lenntech.com).

Plate-and-frame module

In this module type flat sheet membranes are placed on top of each other and are separated by so-called spacers. The packing density is rather low, about 100-400 m^2/m^3 and therefore this configuration is relatively expensive. It is used normally to treat bad quality water and as the only which can be used in electrodialysis.

Spiral wound module

The spiral wound module is a module configuration in which two flat sheet membranes, separated by a permeate spacer, are glued along three edges to form a "membrane envelope". The open side of this envelope is attached to a central tube (permeate collection tube) on which the membrane envelope is wrapped around. The feed flows axial through the cylindrical module parallel along the central pipe,

whereas the permeate flows radially toward the central pipe. Due to the low fabrication costs and the high packing density (300-1000 m^2/m^3) this module is ver6y popular in applications like nanofiltration, reverse osmosis and gas separation.

Tubular membrane module

Respect to capillaries and hollow fibers, the tubular membranes have a inner diameter larger than 5 mm and are not self-supporting. They are, therefore, placed inside a porous stainless steel, ceramic or plastic tube which acts as support. Generally used for viscous or bad quality fluids. These modules do not need a preliminary pre-treatment of the water. Due to the large diameter of the tube, the low packing density (300 m^2/m^3) and the need to operate cross-flow, the energy requirements is high compared to the other configurations.

Capillary membrane module

With capillary membranes the membrane serves as a selective barrier, which is sufficiently strong to resist filtration pressures. Because of this, the flow through capillary membranes can be both inside out and outside in.

The diameter of capillary membranes is much smaller than that of tubular membranes, namely 0.5 to 5 mm. Because of the smaller diameter the chances of plugging are much higher with a capillary membrane. A benefit is that the packing density is much greater, of about 600-4000 m^2/m^3.

This module are used in applications with low transmembrane pressure driving forces, such as in (diffusion) dialysis or micro- and ultrafiltration.

Hollow fiber membrane module

The only difference between the capillary membranes and the hollow fiber is the diameter of the fibres which for the latter module is less than 0.5 mm. Because of this small inner diameter, this membranes can only be used for the treatment of water with a low suspended solids content. Hollow fiber module are used in reverse osmosis, gas separation and dialysis.

I.2.2 Transport through membranes

I.2.2.1 The driving force

Membrane separation processes are characterized by the ability of the membrane to transport one component more readily than other thanks to a differences in physical and/or chemical properties between the membrane and the permeating components. The transport occurs as a result of a driving force which acts on the components in the feed phase. The driving force can be a gradient in pressure, concentration, electrical potential or temperature and is proportionally related to the flux (J) by the general phenomenological equation (Mulder, 1991):

$$J = -A\frac{dX}{dx}$$

where A is called the phenomenological coefficient and (dX/dx) is the driving force, expressed as the gradient of X along a coordinate x perpendicular to the transport barrier. As reported in Table I.4, this equation can be used to describe fluxes of mass, volume, heat, etc.

Table I.4: Phenomenological equations for the membrane processes (Mulder, 1991).

	Equation	**Law**	**Phenomenological coefficient (A)**
Mass flux	$J_m = - D\ dc/dx$	Fick	Diffusion coefficient
Volume flux	$J_v = -L_p\ dP/dx$	Darcy	Permeability coefficient
Heat flux	$J_h = -\lambda\ dT/dx$	Fourier	Thermal diffusivity
Momentum flux	$J_n = -\upsilon\ dv/dx$	Newton	Kinematic viscosity
Electrical flux	$J_i = -1/R\ dE/dx$	Ohm	Electrical conductivity

I.2.2.2 Membrane functions

As reported by Sirkar et al. (1999), the membrane inside the reactor can served a variety of functions. It is important to underline that a given membrane in a given reactor is not able of all functions, but under appropriate circumstances can perform more than one generic role.

The functions of the membrane in a reactor can be summarized as follow (Figure I.5):

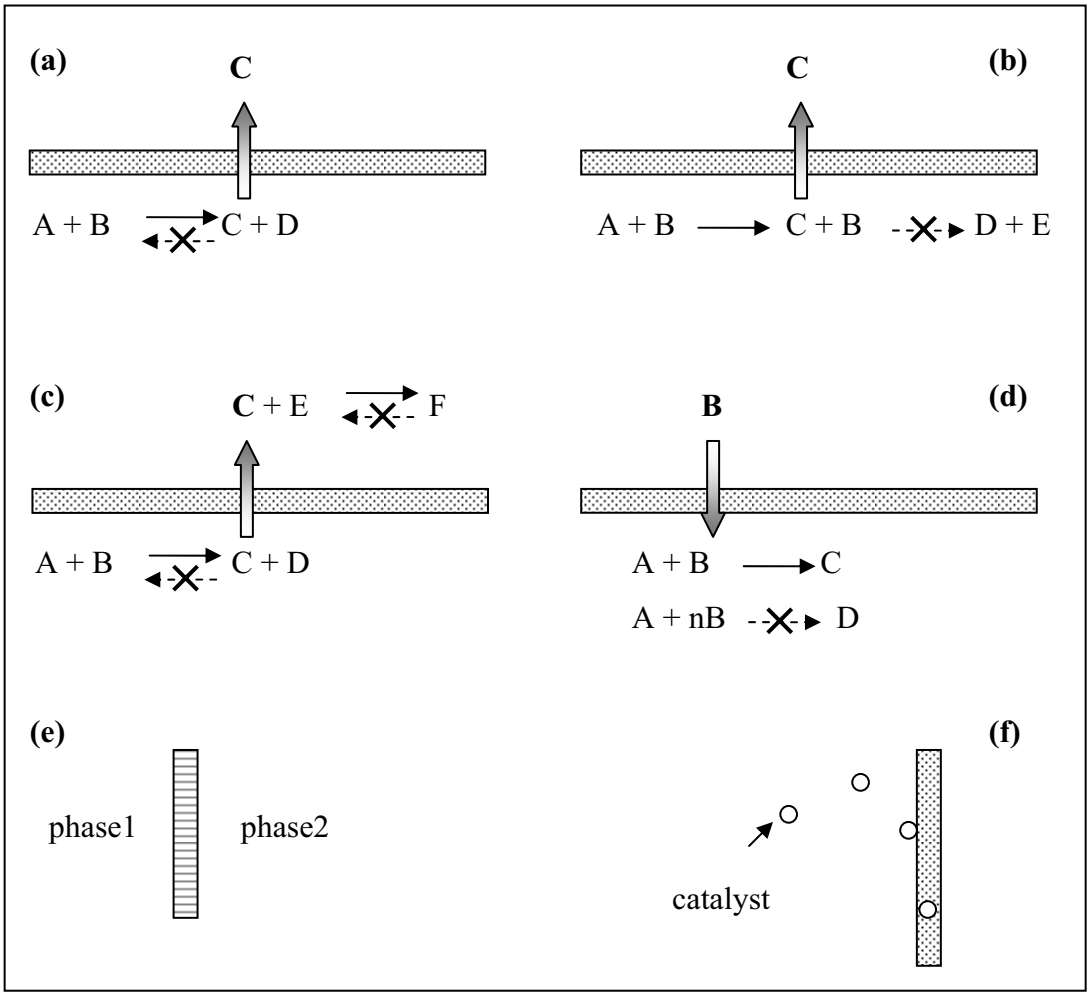

Figure I.5: Schematic of possible functions of a membrane.

Separation of products from the reaction mixture: this is one of the most common functions of a membrane in a reactor in which the separation may be purification, enrichment or concentration. Thermodynamically limited reactions can reach a conversion value higher than that obtainable in a traditional reactor. The application of this concept would be positive in many equilibrium-limited systems in which the reaction is shifted to the right (Figure I.5a).

Besides, if there is an undesirable reaction between the product I and one of the reagent (e.g. B), the separation of product C from the reaction mixture reduces the

loss of B and increases the conversion to C, avoiding or minimizing the production of by-products (Figure I.5b).

Separation of a product for introduction in another reactive environment: the membrane separates two reaction zones in the same reactor (Figure I.5c). In this case only one of the products of the first reaction can, selectively permeating through the membrane, approach the second zone where it reacts.

Controlled addition of one reactant: in this case the addition of a reagent is controlled through the membrane in order to maintain its concentration in the reaction volume low, limiting side reactions or eventual consecutive reactions of the products (Figure I.5d). The controlled feeding can also be used to prevent catalyst deactivation.

Nondispersive phase contacting: in many reactions, two immiscible phases are frequently used together. In this conditions a porous membrane can be useful to keep the two phases on the two sides of the membrane with their interfaces immobilized at the membrane pore (Figure I.5e).

Catalytic membrane reactor: when the membrane is incorporated in a catalytic reaction system it can assume various function. It can maintain the catalyst in the reaction environment, allowing is recovery and reuse in continuous systems, it can have the catalyst immobilized on/within its structure or it can operate itself as catalyst (Figure I.5f).

I.2.3 Membrane processes

The membrane processes are classified in four main categories according to their driving forces which can be a difference in pressure, concentration, temperature or electrical potential (Mulder, 1991).

I.2.3.1 Pressure driven membrane processes

In these processes the solvent is the continuous phase and the concentration of solute is relatively low. Depending on the particle size and chemical properties of the solute the properties and the structure of the employed membrane change. Considering the

membrane pore size the pressure-driven membrane processes can be subdivided in: microfiltration, ultrafiltration, nanofiltration and reverse osmosis (Figure I.6).

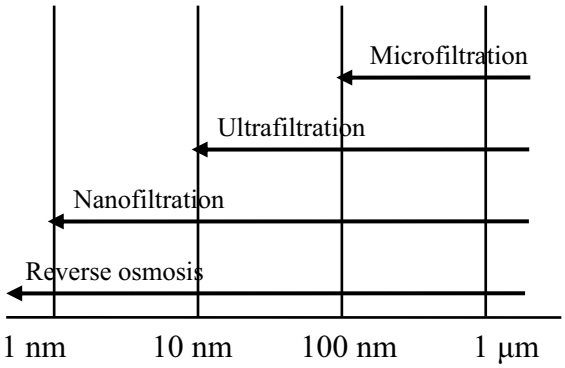

Figure I.6: Pressure driven membrane processes (adapted from www.lenntech.com).

When the size of particles or molecules separated diminishes, the pore sizes in the membrane must become smaller, and, consequently, increasing the resistance of the membrane to mass transfer it is required a higher applied pressure to obtain the same flux.

In Table I.5 a comparison of various pressure driven membrane processes are reported

Table I.5: Pressure driven membrane processes.

	membranes	**pore sizes**	**thickness (μm)**	**pressure (bar)**	**separation principle**
Microfiltration	(a)symmetric porous	0.05-1.0 μm	10-150	< 2	sieving
Ultrafiltration	asymmetric porous	1.0-100 nm	150	1-10	sieving
Nanofiltration	composite	< 2 nm	sublayer 150 toplayer 1	10-25	sieving/solution-diffusion
Reverse osmosis	asymmetric or composite	< 2 nm	sublayer 150 toplayer 1	15-80	solution-diffusion

I.2.3.2 Concentration driven membrane processes

In this type of membrane processes, the transport through the membrane proceeds via spontaneous diffusion of the molecules from a high to a low chemical potential. Gas separation, pervaporation, dialysis, carrier mediated processes and membrane contactors represent the main membrane processes in which a concentration difference acts as the driving force (Table I.6). Each of this separation systems differs considerably from the others, although for all the membrane used is a nonporous membrane.

Table I.6: Concentration driven membrane processes.

	membranes	**pore sizes**	**thickness (μm)**	**separation principle**
Gas separation	asymmetric or composite	nonporous	toplayer < 0.1	solution-diffusion
Pervaporation	composite	nonporous	toplayer < 0.1	solution-diffusion
Carrier mediated	liquid membrane	-	1-20	affinity to carrier
Dialysis	homogeneous		10-100	diffusion rate
Membrane contactor	(a)symmetric	nonporous or 0.05-1.0	20-100	distribution coefficient

I.2.3.3 Thermally driven membrane processes

When two phases, at different temperatures, are separated by a membrane, heat flows from the high-temperature side to the low-temperature side and the transport of heat is expressed by the Fourier's low (see Table I.4).

Membrane distillation is a particular types of thermally driven membrane process in which a porous membrane separates two liquid or solution at different temperatures that do not wet it. If a temperature difference exists across the membrane, the resulting vapour pressure difference causes vapour molecules to permeate from the high-temperature phase to the low-temperature phase.

In this condition the membrane acts only as a barrier between the two phase and it is not directly involved in the separation process, which is determined by the vapour-liquid equilibrium involved. Symmetric or asymmetric porous membrane with pore

size of 0.2 – 1.0 μm are used in these systems which are applied for the production of pure water and for the removal of VOC's.

I.2.3.4 Electrically driven membrane processes

In electrically driven membrane processes an electrical potential difference acts as driving force which take advantage of the ability of charged species to conduct an electrical current. In this case electrically charged membranes are used to separate electrically charged components from their uncharged counterparts. The membranes, which are electrically conductive, can be distinguished in cation-exchange membranes, that permit the passage of cations, and anion-exchange membranes, allowing the transport of negatively charged anions.

Membrane processes in which the charged membrane acts as selective barrier where ions are either rejected or transported dependent on the ionic charge and the membrane charge, are fuel cells, membrane electrolysis, electrodialysis and bipolar membranes. The first process convert chemical energy into electrical energy, while in the others an electrical potential difference acts as driving force.

I.3 PHOTOCATALYTIC MEMBRANE REACTORS (PMRS)

I.3.1 Photocatalysis coupled to Membrane Processes

In a Photocatalytic Membrane Reactor (PMR) a synergic effect can be obtained combining the advantages of classical photoreactors (catalyst in suspension) and those of membrane techniques (one-step separation).

In a photocatalytic slurry reactor the recovery of the unsupported catalyst from the treated solution is one of the key challenges for large-scale application.

A membrane process is a physical separation technique which do not involve a phase change and allows to operate in continuous mode. When a suitable membrane is coupled to the photocatalytic process, it is possible not only the recovery and reuse of the catalyst, but also the separation of the treated solution and/or of the reaction products.

Therefore, the choice of the membrane module configuration is mainly determined by the type of photocatalytic reaction and the membrane can assume many roles in the system, as catalyst recovery, separation of the products, rejection of the substrate, etc.

Besides, membrane photoreactors allow operation in continuous systems (Molinari et al., 2006a) in which the reaction of interest and the selective separation of the product(s) simultaneously occur, avoiding in some cases the formation of by-products, resulting competitive with other separation technologies for what concerns material recovery, energy costs, reduction of the environmental impact and selective or total removal of the components (Molinari et al., 2001).

Interesting solutions involving the use of a membrane to enhance the performance of the photocatalytic processes have been proposed by several authors, although the few works present in literature demonstrate that the research on the PMRs is not sufficiently developed yet.

I.3.2 Variables influencing the performance of PMRs

From a practical point of view, the selection of the appropriate operative conditions is of critical importance to obtain a good performance of the PMR, as is common for all other membrane and photocatalytic technologies.

In the development of a photocatalytic membrane reactor it is important to take into account some parameters that influence the performance of the system and its applicability at industrial level.

The main purpose in the combination of a membrane process with a photocatalytic reaction is the necessity to recover and to reuse the catalyst. Besides, when the process is used for the degradation of organic pollutants, the membrane must be able to reject the compounds and their intermediate products, while if photocatalysis is applied to a synthesis, often the role of the membrane is the separation of the product(s) from the reaction environment.

In the former case, a useful parameter which expresses the ability of the membrane to maintain the substrate and its intermediates in the reactive environment is the Rejection (R) or retention coefficient, defined as:

$$R = \frac{C_f - C_p}{C_f} = 1 - \frac{C_p}{C_f}$$

where C_f and C_p are the solute concentrations in the feed and permeate, respectively.

High rejection values can be achieved when membranes with pore size smaller than the size of the molecules to be retained are used. Besides, it is possible to increase the retention of the substrates controlling other factors influencing the separation properties of a membrane, such as the pH, which influences the acid-basic properties of the membrane and of the molecules, the residence time of substrates and the concentration polarisation phenomenon.

In particular, some membranes can become electrically charged changing the pH and this property can be exploited to retain in the reactive environment molecules that otherwise can pass freely in the permeate. Thanks to Donnan effects, in fact, repulsive or attractive interactions between the substrate molecules and the membrane surface may occur if the charges are of the same or of different sign,

respectively. In this condition, repulsive interactions increase rejection values whereas attractive ones decrease them.

The residence time of substrate in the photocatalytic system is another important factor which influences the efficiency of photodegradation. Longer retention times, obtained reducing the permeate flux, resulted in a better organic removal (Chin et al., 2007). This aspect can be explained considering that a longer residence time allows a greater contact between the molecules to be degraded and the catalyst.

However, since the PMR must be able to offer an high water permeate flux, it is important to find a good compromise among the permeate flux and the residence time in order to achieve a system for application purpose.

In a pressure driven membrane process, the rejection phenomena allows to obtain a permeate in which the concentration of the substrate results lower than that in the retentate. Nevertheless, when an accumulation of excess particles takes place at the membrane surface, with the formation of a boundary layer, the concentration polarisation occurs which causes a different membrane performance. Solutes with low molecular weight, deposited on the membrane, pass in the permeate leading to negative rejection values. Moreover, the layer deposited on the membrane surface increases the resistance to solvent flow and, therefore, reduces the permeate flux. This problem can be reduced generating a turbulent flow on the membrane surface which avoids or minimizes catalyst and drug deposition.

When the membrane is used to separate one or more products, it is more convenient to express the performance of the system in terms of a selectivity factor (α). For a mixture consisting of two components A and B, with concentrations in the retentate x_A and x_B and in the permeate y_A and y_B, respectively, $\alpha_{A/B}$ is given by:

$$\alpha_{A/B} = \frac{y_A / y_B}{x_A / x_B}$$

In this case, the selectivity of the membrane towards the products becomes an important aspect of the separation process. The membrane must be able not only to selectively and quickly separate the product of interest, avoiding secondary reactions

that would cause the formation of undesirable by-products, but also to maintain in the reactive ambient the catalyst and the other photocatalytic products.

I.3.3 Membrane Photoreactor Configurations

Various types of membrane photoreactors were realized with the purpose of having an easy separation of the catalyst from the reaction environment and an efficient removal of pollutants from water and air.

In this section some of the most recent studies on PMRs reported in literature, divided on the base of the membrane module configuration used for the separation, will be presented.

I.3.3.1 Pressurized membrane photoreactors

In literature the most studied configurations of membrane photoreactors were pressurized systems in which a pressure membrane technique, such as nanofiltration (NF), ultrafiltration (UF) and microfiltration (MF), was combined with a photocatalytic process. In these systems the catalyst, used both in the suspended configuration and immobilized on the membrane, is confined in the pressurized side of the permeation cell.

The firsts works reported in literature (Sopajaree et al., 1999a-b; Molinari et al., 2000-2001) were performed with the aim to choose an useful membrane material, stable in the reactive environment, and to identify the variables influencing the performance of the membrane photoreactor.

Molinari et al. (2002) studied the performance of various photocatalytic membrane systems in the degradation of 4-nitrophenol using TiO_2 as catalyst. In particular, two configurations were investigated in which the irradiation source was placed on the recirculation tank or on the cell containing the membrane. Besides, in the last configuration the efficiency of the process was investigated with the catalyst suspended, coated or included in the membrane. Although the system in which the membrane was used only as a support for the catalyst showed a good synergy between the photocatalytic and the separation process, the configuration with the suspended catalyst and the irradiation of the recirculation tank resulted more

interesting in terms of irradiation efficiency and membrane permeability, allowing also to select the membrane type depending on the photocatalytic process under study.

Further studies (Molinari et al., 2004) demonstrated that the rate of pollutant photodegradation was strongly affected by the UV irradiation mode. Comparing the results obtained in two types of photoreactor, with external lamp and with immersed lamp, it was observed that the rate of photodegradation with the immersed lamp resulted three times higher than that of suspended one, although the power of the last was four times greater.

In the perspective to solve the limitations of membrane technology in water treatments due to membrane fouling caused by solute content in wastewater, Shon et al. (2008) proposed an integrated photocatalysis – MF hybrid system in which photocatalytic reactions were exploited to degrade and modify organics giving a membrane fouling.

However, one of the major problems observed with pressurized flat sheet membrane systems is the membrane flux decline due to catalyst deposition and membrane fouling (Lee et al., 2001; Molinari et al., 2006a-2008; Le-Clech et al., 2006).

Choo et al. (2008), using an integrated photocatalysis/hollow fiber microfiltration system for the degradation of trichloroethylene in water, observed that membrane permeability was strongly affected by hydraulic conditions. In particular, they reported a reduction of permeability decreasing the cross flow velocity due to deposition of TiO_2 particles on the membrane surface, leading to membrane fouling.

Therefore, this drawback, which makes the pressurized systems unsuitable for industrial applications, addressed the research towards the use of other configurations of membrane photoreactors.

I.3.3.2 Submerged (de-pressurized) membrane photoreactors

In the last years several studies were performed using submerged membrane modules coupled to photocatalytic systems for the removal of organic pollutants such as fulvic acid (Fu et al., 2006), bisphenol-A (Chin S.S. et al., 2007), para-chlorobenzoate (Huang X. et al., 2007).

In the Submerged Membrane Photocatalytic Reactor (SMPR), the catalyst is suspended in an open-air reaction environment, the membrane is immersed in the batch and the permeate is sucked by means a pump.

Fu et al. (2006), studied the degradation of fulvic acid by using synthesized nano-structured TiO_2/silica gel catalyst particles in a submerged membrane photoreactor. They investigated the effects of some operative conditions, such as catalyst concentration, pH and airflow on the performance of the overall process and demonstrated that a reduction of membrane fouling, and therefore, an improvement of the permeate flux rate, can be obtained using nano-strctured TiO_2. This synthesized catalyst has an average particle size of 50 μm, which resulted small enough for the suspension, but big enough to avoid membrane fouling and to allow its easy separation.

Besides, controlling the hydrodynamic conditions near membrane surface it is possible to prevent catalyst deposition, reducing the membrane fouling which causes the membrane flux decline. An useful strategy in this context is gas sparging at the bottom of the membrane (Ghosh, 2006; Chan et al., 2007).

The efficiency of a hybrid system, combining a low-pressure submerged module in direct contact with the photocatalytic environment, was studied by Chin et al. (2007) for the removal of bisphenol-A in water. In particular, studying the factor affecting the performance of the SMPR, they observed that the aeration, allowing a mechanical agitation, reduces the fouling of the membrane and keeps the TiO_2 well suspended in the solution, acting also on the size of catalyst aggregates. However, beyond an aeration of 0.5 L min^{-1} no enhancement of photodegradation rate was achieved, probably due to the presence of bubble clouds that could attenuate UV light transmission in the photoreactor.

Besides, in this study the effect of another strategy was investigated; an intermittent permeation method was applied reducing membrane fouling thus maintaining high flux at low aeration rate.

When suction is stopped, the aeration can shear the membrane surface facilitating the detachment of catalyst particles and, therefore, avoiding their accumulation on the membrane.

The advantages of this approach were also investigated by Huang X. et al. (2007) in a study on the operational conditions of SMPR, in which it was demonstrated that suspending catalyst dropping out can be controlled by applying fine-bubble aeration and an intermittent membrane filtration.

An intermittent operative procedure was also employed by Choi W. (2006) in a work on the performance of submerged membrane photoreactors for 4-chlorophenol degradation. A pilot-scale photocatalysis-membrane hybrid reactor was constructed and characterized in terms of degradation efficiency and degree of membrane fouling. A complete degradation of the pollutant was achieved in 2 hours and, in continuous runs, no fouling of the membrane was observed when an intermittent operation was used.

Although the high fluxes and good removal efficiency of organic molecules obtained using ultrafiltration or microfiltration membrane in the described SMPR, nevertheless a common drawback reported is the low rejection of compounds with low molecular weight.

To overcome this problem, Choi J.H. et al. (2007) proposed the use of nanofiltration submerged membranes in a bioreactor for domestic wastewater treatment. The NF cellulose acetate membrane used in this work allowed to achieved a very good-quality permeate for a long-term operation, with a DOC concentration in the permeates which remained in the range 0.5 - 2.0 mg L^{-1} for the first 130 days. Nevertheless, after 80 days, the relative flux of the NF membrane increased gradually and the transmembrane pressure decreased, probably due to the hydrolysis of the cellulose acetate in wastewater which, increasing the pore size and porosity, caused a deterioration of permeate quality.

I.3.3.3 Photocatalytic membrane contactors

Other types of membrane separation processes that can be useful when they are coupled with a photocatalytic system are the membrane contactors.

In a membrane contactor the separation performance is determined by the distribution coefficient of a component in two phases and the membrane acts only as an interface.

They can be divided in gas-liquid (G-L) and liquid-liquid (L-L) membrane contactors. In the first configuration one phase is a gas or a vapour and the other phase is a liquid, while in the second one both phases are liquids.
Dependent on the type of membrane, the membrane phase may contribute to the overall mass transfer resistance.
Several photocatalytic hybrid systems in which the permeation module consists of a membrane contactor are reported in literature for photodegradation processes, and their potentialities are greater than those of the systems previously described. In fact, they can be a useful solution to separate the product(s) of interest during a photosynthetic process and in particular, if a suitable membrane and a proper strip phase are chosen, it is possible to obtain a selective separation of the product(s) before the occurrence of secondary reactions. Despite the advantages of these integrated systems, to our knowledge, in literature few studies report the use of a membrane contactor module coupled to photocatalytic synthetic pathways. (Mozia et al., 2006-2007; Camera-Roda et al., 2007; Azrague et al., 2007)

- I.3.3.3.1 Photocatalysis and direct contact membrane distillation

To solve the problems observed with pressure driven membrane reactor, an useful alternative PMR was proposed by Mozia et al. (2006-2007) studying the photodegradation of azo-dyes in aqueous solutions using a membrane distillation module to separate distilled water and TiO_2 Aeroxide® P25 as photocatalyst.
The separation in a membrane distillation process is based on the principle of vapour-liquid equilibrium, therefore, ions, macromolecules, cells and other non-volatile components are retained on the feed side, whereas the volatile components are separated by means of a porous hydrophobic membrane and then condensed in cold distillate (distilled water).
The results reported in these studies showed a complete rejection of the dye and other non volatile compounds (organic molecules and inorganic ions), thus the permeate was practically pure water. Some volatile compounds passed through the membrane, as indicated by TOC measurements in the distillate, although their concentration remained in a range of 0.4 – 1.0 mg L^{-1}. Besides, it was found that the addition of TiO_2 (in concentration of 0.1, 0.3 or 0.5 mg dm^3) to the feed solution did

not affect the permeate flux at least in the range investigated, which was about 0.34 m^3 m^{-2} d^{-1}, similarly to those obtained during the process in which ultrapure water was applied. This last aspect results very interesting because it avoids the significant fouling observed with pressure-driven membrane processes, although the higher energy consuming constitute a disadvantage in terms of process costs.

- I.3.3.3.2 Photocatalysis and Pervaporation system

To reduce the heating cost of the solution needed to perform a separation with a membrane distillation module, an approach could be to combine photocatalysis with pervaporation. In pervaporation the separation is not based on the relative volatility of the components in the mixture, but only depends on the relative affinity of the components for the membrane. Keeping a vacuum on the permeate side of the membrane and maintaining the feed side at atmospheric pressure, a pressure differences is created which results the driving force of the process. In this case, therefore, the choice of the membrane material is important to obtain a selective separation of the molecules.

Camera-Roda et al. (2007) proposed an integrated system in which photocatalysis is coupled with pervaporation as process intensification for the photocatalytic degradation of 4-chlorophenol (4-CP) in aqueous solutions. Aim of this work was to remove the intermediate organics formed in the first steps of the photodegradation of 4-CP which negatively affect the reaction rate, hindering the mineralization of the pollutant. To this purpose, organophilic pervaporation membranes were used so that most of the organic oxidation by-products permeated preferentially with respect to water.

- I.3.3.3.3 Dialysis – Photocatalysis

Another interesting separation approach was described by Azrague et al. (2007) that proposed a particular type of membrane contactor photoreactor in which a dialysis membrane (used as a contactor) was combined with a photocatalytic system for the depollution of turbid waters. This study was addressed to solve the problem of light scattering observed when solid particles are present in the solution which decrease the rate of photocatalytic degradation of pollutant in water. On this basis the

membrane dialysis module was used to keep the solid particles in their initial compartment and, contemporarily, to concentrate the pollutant, thanks to a different concentration, on the other side of the membrane where the photocatalytic reaction took place until total mineralization. Since the separation occurs thanks to a diffusion of the pollutant through the membrane, no transmembrane pressure is needed, avoiding the fouling of membrane which is an expensive problem in case of pressure driven membrane processes.

I.3.4 Future perspectives: solar energy

As previously described, many studies have been performed with the purpose to develop photocatalyst and photocatalytic systems able to exploit the sun as a source of light (Fernandez et al., 2005; Sarria et al., 2004).

Solar energy is important for achievement of sustainable processes because it constitutes a renewable, cheap and clean energy source.

Although the use of sunlight makes the photocatalytic membrane reactors promising in industrial and environmental fields, very few are the studies performed in this way.

A hybrid system consisting of a solar photoreactor with the catalyst suspended coupled with a membrane reactor was reported by Augugliaro et al. (2005) in a study on the photodegradation of lincomycin. The photo-oxidation experiments were carried out using compound parabolic collectors (CPC), installed at the "Plataforma Solar of Almerìa" (PSA, Spain).

By means of some preliminary tests performed without the membrane it was determined that photooxidation rate of lincomycin followed a pseudo-first order kinetics with respect to the substrate concentration under the used experimental conditions. The high membrane rejection values measured for lincomycin and its degradation products demonstrated that the hybrid system allowed the separation of these species and also of the photocatalyst particles, although in the experiments carried out in continuous mode, it was observed an accumulation of organic molecules in the system. This finding, which was dependent on solar irradiance and initial lincomycin concentration, can be explained by considering that the amount of

photons entering in the system were not sufficient to mineralise the organic carbon fed in the photoreactor.

Moreover, the experimental results obtained in continuous mode showed that the presence of the membrane allowed to reduce both the substrate and intermediates down to very low concentration levels, proving that the hybrid system could be very interesting from an economic point of view.

The photodegradation of pesticides in a solar pilot scale photocatalytic system coupled to a separation process was also reported by Malato et al. (2003). In this work, performed also at the Plataforma Solar de Almerìa, the TiO_2 recycling was realized by an accelerated sedimentation process, while the treated clean water was discharged through a microfiltration membrane to remove any small remaining catalyst residue.

I.4 OUTLINE ON KINETIC MODELS IN PHOTOCATALYSIS AND MODELING OF PMRS

I.4.1 Kinetic parameters

The development of fundamental kinetic models represents an important topic in the field of photocatalytic processes because, as emphasized by Ollis (2005), the discovered of credible rate equation can allow the scale-up or reconfiguration of photocatalyst systems. In fact, one of the problems that hinders the use of this technology at industrial level is the lack of validated kinetic models that allow the design of appropriate reactors reducing expensive and time-consuming steps required by the traditional empirical methodology for scaling-up.

On these basis, Imoberdorf et al. (2007) reported a kinetic study which predicts with good accuracy the performance of a pilot scale photoreactor starting directly from laboratory experiments.

The development of a full scale-up procedure employing laboratory kinetic information was presented also by Satuf et al. (2007) in a study on the photodegradation of 4-chlorophenol in a small slurry photoreactor. The kinetic model obtained describes the evolution of 4-CP as well as the formation and degradation of the main intermediate products. The intrinsic kinetic parameters estimated were used to model a bench scale reactor in which the experimental data obtained were in good agreement with the simulation results.

Therefore, knowledge of the reaction mechanism and of the effects of different variables on the reaction rate permits to obtain a kinetic model which can describe the process independently of the shape and configuration of the reactor allowing the development of a photocatalytic technology for industrial application.

As previously described, the photocatalytic process can proceed through the adsorption of the substrate (S) on the catalyst surface (Cat), although this phenomena is not a requirement for the reaction since the oxidizing species can diffuse into the bulk and react with the molecules.

When the reaction occurs on the catalyst surface, two consecutive reactions can be written:

$$S + Cat \underset{k_{-1}}{\overset{k_1}{\rightleftharpoons}} S\text{-}Cat \quad (1)$$

$$S\text{-}Cat \xrightarrow{k_S} P \quad (2)$$

In this condition, the rate of the photocatalytic process (r_S) depends on the amount of substrate S adsorbed on the catalyst surface.

I.4.2 Adsorption kinetics

The catalyst fractional sites covered by S is expressed by the parameter θ reported as:

$$\theta_S = \frac{Q_{ads}}{Q_{\max}} \quad (3)$$

where Q_{ads} is the amount of substrate adsorbed onto the catalyst (mol g^{-1}) and Q_{max} is the maximum number of molecules that can be adsorbed onto a gram of catalyst (e.g. TiO_2):

$$Q_{ads} = \frac{C_{in} - C_{eq}}{C_{cat}} \qquad Q_{\max} = \frac{C_{in}}{C_{cat}} \quad (4)$$

where C_{in} and C_{eq} are the initial and equilibrium concentrations of substrate (mol L^{-1}) and C_{cat} is the amount of catalyst per unit amount of solution (g L^{-1}).

θ_S depends on the substrate concentration in the reactive environment and it can be defined (at constant temperature) by the Langmuir Adsorption Isotherm, when the following assumptions are considered (Guettai et. al, 2005): (i) the number of adsorption sites on the catalyst surface is limited and homogeneously distributed, (ii) only one molecule can be adsorbed on a site, (iii) the coverage of catalyst is a monolayer, (iv) no interactions occur between the adsorbed molecules.

The Langmuir adsorption equation can be derived considering that:
- the rate of the adsorption step (r_1) is proportional to substrate concentration and to fractional free catalyst sites:

$$r_1 = k_1 C_{eq} (1- \theta_S) \tag{5}$$

- the rate of the deadsorption (r_{-1}) depends on the coverage catalyst surface:

$$r_{-1} = k_{-1} \theta_S \tag{6}$$

When equation (1) reaches the equilibrium condition ($k_2 <<< k_1$), r_1 and r_{-1} are equal, therefore:

$$k_1 C_{eq} (1- \theta_S) = k_{-1} \theta_S \tag{7}$$

thus:

$$\theta_S = \frac{k_1 C_{eq}}{k_{-1} + k_1 C_{eq}} = \frac{K_{ads} C_{eq}}{1 + K_{ads} C_{eq}} \tag{8}$$

in which $K_{ads} = k_1/k_{-1}$ is the Langmuir adsorption constant.
Substituting equation (3) into equation (8) gives the following expression:

$$Q_{ads} = \frac{Q_{\max} K_{ads} C_{eq}}{1 + K_{ads} C_{eq}} \tag{9}$$

The linear transformation of equation (9) can be expressed as the function $C_{eq}/Q_{ads} = f(C_{eq})$ (Guettai et al., 2005; Gora et al., 2006):

$$\frac{C_{eq}}{Q_{ads}} = \frac{1}{Q_{\max} K_{ads}} + \frac{C_{eq}}{Q_{\max}} \tag{10}$$

The ordinate at the origin of the straight line obtained is equal to $1/(Q_{max} K_{ads})$, whereas Q_{max} can be calculated from the reciprocal of the slope $\alpha = 1/Q_{max}$.

I.4.3 Photocatalytic kinetics

The widely accepted equation used to describe the photocatalytic kinetics is the Langmuir-Hinshelwood (L-H) kinetic model, in which the rate of oxidation is the limiting reaction rate at maximum coverage of catalyst. It is related to the substrate concentration by the parameter θ_S:

$$r_S = -\frac{dC}{dt} = k_S \theta_S = k_S \frac{K_{LH} C}{1 + K_{LH} C} \tag{11}$$

As demonstrated in many studies (Djikstra et al., 2001; Bhatkhande et al., 2004; Doll et al., 2004; Herrmann, 2005; Guettai et al.,2005), for diluted solutions in which the substrate concentration is $<10^{-3}$ M, the values of $K_{LH}C << 1$ and the L-H equation is simplified to a pseudo-first order kinetic law with respect to C (equation 12). At higher initial substrate concentrations ($C > 5\ 10^{-3}$ M), $K_{LH}C >> 1$ and the reaction rate is of apparent zero order (equation 13):

$$r_S = k_S K_{LH} C = k_{app} C \tag{12}$$

$$r_S = k_S \tag{13}$$

The dependence of the initial photocatalytic rate on the respective initial concentration (C_0) of substrate can be obtained by the linear form of the L-H model:

$$\frac{1}{r_S} = \frac{1}{k_S} + \frac{1}{k_S K_{LH}} \cdot \frac{1}{C_0} \tag{14}$$

Plotting the inverse of the initial rate against the inverse of the initial concentration a straight line is obtained in which the intercept gives the k_S value and the slope the K_{LH} value.

As reported in several studies (Ollis, 2005; Guettai et al., 2005) a discrepancy between K_{ads} obtained in the adsorption isotherm and K_{LH} obtained from photocatalytic reaction can be observed. This aspect can be explained considering that the photocatalytic process is influenced by various parameters, such as oxygen,

formation of by-products, light intensity, number of adsorption sites, reaction mechanism and changes of electronic properties of catalyst surface under irradiation. For these reasons, when the kinetic of the photocatalytic process is expressed by the L-H kinetic model, some assumptions must be take into account.

Since the surface of TiO_2 catalyst is covered with hydroxyl groups and water molecules, they can compete with the substrate for the same active sites (Guettai et al., 2005), equation (11) should be expressed as:

$$r_S = k_S \frac{K_{LH} C}{1 + K_{LH} C + K_w C_w} \tag{15}$$

where K_w is the solvent adsorption constant and C_w its concentration.

However, since the C_w is constant and it is >> C, the part of the catalyst covered by water is unalterable over the whole range of concentration. Therefore, if the others experimental conditions (such as pH, catalyst dosage, photointensity, etc.) are the same, C is only variable in the initial reactions and the rate can be calculated by the equation (11).

The rate determining step of the photocatalytic oxidation is the reaction between the OH radicals and the substrate. Augugliaro et al. (2005) hypothesized that two different types of active sites exist over the catalyst surface. The first ones are able to adsorb the substrate while the others are able to adsorb oxygen molecules that acts as electron trap generating OH radicals.

The reaction rate may be written in terms of modified L-H kinetic as:

$$r_S = k'' \theta_S \theta_{O_2} \tag{16}$$

in which k'' is the surface second-order rate constant and and θ_{O_2} the fractional sites coverages by oxygen:

$$\theta_{O_2} = \frac{K_{O_2} C_{O_2}}{1 + K_{O_2} C_{O_2}} \tag{17}$$

If the oxygen is regularly supplied, it can be assumed that the fractional sites coverage by hydroxyl radicals is constant and it can be integrated in the apparent rate constant (Bhatkhande et al., 2004; Herrmann, 2005):

$$r_S = k''\theta_S\theta_{O_2} = k_{app}\theta_S \tag{18}$$

Another important aspect, which must be taken into account studying the kinetic mechanisms of a photocatalytic process, is the presence in the reactive environment of other species, mixture or intermediates by-products, which may interfere in the adsorption and oxidation mechanism of the main substrate.

When *n* intermediate products are formed during a photocatalytic reaction, the L-H models assumed the form (Gora et al., 2006; De Heredia et al., 2001):

$$r_S = k_S \frac{K_S C_S}{1 + K_S C_S + \sum_{i=1}^{n} K_i C_i} \tag{19}$$

where K_i is the binding constant of the intermediate products adsorbed onto catalyst surface and C_i their concentration. Assuming that C_i adsorbed can be neglected respect to C_S and that the binding constants of the intermediates is the same to that of S, $K_{i=1} = K_{i=2} \ldots = K_S$, equation (19) can be approximated to the L-H model.

The kinetic model of a multicomponent system can be obtained making the same considerations.

Biard et al. (2007) in a study on the photodegradation rates of a binary mixture of propionic and butyric acids, demonstrated that the degradation is inhibited when the two compounds are mixed in comparison to the pure acids due to a competitive adsorption on the catalyst active sites.

When the molecules or their by-products react together (chemical interaction) the proposed L-H kinetic equation is (Wang et al., 1998; Rideh et al., 1999; Tan S.S. et al., 2008):

$$r_{S1} = k_{S1}\theta_{S1}\theta_{S2} = k_{S1}\frac{K_{S1}C_{S1}K_{S2}C_{S2}}{(1 + K_{S1}C_{S1} + K_{S2}C_{S2})^2} \tag{20}$$

If between two (or more) substrates no molecular interactions occur, equation (20) can be simplified as (Li Puma et al., 2007; Biard et al., 2007; Zmudzinski et al., 2007):

$$r_{S1} = k_{S1}\theta_{S1} = k_{S1}\frac{K_{S1}C_{S1}}{1 + K_{S1}C_{S1} + K_{S2}C_{S2}} \tag{21}$$

I.4.4 Quantum yield and relative photonic efficiency

As observed by Xu Y. et al. (2000), modifications in the characteristics and adsorption capacity of the catalyst sites can occur when the surface is irradiated with UV photons, causing different values of adsorption constants in the dark and in the photocatalytic reaction.

As reported in literature (Emeline et al., 2000; Brosillon et al., 2008a) the rate of reaction is related to the photon flux ρ by the following equation

$$\frac{dC}{dt} = r \propto \rho^n \tag{23}$$

At low light intensities, a linear reaction rate is observed with the photon flux (n=1); nevertheless, increasing the light intensity a plateau is reached and the rate becomes proportional to the square root of ρ (n=1/2). For a very high value of photon flux, the rate of reaction assumes a kinetic of zero order with respect to the light intensity (n=0).

The relation between the rate of reaction and the photon flux can be expressed as "quantum yield" Φ, equal to the ratio of reaction rate to the theoretical maximum rate of photon absorption (Serpone,1997; Hoffmann et al., 1995; Djikstra et al., 2001):

$$\Phi_S = \frac{dN_S / dt}{d[h\nu]_{inc} / dt} \tag{22}$$

where N_S is the number of molecules converted and $[h\nu]_{inc}$ the incident photonic flux.

Its theoretical maximum value is equal to 1 and it can vary with the nature of the catalyst, the experimental conditions and the reaction considered (Herrmann et al., 2005).

As observed by Serpone (1997), the measurement of Φ requires the knowledge of action spectrum in the spectral region of interest on the examined reaction. When the action spectrum is unknown, it is preferable to use the "quantum efficiency" η, defined as the ratio of number of molecules which undergo a given event to the total number of photons absorbed in the spectral region used. This difference takes into account that only the photons actually absorbed induce the photocatalytic process, although in literature these two parameters are often reported with the same meaning. Since the rate of absorption of photons is very difficult to assess due, in particular, to the light scattered by the molecules in the dispersion, it was proposed another parameter, the "photonic efficiency" (ζ), defined as the number of reactant molecules transformed or produced divided by the number of photons, at a given wavelength, incident inside the front window of the cell (Serpone, 1997):

$$\zeta = \frac{\mathrm{N_{molecules}\,(mol\,s^{-1})\ transformed/produced}}{\mathrm{N_{photons}\,(einstein\,s^{-1})\ incident\ inside\ reactor\ cell}} \tag{23}$$

To avoid unnecessary errors and to propose a method that could be used to cross-reference experiments independently from the reactor used, several authors (Serpone, 1997; Okte et al., 2000) used a "relative photonic efficiency" (ζ_r) which is related to an acceptable standard process.

Besides, the ζ_r values can be converted into the quantum yield Φ, once a standard quantum yield $\Phi_{standard}$, (for the given photocatalyst and the given substrate), has been determined, by the relation:

$$\Phi = \zeta_r\, \Phi_{standard} \tag{24}$$

Zhang et al. (2002), in a study on the photocatalyzed N-demethylation and degradation of methylene blue (MB) in TiO_2 dispersions exposed to concentrated sunlight, used the relative photonic efficiency to demonstrate that MB

photodecomposition under concentrated sunlight irradiation, measured against phenol, is identical with the efficiency measured under UV radiation, independent of photoreactor geometry, of light sources and of the operating mode used.
The understanding of these relations is fundamental to compare the activity of different catalysts for a same reaction and to estimate the energetic yield and the cost of the photocatalytic process.

I.4.5 Modeling of PMR

Although the great potentialities of membrane photoreactors, very few studies have been performed with the aim to understand the kinetic models influencing the performance of the separation process in these systems.
Models predictions can be used to optimize the performance of the reactor, to design the reactor and to evaluate the performance of different membranes.
Depending on the photocatalytic reaction involved and on the type of membrane module used, the kinetic model changes its form, therefore modelling a membrane photoreactor requires knowledge of the kinetic equations of the catalyst, the membrane and the reactor configuration.
Azrague et al. (2007) proposed a mathematical model (Scheme I.1) for a system in which a photocatalytic reactor was combined with a dialysis membrane, used to concentrate organic pollutants from the feed tank in the photocatalytic reactor where they were degraded. By a preliminary study they demonstrated that, starting from the L-H kinetic model, the rate of the photocatalytic degradation followed a pseudo-zero order kinetics (eq. a). Besides, performing dialysis experiments (without irradiation), they assumed that mass transport of solutes was due to diffusion only and no occurring exchange of solution between the two compartments and they described the variation of concentration in the feed tank and in the reactor by differential equations (eq. b).
On these basis, for the described PMR, a model based on diffusion through the membrane and zero-order reaction in the reactor was proposed (eq. c). A good agreement with the experimental data, in a wide range of operating conditions, was demonstrated.

Photocatalytic kinetics

$$C_s = C_s^0 - k_{app} t \qquad (a)$$

Separation kinetics

$$\frac{dC_s}{dt} = -\psi(C_s - C_a) \qquad \frac{dC_a}{dt} = \omega(C_s - C_a) \qquad (b)$$

Modeling of PMR

$$\frac{dC_s}{dt} = -\psi(C_s - C_a) \qquad \frac{dC_a}{dt} = \omega(C_s - C_a) - k_{app} \qquad (c)$$

where C_s and C_a are the pollutant concentration in the feed tank and in the photoreactor, respectively; C_s^0 is the initial substrate concentration in the feed tank; k_{app} the apparent zero-order rate constant; t is the irradiated time; $\psi=kA/V_s$ and $\omega=kA/V_a$ are abbreviations without name used to simplify the mathematical expressions; V_s and V_a are the volumes of the solutions in the feed tank and in the photoreactor, respectively; A the membrane area; k the average overall mass-transfer coefficient.

Scheme I.1: Modeling of a dialysis membrane photoreactor proposed by Azrague et al. (2007).

Chin et al. (2007) used pseudo-first order reaction kinetics combined with the ideal CSTR (Continuous stirrer tank reactor) model to evaluate the effect of initial concentration of pollutant on the performance of a submerged membrane photocatalytic reactor for the degradation of bisphenol-A in water (Scheme I.2). This CSTR model, which takes into account the importance of the residence time of the organic substrate in the system (assuming the membrane has zero retention of substrate), however, had only limited success. The discrepancies observed with the experimental data were attributed both to the effect of adsorption/desorption of organics on the membrane and to the variation of their rate constants.

Equation in an isothermal stirred tank reactor

$$C_A - C_{Af} = -kC_A\vartheta$$

Differentiation

$$\frac{dC_A}{dt} = \frac{1}{\vartheta}(C_{Af} - C_A) - kC_A$$

Analytical solution

$$C_A(t) = C_A^0 e^{-(1/\vartheta+k)t} + \frac{C_{Af}}{1+k\vartheta}[1 - e^{-(1/\vartheta+k)t}]$$

where C_A is the substrate concentration at time t; C_{Af} the feed concentration; θ is the residence time of substrate.

Scheme I.2: Modeling of a submerged membrane photoreactor proposed by Chin et al. (2007).

SECTION II

TOTAL OXIDATION REACTIONS IN PHOTOCATALYTIC MEMBRANE REACTORS: DEGRADATION OF PHARMACEUTICAL COMPOUNDS IN WATER*

II.1 PHARMACEUTICAL ACTIVE COMPOUNDS AS TOXIC POLLUTANTS

II.1.1 Occurrence of pharmaceuticals in the aquatic environment

Pharmaceutically active compounds (PhACs) are an important group of toxic organic contaminants that recently has attracted much attention to the international scientific community because of their presence in the aquatic environment (Heberer et al., 2002; Nikolaou et al., 2007; Gomez et al., 2007).

The problem is further exacerbated considering the lack of knowledge on the biological effects of these contaminants.

Concentrations of human pharmaceuticals are typically highest in wastewaters but can also be relevant in surface waters, where, despite their low levels, they might give rise to undesirable effects on living organisms. Since surface waters are often used as source for drinking-water production, and treated wastewaters are utilized to recharge groundwater tables in regions affected by freshwater scarcity, there is a growing interest in understanding the fate of pharmaceuticals during drinkingwater treatment (Canonica et al., 2008).

These compounds reach the aquatic environment as refusals of the hospital structures, pharmaceutical industries, municipal sewage treatment plants, as well as residues of their use in agriculture and breeding (Nikolaou et al., 2007).

---

* This part of work has been published as:

Molinari R., Caruso A., Argurio P., Poerio T., "Degradation of the drugs Gemfibrozil and Tamoxifen in pressurized and de-pressurized membrane photoreactors using suspended polycrystalline TiO_2 as catalyst", *Journal of Membrane Science*, 2008, Vol. 319, pp. 54-63.

The number of pharmaceutical compounds licensed for human use and their annual consumption have increased dramatically over the past number of years. As reported by Comeau et al. (2008), the worldwide use of prescription and non prescription drugs are estimated in the thousands of metric tons per year. The principal sources of these organic contaminant present in the environment originate from the medical and therapeutic treatment of humans and animals. The drugs are usually absorbed and metabolized (completely or partially) by the body and residues of the active ingredients and metabolites are excreted in the urine and feces which, therefore, flushed directly into domestic septic systems or into municipal wastewater treatment infrastructure. Treated effluents and, in some cases, untreated wastewater are then discharged into a receiving body of water, including small streams, rivers, lakes, and the marine environment.

As widely discussed by Eriksson et al. (2008), the large part of the population in EU is connected via sewerage systems to treatment plants, which treat the municipal wastewater. The municipal wastewater generally consists of a mixture of domestic, industrial wastewater and stormwater. More than 50,000 wastewater treatment plants (WWTP) are operating in the European Union, producing more than 8.1 millions tons of dry solids per year. The main disposal routes for sewage sludge deriving from WWTP are application to land, composting, disposal in a landfill and incineration as well as sea disposal. Sewage sludge has been used in agriculture as fertilizer as sustainable practice utilizing, recycling the nutrients back to land and to improve soil quality. Nevertheless, despite the benefits, applications on agricultural land have some disadvantages due to the presence of xenobiotics and pathogenic microorganisms which represent a risk for humans and animals.

On this basis, the Urban Waste Water Treatment Directive (91/271/EEC) implemented, in both the old and the new EU member states, the demand for more extensive wastewater treatment will eventually result both in the safeguarding of the receiving waters as well as in the production of more sewage sludge than produced today. Although in the 15 old member states the 75% of the wastewater treatment plants comply with the directive, in the new states, the number is estimated to be significantly lower.

Since the demand for sustainable solutions requires that the modern societies make safe use of all recyclable resources, toxic xenobiotic organic compounds (XOCs) which are found in concentrations that constitute a risk to living organisms should be identified and eliminated before application to land or other dispersal in the environment via various land applications. Although there is no extensive evaluation of environmental risk assessment of XOCs, some European countries have been implementing additional limit values for these contaminants in sludge.

Besides, wastewater treatment plants have been identified as a major point source of pharmaceuticals and personal care products entering in the aquatic environment both as the parent compound or as an array of metabolites. Removal efficiencies in WWTPs are often low, for example, removal rates for carbamazepine in a German WWTP was 7% while the average removal rate for the 14 compounds investigated was 65% (Lacey et al., 2008).

Compounds not removed are, therefore, released to receiving water bodies in WWTP effluent streams.

Studies have reported on the presence of more than 80 drugs, including active and inactive metabolites in the surface waters of various countries of the European Union, the United States, Brazil, and Canada.

Generally, these pharmaceutical compounds are detectable in receiving waters in concentration range of ng L^{-1} to μg L^{-1} (Zwiener et al., 2003; Comoretto et al., 2005; Kolpin et al., 2004). Despite such values are lower than maximum concentrations found for other industrial contaminants, they are considered among the pollutants which cause greater health risks for humans and members of terrestrial and aquatic ecosystems (Bendz et al., 2005). Pharmaceuticals are designed to produce biological and therapeutic effects in humans and animals at low doses. Little is known on potential effects of these biologically active compounds on the much smaller organisms living in the ecosystem. Another issue at the ecosystem level is that of continual exposure of organisms due to the continuous discharge of sewage contaminants into receiving waters (Comeau et al., 2008) which can cause toxicological chronic effects.

Kim et al. (2007) evidenced that some treatment processes are clearly more effective than others for reducing the concentration of a broad range of trace contaminants.

Traditional methods, like coagulation, flocculation and precipitation, are largely ineffective for removing dissolved organic contaminants, while oxidative processes such as chlorination and ozonation are effective for reducing their concentrations, although removal efficacy is a function of the contaminant structure and oxidant dose.

Biological processes, such as activated sludge, biofiltration, and soilaquifer treatment, have been shown to greatly reduce the concentration of compounds which are biodegradable and/or readily bind to particles. Activated carbon can remove nearly all organic contaminants; however, removal capacity is limited by contact time, competition from natural organic matter, contaminant solubility, and carbon type. Also membrane processes are identified as an attractive solution. Reverse osmosis (RO) and nanofiltration (NF) membranes provide effective barriers for rejection of contaminants, while microfiltration and ultrafiltration (UF) membranes provide selective removal for contaminants with specific properties.

On this basis the demand to develop efficient systems, alternative to the traditional purification methods, for removing these compounds from waters, has assumed a great research interest.

II.1.2 Photocatalytic membrane reactors as purification tecnique

Hybrid processes coupling membranes and photocatalysis could represent an useful solution to the above mentioned problems (Molinari et al., 2006a) because the membrane could play the role of confining the photocatalyst and, if a suitable membrane is used, of selective barrier for the species to be degraded.

Photocatalytic degradation processes have been studied in the mineralization of toxic organic compounds (Wu et al., 2005; Bhatkhande et al., 2004), herbicides (Topalov et al., 2000; Singh et al., 2007; Sleiman et al., 2007), pesticides (Lhomme et al., 2007; Abu Tariq et al., 2007), hormones (Zhang et al., 2007), dyes (Molinari et al., 2004; Mascolo et al., 2007), pharmaceuticals (Molinari et al., 2006a; Augugliaro et al., 2005), etc (see also section I.1.3.1). As represented in Scheme II.1, thanks to the high and unselective reactivity of the hydroxyl radicals these organic molecules are converted into harmless inorganic species.

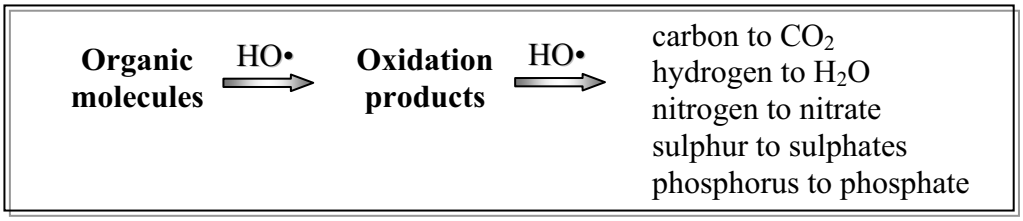

Scheme II.1: Schematization of the oxidative pathway of organic molecules into the corresponding inorganic species.

Besides, as reported by Augugliaro et al. (2006), in order to improve the performance of the photodegradation process, heterogeneous photocatalysis has been combined with physical or chemical operations, such us ozonation (Addamo et al., 2005; Hernandez-Alonso et al., 2002), ultrasonic irradiation, electrochemical treatment, biological treatment (Parra et al., 2000; Pulgarin et al., 1999), membrane reactor (Molinari et al., 2006a; Mozia et al., 2006), etc., with an increase of the efficiency of the photocatalytic process or/and of the overall process.

In particular, in hybrid system in which photocatalysis is coupled with membrane module, the membrane can allow to recovery and reuse the photocatalyst and to maintain the substrate and its oxidation products in the reactive environment, obtaining the clarified solution as permeate (Figure II.1).

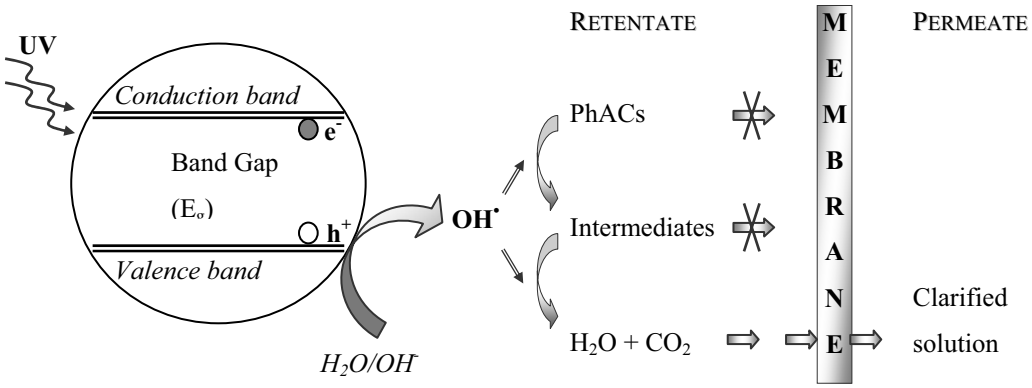

Figure II.1: Schematic representation of a photodegradation process in a membrane reactor for pharmaceutical pollutants.

II.1.3 The aim

Aim of this work was to study the possibility to use photocatalytic membrane reactors in the degradation of pharmaceutical compounds in water using two membrane module configurations, **Pressurized (PPMR) and Submerged (SPMR) Photocatalytic Membrane Reactors**.

In the first module the catalyst is suspended and recirculated in the pressurized side of the membrane, while in the second one the catalyst is suspended outside the membrane immersed in the batch reactor and the permeate is sucked by a de-pressurization. Both these systems permit to work in continuous, but the immersed membrane photoreactor should be more interesting on the application point of view.

Two drugs, Gemfibrozil and Tamoxifen, not studied before in membrane photoreactors, were used as target pharmaceutical pollutants and suspended TiO_2 was used as photocatalyst.

Initially, to optimize the performance of membrane photoreactors the effects of some parameters on the photodegradation and on the separation processes were studied separately.

The influence of the pH of aqueous TiO_2 suspensions on the passage of the catalyst through the membrane pores was investigated in order to minimize its presence in the permeate. Particular attention was addressed to some aspects that affect the behaviour of the membranes in terms of rejection, flux and fouling, such as recirculation flow rate and membrane clean-up.

These results were then used to perform the photodegradation experiments in the batch and in the continuous membrane photoreactors (with pressurized and sucked (submerged) membranes) to study the catalytic efficiency of the photodegradation process. In particular, the submerged membrane, differently from the configurations reported in literature, is placed in a permeation cell located separately from the irradiation zone.

II.2 EXPERIMENTAL

II.2.1 Materials

Gemfibrozil (GEM) is the 5-(2,5-dimethylphenoxy)-2,2-dimethylpentanoic acid (is a fibrate hypolipidemic agent) (Figure II.2a), $C_{15}H_{22}O_3$, MW = 250.35 g mol^{-1}, from Sigma. Gemfibrozil solutions were prepared by dissolving 10 mg of the drug in 1 L of ultrapure water (Elix 5, Millipore).

Tamoxifen (TAM) is the 2-[4-(1,2-diphenylbut-1-enyl)phenoxy]-N,N-dimethyl-ethanamine (an antineoplastic agent used for the treatment of breast cancer) (Figure II.2b), $C_{26}H_{29}NO$, MW = 371.53 g mol^{-1}, from Sigma. Tamoxifen solutions were prepared by dissolving 8 mg of the drug in 1 L of ultrapure water (Elix 5, Millipore) and adding hydrochloric acid or citric acid.

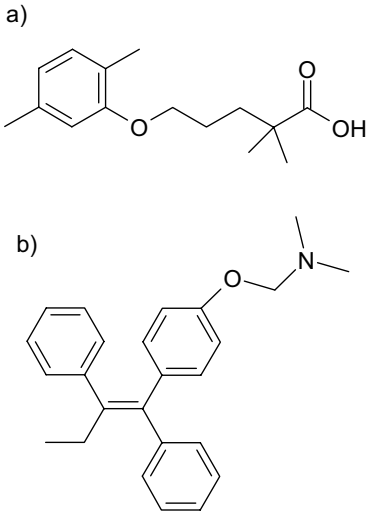

Figure II.2: Chemical structures of Gemfibrozil (a) and Tamoxifen (b).

Sodium hydroxide (NaOH, MW = 40.00 g mol^{-1}, purity = 98 %) from Sigma, hydrochloric acid 37 % w/w (HCl, MW = 36.46 g mol^{-1}) from Riedel-de Haen and citric acid ($C_6H_8O_7 \bullet H_2O$, MW = 210.14 g mol^{-1}, purity = 99.8 %) were used to correct the pH of aqueous phases.

In every test, the photocatalyst was TiO_2, Degussa P25 type (specific surface area = 44 m^2 g^{-1}, crystallographic phase ca. 80 % anatase and 20 % rutile, band gap 3.2 eV).

Commercial flat sheet nanofiltration membranes NTR 7410 (Nitto Denko, Tokyo) were used in the rejection and photocatalytic tests in the configuration where the catalyst was recirculated in the pressurized side of the membrane. They were made of sulfonate polyethersulfone polymer with 600/800 Da cut-off (rejection 10 % with 0.2 % NaCl at 4.9 bar, 25 °C, pH 6.5). After each run, the membranes were regenerated by immersion in an aqueous solution containing 0.2 % (w/w) of an enzymatic detergent (Ultrasil 50 by Henkel).

Commercial capillary membranes made by hydrophilic polyethersulfone (PES) (X-Flow, Norit), 2.9/1.9 mm outside/inside diameter and 0.05 - 0.1 μm average pore size were used in the configuration with immersed membrane.

II.2.2 Methods

Gemfibrozil and Tamoxifen concentration and the relative area of peaks of their degradation products were detected by high performance liquid chromatography (HPLC, Agilent 1100 Series instrument) using a Phenomenex Synergi 4u Fusion – RP 80 A (4.60 × 250 mm, 4 μm) column by UV readings at 220 nm and 235 nm wavelength for GEM and TAM, respectively. The mobile phase consisted of an acetonitrile/phosphate buffer at pH 3.1 solution 70/30 v/v fed to a flow-rate of 1.0 mL min^{-1}. The column pressure was 82 bar and the injection volume was 20 μL.

Gemfibrozil and Tamoxifen mineralization was evaluated by Dissolved Organic Carbon (DOC) measurements, performed by using a TOC-VCSN from Shimadzu.

All the samples used were filtered by means of a low-adsorbing membrane (mean pore size 0.2 μm) before carrying out the analyses.

The properties of TiO_2 suspensions, at different pH and concentrations, filtered with 0.2 μm membranes, were determined by light scattering analyses, using the 90 - Plus particle size analyzer (Brookhaven Instruments).

A pH meter (WTW Inolab Terminal Level 3) with a glass pH-electrode SenTix 81 (WTW), was used for pH measurements.

II.2.3 Apparatus

In order to determine the best operative condition to employ in the membrane photoreactor, some experimental runs were carried out in the batch photoreactor (b) (without membrane) reported in Figure II.3.

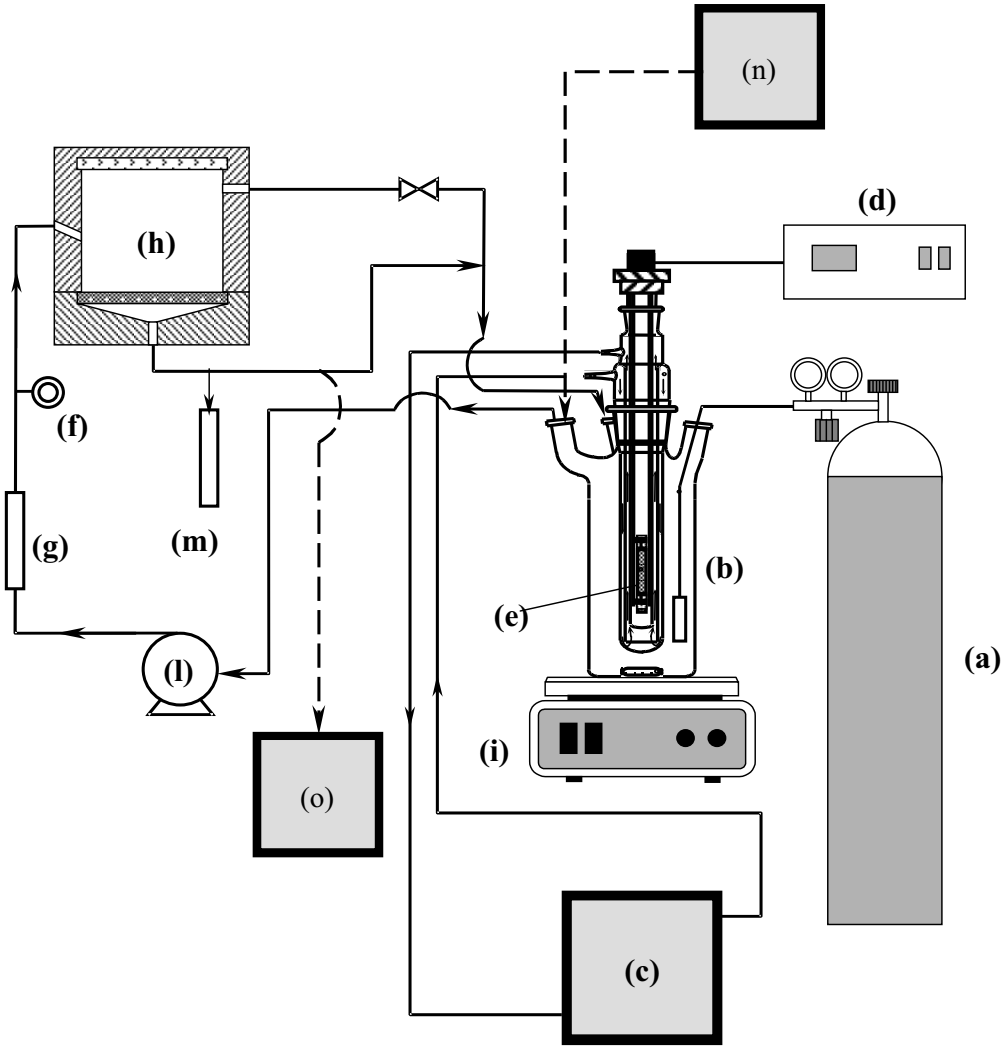

Figure II.3: System set-up with the pressurized membrane module:
(a) oxygen cylinder; (b) photoreactor; (c) thermostatic bath with cooling water; (d) power supply; (e) medium pressure Hg lamp with cooling jacket; (f) manometer; (g) rotameter; (h) pressurised cell containing the membrane; (i) magnetic stirrer; (l) pump; (m) graduated cylinder for permeate sampling; (n) feed tank (continuous regime); (o) waste tank (continuous regime).

It consisted of a cylindrical Pyrex glass reactor with a 125 W immersed medium pressure Hg lamp (e) (Helios Italquartz). The annular photoreactor, whose volume was 700 mL, had ports in its top section for sampling the suspension and bubbling of gas. The UV lamp was positioned axially inside the reactor and the circulation of distilled water, in the Pyrex glass jacket surrounding it, allowed to maintain the system at a temperature of 30 °C.

Oxygen (a) was bubbled into the reacting mixture to maintain a constant concentration of 22 ppm, determined by means of a dissolved oxygen meter (Mod. HI 9143, Hanna Instruments) with a membrane selective electrode.

When the flat sheet membrane was used, the photodegradation and rejection experiments were carried out in the whole system set-up.

This system set-up was realized by coupling the membrane cell containing the flat sheet membrane (h) to the batch photocatalytic reactor before described. The nanofiltration membrane, with exposed membrane surface area of 19 cm^2, was placed on a porous disk of sintered stainless steel in the bottom of a cylindrical cell, made with stainless steel, closed at the top with a transparent polycarbonate septum. The cell, with a volume of 95 mL, was maintained under pressure by means of a diaphragm pump (l) (Cole-Palmer (Lewa MD 0.18) Qmax = 60 L h^{-1}, Pmax = 14 bar) that allowed the recirculation of the aqueous solution. Pressure regulation on the membrane was obtained by means of a valve located between the exit of permeation cell and the batch reactor. The suspension entered the cell downward tangentially, generating a turbulent flow which minimised catalyst deposition on the membrane surface.

The submerged membrane photoreactor (SPMR) was built from a modification of the previous one described by simply changing the permeation cell connected to the batch photoreactor. The pressurized membrane permeation cell was substituted with the permeation system reported in Figure II.4. It is constituted by a module containing four capillary membranes in polyethersulphone (PES) useful length 11.5 cm. The capillary membranes were vertically assembled in a cylindrical shell made with a polypropylene tube by using a two component epoxy encapsulant (Stycast 1266 from Emerson & Cuming). The external exposed membrane surface area was $4.19 \cdot 10^{-3}$ m^2. The oxidant (O_2) was not fed directly in the photocatalytic reactor but it

was insufflate in the permeation module as evidenced in Figure II.4, providing some turbulence on the external membrane surface and therefore reducing catalyst deposition on the membrane. Oxygen freely crossed from inside to outside the holes of the shell thus oxygenating also the aqueous medium recycled back to the batch photoreactor.

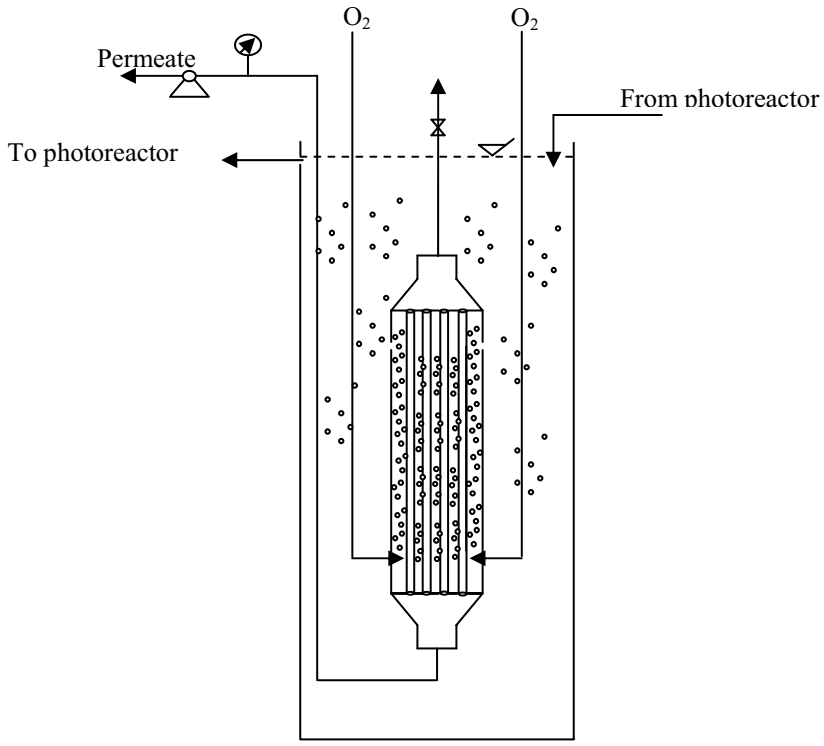

Figure II.4: Scheme of the permeation cell with submerged membranes.

The permeate was continuously withdrawn (sucked) from the module through the depression provided by a peristaltic pump (Masterflex Easy Load, Model 7518-12), splined to a shaft operated by an electric engine (Masterflex Console Drive, Cole-Parmer Instruments Company).

The permeation cell with submerged membrane was fed by means of a diaphragm pump withdrawing the solution from the batch photocatalytic reactor. The retentate come back in the photoreactor by gravity.

II.2.4 Parameters investigated

The efficiency of the photocatalytic process was evaluated in terms of drugs abatement and mineralization. In particular the abatement percentage (Abt %) was calculated, by means of HPLC analysis, as:

$$\text{Abt}\% = \frac{C^i - C^t}{C^i} * 100$$

were C^i and C^t are the concentration of the drug at the time "0" and "t", respectively.
The mineralization was estimated by TOC measurements as:

$$\text{Min}\% = \frac{TOC^i - TOC^t}{TOC^i} * 100$$

were TOC^i and TOC^t are the total organic concentrations in solution at the time "0" and "t", respectively.
In the experiments with the membrane modules, the performance of the system was investigated in terms of substrate rejections and permeate fluxes.
Membrane rejection (R%) was calculated as

$$R\% = \left(1 - \frac{C_p}{C_r}\right) * 100$$

where C_p and C_r are the concentrations of the drug present in the permeate and in the retentate, respectively.
The permeate flux (J_p) was reported as:

$$J_p = \frac{V_p}{t * S}$$

were V_p is the volume of permeate (L) collected at the steady state in the time t (h) and S is the membrane surface area (m^2).

II.3 RESULTS AND DISCUSSION

II.3.1 Determination of optimal operative conditions

Before carrying out the tests on the batch and membrane photoreactors, some preliminary tests were carried out in order to determine the influence of pH and concentration of aqueous suspensions of TiO_2 on particle aggregation and adsorption of organics.

II.3.1.1 pH of aqueous TiO_2 suspensions

The pH plays an important role on the dispersion of the catalyst in the aqueous suspension. In particular, the formation of aggregate of catalyst particles and their precipitation was observed at acidic values; this aspect, determining a reduction of the catalytic active sites, decreases the catalyst activity. On the other hand increasing the pH, particle size decreases but it is necessary that particles are rejected by the membrane in order to confine them in the reaction zone.

The optimal pH value was determined by means of Light Scattering analyses on TiO_2 suspensions, at different pH and concentrations, filtered with 0.2 μm membranes.

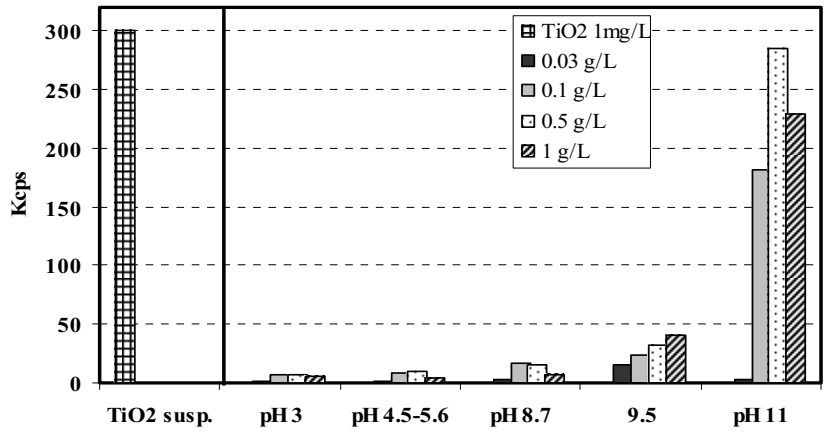

Figure II.5: Comparison between count of particles per second (Kcps) vs pH for different catalyst concentrations after filtration through a 0.2 μm membrane (TiO_2 susp. is not filtered, pH ca. 5).

Figure II.5 compares the kcps values (kilocount per second of the particles that the instrument measures in the suspension) in the different conditions. It can be observed that alkaline pH, greater than 10, causes the passage of particles through the 0.2 μm membrane indicating their excessive desegregation. The reported results suggest a preferable pH range of 7 ± 3 to perform the experiments.

II.3.1.2 Catalyst concentration

An important step of a photocatalytic process is the adsorption of organic compounds onto the catalyst surface, where the hydroxyl radicals can oxidize the substrate.
In order to verify the adsorption behaviour of Gemfibrozil on the TiO_2 surface, some tests on GEM solutions at initial concentration of 10 mg L^{-1} and pH 9.15, using different concentration of the catalyst, were carried out. The steady-state conditions were reached for all the solutions after about 60 minutes. The tests were carried out in duplicate.
The obtained adsorption values, measured at the steady-state, showed a negligible adsorption that did not increase with increasing the catalyst amount (Table II.1).

Table II.1: Gemfibrozil adsorption (Ads %) on catalyst surface (C_{GEM} = 10 mg L^{-1}; T = 30 °C; V = 500 mL; pH = 9.1).

TiO_2 (g L^{-1})	**Ads %**
0.01	13.0
0.05	12.9
0.10	14.0
0.50	16.0
1.00	22.1

This behaviour can be explained by considering that TiO_2 catalyst is neutral at the isoelectric point (PZC TiO_2 in the pH range 4.5 – 6.2), above this one its surface is charged negatively and below it is positive (Molinari et al., 2006a; Bekkouche et al.; 2004). Thus, at the alkaline pH, used in the adsorption tests, the catalyst surface is negatively charged and the carboxylic group of GEM is in the anionic form causing a repulsion phenomenon that could explain the low adsorption values.

Therefore, the reported results suggest to work at low concentration of TiO_2, which is an useful condition both from an economic and reaction efficiency point of view, because an increase in opacity and light scattering of TiO_2 particles occurred at high concentrations, leading to the decreased passage of radiation through the suspension.

II.3.2 Degradation tests in the batch reactor

Based on the previous results the operative conditions selected for the photodegradation tests in the batch reactor were: Gemfibrozil concentration in the feed 10 mg L^{-1}; suspended TiO_2 concentration 0.1 g L^{-1} or 1 g L^{-1}; pH in the range 7 - 10; temperature in the reactor thermostatted at 30 °C; volume of solution 700 mL, oxygen continuously bubbled at 0.5 bar to obtain a saturation concentration of 22 ppm determined by means of a dissolved oxygen meter.

II.3.2.1 Photolysis tests

To understand the behaviour of GEM using only UV light, photolysis tests in absence of the catalyst were performed. Although the HPLC analyses showed a complete drug degradation in about 30 minutes, TOC measurements revealed the occurrence of oxidation products that were not degradated, with a mineralization of 17.2 % after 2 hours (Figure II.6).

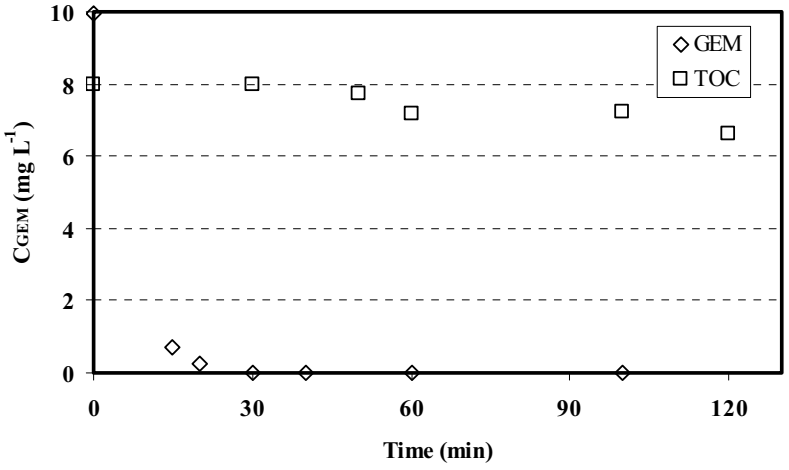

Figure II.6: Trends of GEM and TOC concentrations in photolysis tests (C_{GEMin} = 10 mg L^{-1}; pH_{in} = 10.1; V = 700 mL; T = 30 °C; P_{O_2} = 0.5 bar).

The presence of these intermediate products was also confirmed by the areas of some HPLC peaks observed at retention times lower than that of the Gemfibrozil. Besides, the pH decreased from an initial value of 10.3 to about 7.5 at the end of the tests. This behaviour was probably due to the formation of acidic species during the oxidation of Gemfibrozil.

II.3.2.2 Photocatalysis tests

Photocatalytic experiments in the batch reactor without the membrane, with the catalyst in suspension, were carried out with the aim to determine the efficiency of this process for the degradation of Gemfibrozil. Some parameters, such as pH and catalyst concentration were studied during the tests.

In Figure II.7 the trend of Gemfibrozil concentration during two photocatalytic runs is reported; TiO_2 amount is 1 g L^{-1} and the obtained data refer to tests: i) in which the pH was maintained constant to the value of 9.5 and ii) with the pH freely decreasing from 9.6 to 7.4.

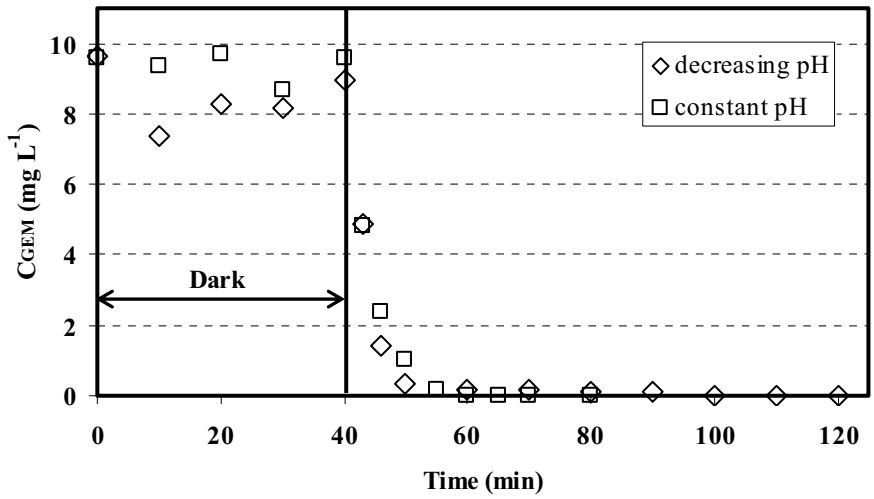

Figure II.7: Gemfibrozil concentration vs. irradiation time for runs carried out in different pH conditions (C_{GEMin} = 10 mg L^{-1}; TiO_2 = 1 g L^{-1}; pH_{in} = 9.5; V = 700 mL; T = 30 °C; P_{O_2} = 0.5 bar).

It can be observed that kinetic trend of Gemfibrozil oxidation does not change with the variations of pH, with a complete degradation of the drug in about 20 minutes.
Besides, TOC measurements during the experiments showed a mineralization of the drug of 92.3 % in 120 minutes which confirms that the photocatalytic reaction (in presence of TiO_2 at concentration of 1 g L^{-1}) allows the degradation of Gemfibrozil and also of its intermediates.
Other tests, with 0.1 g L^{-1} of suspended TiO_2, were addressed to investigate the influence of TiO_2 concentration on the degradation process (Figure II.8).
The time-course of degradation and mineralization of GEM were exactly the same of that obtained with 1 g L^{-1} TiO_2; e.g. the mineralization at 120 minutes was 92.8 % with TiO_2 at 0.1 g L^{-1}.

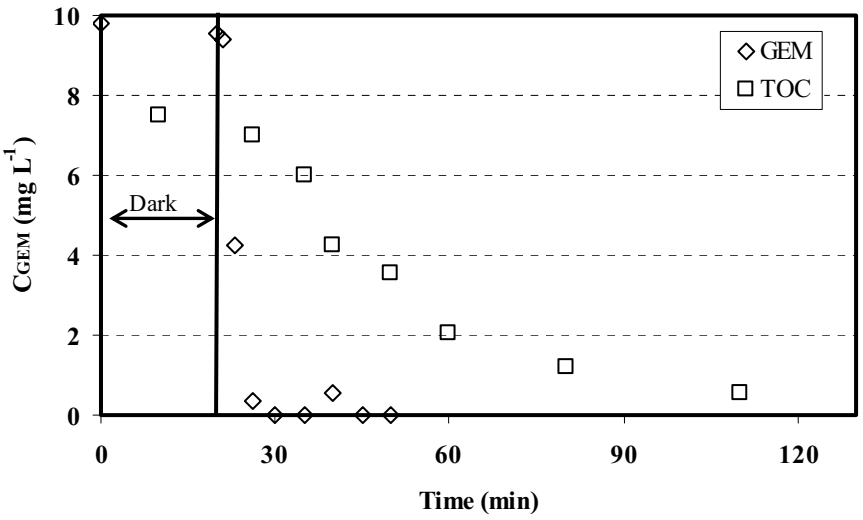

Figure II.8: Trends of GEM and TOC concentrations in photocatalytic tests with suspended TiO_2 at concentration of 0.1 g L^{-1} (C_{GEMin} = 10 mg L^{-1}; pH_{in} = 9.8; V = 700 mL; T = 30 °C; P_{O_2} = 0.5 bar).

This behaviour could be explained considering that reaction kinetics follows the widely accepted Langmuir -Hinshelwood model (see Section I.4), in which the photodegradation rate depends on the initial substrate concentration in the bulk, on the adsorption equilibrium constant and the oxidation reaction constant. Considering that in our operative conditions the adsorption phenomena was negligible, then photodegradation kinetics depends only on the initial GEM concentration.

II.3.3 Characterization and performance of the membrane photoreactor without irradiation

One of the main advantages in the use of a membrane photoreactor is the possibility of selective confining of photocatalyst, substrate and its oxidation products in the reaction ambient, while the treated water is withdrawn as permeate. Therefore, the choice of a suitable membrane should meet some criteria such as high rejection towards the compounds to be oxidized and their by-products so as high membrane water flux (permeate). The use of a nanofiltration membrane can allow, in principle, to get these objectives.

To identify membrane behaviour changing catalyst concentration, system flow rate and pressure in the permeation cell, some tests were performed in the membrane photoreactor without UV light. During the experiments particular attention was devoted to some phenomena, i.e. membrane fouling, Donnan effect and concentration polarisation.

II.3.3.1 Membrane characterisation

The NTR-7410 membrane was used in this work on the basis of previous studies with other drugs (Molinari et al., 2006a). Its flow characterization was carried out before each experiment of degradation and/or rejection by permeability tests with ultrapure water at three different pressures: 8, 6 and 4 bar.

In Figure II.9 the water fluxes measured at 6 bar for three membranes pieces (NTR-7410 type), used in about one year, indicated as “a”, “b” and “c”, are reported. In particular: “a”, “b” and “c” indicate the new membrane and I, II, III, IV the successive characterization of each one after use in the photoreactor.

The first characterization performed on the new membranes gave a flux of 54 ± 4 L h^{-1} m^{-2}. After their use in the photoreactor system, the membranes were immersed in an aqueous bath of an enzymatic detergent (Ultrasil 50, 0.2 % w/w) for about 2 weeks and washed in the system with ultrapure water.

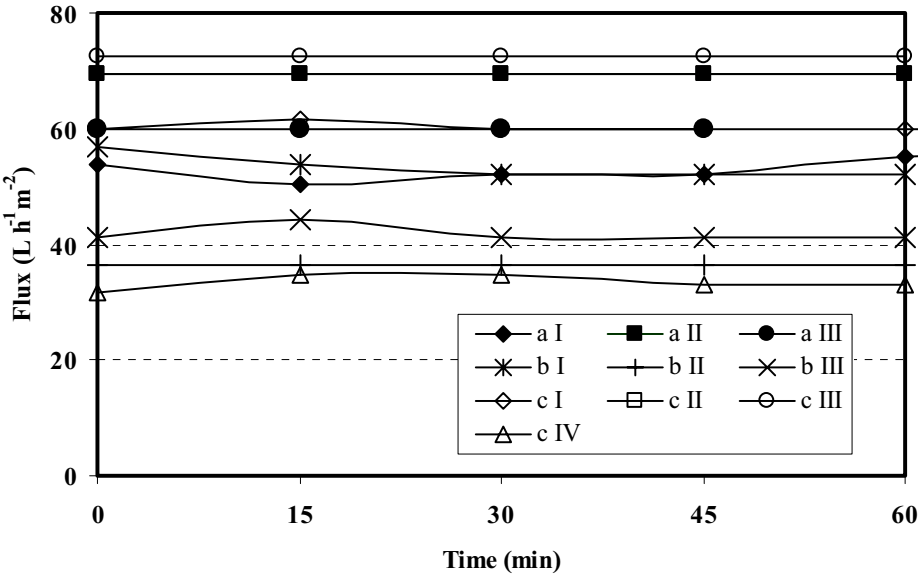

Figure II.9: Fluxes of ultrapure water vs. time measured for different pieces (a, b, c) of NTR-7410 membrane at 6 bar after repetitive uses (I, II, III, IV).

As showed in Figure II.9, in the successive characterizations the measured fluxes were high reaching values also higher than that observed in the first characterization. Although it can be observed a decrease of the permeability after their repeated use (3 - 4 set of experiments) caused by the membrane fouling, the fluxes remained always above 33 L h^{-1} m^{-2}. This means that the washings with the enzymatic detergent were able to remove some particles of catalyst and organic substances entrapped in the pores of the membrane or deposited on its surface.

II.3.3.2 Flux and rejection tests with GEM solutions

One advantage in using a membrane process coupled to the photocatalytic system should be to retain in the reaction ambient not only the catalyst, but also the molecules to be oxidized, controlling and enhancing their residence time in the reactor. To this aim the membrane should have high rejection and high flux.

To verify the rejection property, tests with GEM solutions at initial concentration of 10 mg L^{-1} were carried out in the membrane photoreactor, without catalyst and UV light.

The membrane showed 42.6 % retention of Gemfibrozil at steady state.
Since the molecular weight of the GEM (250.35 g mol^{-1}) is lower than the cut-off of the membrane (600 - 800 Da), a complete passage of the drug in the permeate should be expected. However, the separation properties of a membrane are characterised also by other parameters, such as the shape and flexibility of the solute molecule, its interaction with the membrane material and pore-size distribution of the membrane.
The NTR-7410 membrane is able to retain molecules carrying the same membrane charge (negative), thanks to the Donnan Exclusion. In particular, at alkaline pH the negative charge of the ionised Gemfibrozil interacts with the negative charge of RSO_3^- groups on the membrane generating an electrostatic repulsion. This phenomenon can explain in part the obtained rejection data.
The measured permeate flux (J_p) was 59.2 L $h^{-1}m^{-2}$ at steady state and pressure of 6 bar. This value was practically the same of that obtained in the previous characterization with ultrapure water during a testing period of 80 minutes.
When the same membrane was used for several runs, it was observed an increase of rejections and a decrease of flux values (Table II.2) which were due to membrane fouling. Immersing the membrane in the Ultrasil bath it was possible to return to the initial characteristics.

Table II.2: Values of rejection percentages and fluxes for consecutive tests on a same NTR-7410 membrane.

	Rejection %	**Flux (L h^{-1} m^{-2})**
I test	42.56	59.21
II test	55.66	50.53
III test	94.65	30.95

II.3.3.3 Flux and rejection tests with GEM solutions in presence of the suspended catalyst

With the purpose of determining the influence of TiO_2 particles on the membrane performance (rejection percentages and fluxes), some experiments were carried out with solutions of Gemfibrozil at initial concentration of 10 mg L^{-1} and the catalyst in suspension at different concentration.

In Figure II.10 the rejection percentages and permeate flux values, measured at different TiO_2 amount and using pump recirculation flow rates of 10 and 46 L h^{-1} in the recirculation loop, containing the photoreactor and the membrane cell, are reported.

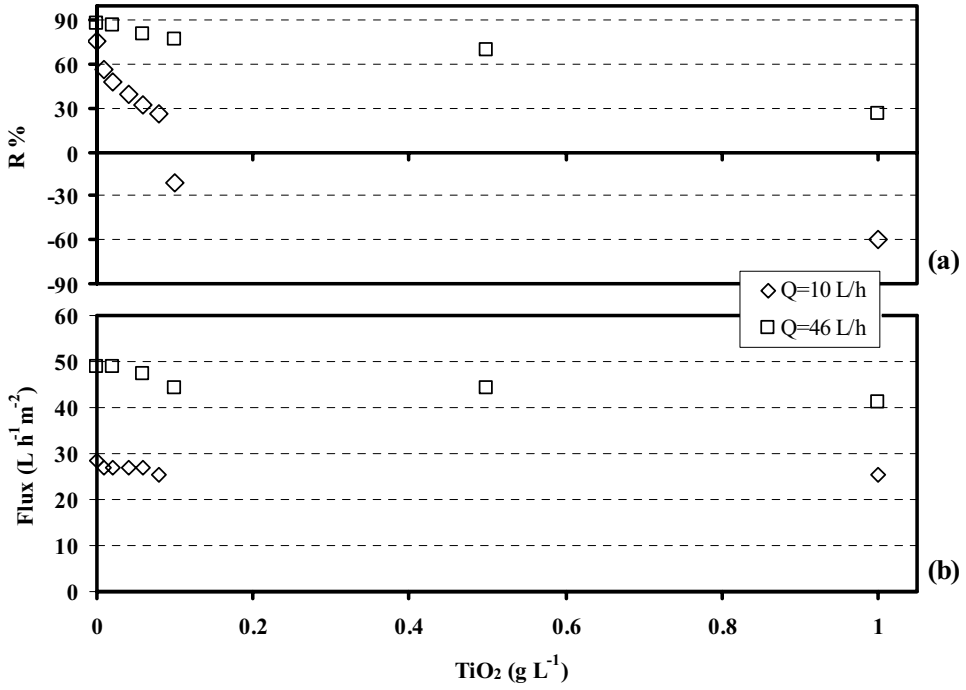

Figure II.10: GEM rejection (a) and permeate flux (b) values vs TiO_2 concentration in the membrane photoreactor without reaction with recycle flow rates of 10 L h^{-1} and 46 L h^{-1}.

The results, obtained at 10 L h^{-1}, show negative rejection when TiO_2 is present at concentration above 0.1 g L^{-1}. These values, caused by higher GEM concentrations in the permeate than retentate, could be explained by means of concentration polarisation phenomenon.

In a membrane process, when a pressure driving force acts on the feed solution, the solute is partially or completely retained by the membrane, whereas the solvent permeates through the membrane. This implies that the concentration of solute in the permeate is lower than the concentration in the bulk (Mulder, 1991). However, the retained solutes can accumulate at the membrane surface where their concentration

gradually increase with a consequent creation of a boundary layer. Because of the increased solute concentration at membrane surface the observed rejection can be lower than the real retention or, sometimes, it could be negative.

This problem could be reduced by increasing the tangential flow in the permeation cell which allows to minimise catalyst and drug deposition on the membrane surface. Therefore, another set of experiments, in the same conditions of previous ones, were performed by increasing the pump flow rate to 46 L h^{-1}.

The obtained data (Figure II.10a) show positive rejection percentages and, in particular, similar to those obtained in absence of the catalyst.

Besides, as shown in Figure II.10b by increasing the pump flow rate the flux through the membrane increases, owing to a smaller deposition of the catalyst on the membrane surface.

II.3.4 Degradation tests in the membrane photoreactor

The behaviour of the membrane photoreactor in the degradation of Gemfibrozil and its intermediates was studied using two different operative procedures. In the first one (closed system) the permeate was continuously recycled, while in the second one the GEM solution, at initial concentration of 10 mg L^{-1}, was fed into the reactor whereas the permeate was continuously removed (open (or continuous) system).

On the basis of previous experiments and considering the results obtained in the tests in the batch reactor, the operative conditions chosen for the experiments in the membrane photoreactor were: aqueous solution of Gemfibrozil at initial concentration of 10 mg L^{-1}; suspended TiO_2 at concentration of 0.1 g L^{-1}; pump flow rate 46 L h^{-1}; pressure in the permeation cell 6 bar.

In addition, the volume of Gemfibrozil solution was 700 mL, the reactor temperature was thermostatted at 30 °C and oxygen was continuously bubbled in the photoreactor at 0.5 bar.

II.3.4.1 Tests in the closed membrane photoreactor

This set of experiments was carried out for determining the ability of the membrane to retain the drug and the oxidation products in the oxidant environment during irradiation.

Figure II.11 shows the trends of Gemfibrozil (a) and TOC (b) concentrations in the retentate and permeate during a photodegradation run.

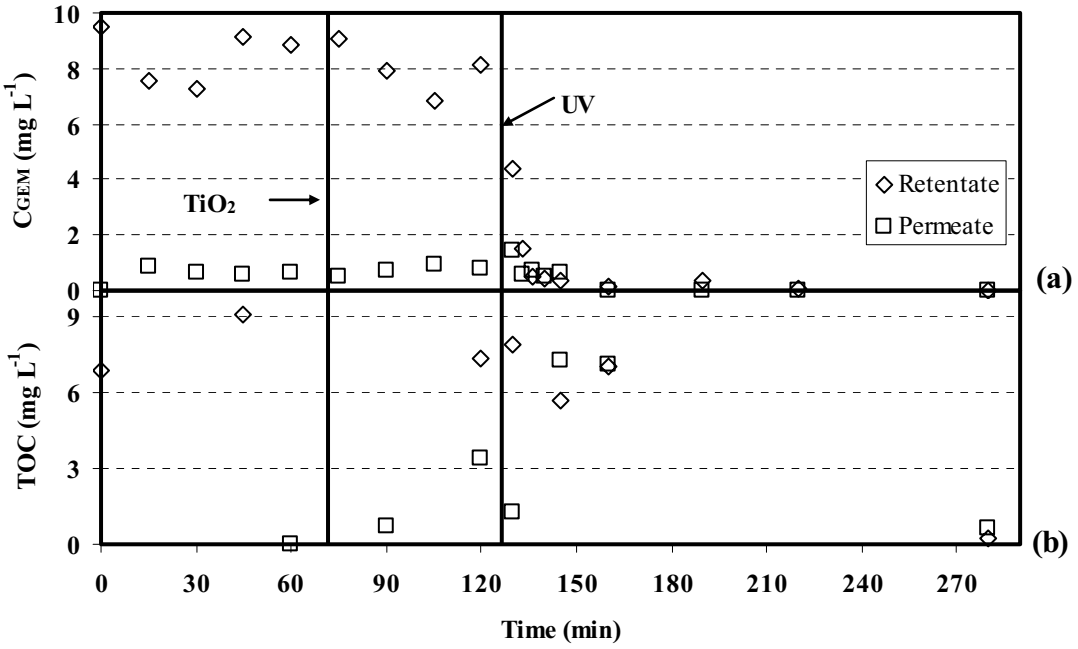

Figure II.11: Gemfibrozil (a) an TOC (b) concentrations in retentate and permeate vs. time for a test in the closed membrane photoreactor.

After 30 minutes of UV light-on a drug abatement of 98.5 % was achieved in the retentate, while a mineralization of 97.1 % was obtained only after 150 minutes.

In particular, analysing the TOC measurements, it was observed that the values in the permeate were near to those of retentate (Figure II.11b). This means a passage of oxidation products through the membrane, as confirmed also by the HPLC peaks area of some intermediates at retention times of 2.5, 3.2 and 3.5 minutes present both in retentate and permeate during the experiment.

II.3.4.2 Tests in the continuous membrane photoreactor

The objective of these tests were to simulate the continuous photodegradation process that could be applied at industrial level. To operate this system the permeate withdrawn from the reactor was replaced by an equal volume of feed solution containing 10 mg L^{-1} of Gemfibrozil.

The tests were performed until reaching a steady state (ca. 190 minutes) in terms of flux and rejection values of intermediates.

The results of GEM concentration versus the time obtained on this system were quite the same of that reported in Figure II.11 for the closed system. The degradation of the drug occurred more quickly than its passage in the permeate, with an abatement in the retentate of 98.9 % in 40 minutes and a constant permeate flux of 38.6 L $h^{-1}m^{-2}$ during the test.

Nevertheless, the trends of TOC, in the permeate and in the retentate (Figure II.12), showed the reaching of a constant mineralization of approximately 80 % and 60 % respectively, after ca. 120 minutes that remained at the steady state until the end of the run.

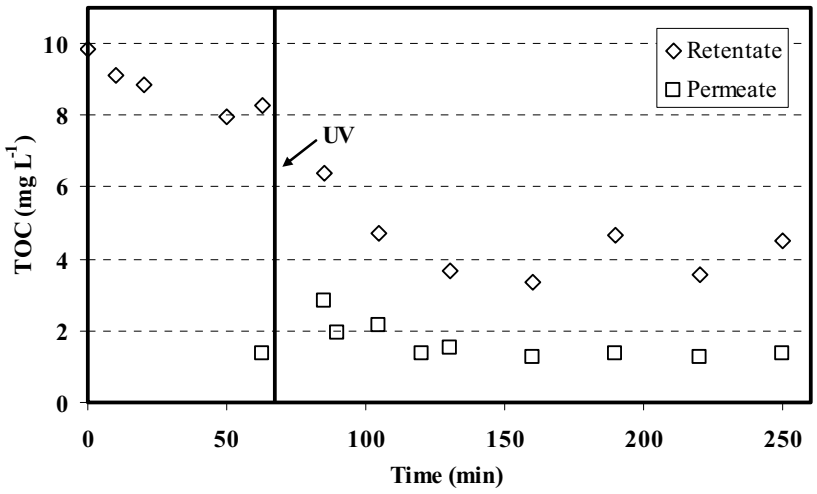

Figure II.12: TOC values versus the time in a degradation test of GEM in the continuous membrane photoreactor.

This means an operating stability of the continuous system (steady-state maintained for more than 1.5 – 2.0 hours). Besides, the different TOC values in the permeate and

the retentate indicated that some intermediates are rejected by the membrane and others not. So the intermediates with slow degradation that pass in the permeate gave a TOC membrane rejection of about (62 ± 5) % at the steady state.

The presence of the intermediates in the permeate was confirmed also by the area of same HPLC peaks at the retention times of 2.5, 3.2 and 3.5 minutes (Figure II.13).

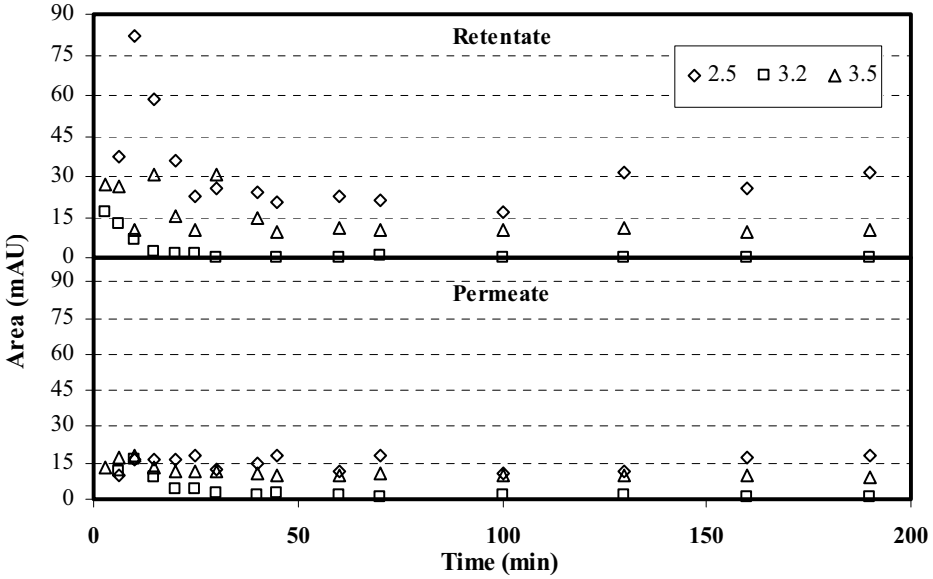

Figure II.13: Area of HPLC peaks of three degradation products (retention times 2.5, 3.2 and 3.5 minutes) in retentate and permeate versus the time in a photodegradation test in the continuous system.

A complete mineralization in the retentate for the degradation product with a retention time 3.2 minutes can be observed; it presents also a negligible area in the permeate. The area of the others two peaks, instead, reached at the steady state constant values that were higher in the retentate compared to the permeate that justify the TOC rejection.

Comparing these results to those obtained in the configurations “batch reactor” and “closed membrane reactor”, it can be noticed that membrane fluxes and abatement values were practically similar. In the continuous system it was not achieved a total absence of the pollutant in the permeate because of a low degradation rate of the oxidation intermediates and because of the not high membrane rejection to intermediates.

II.3.5 Degradation of Tamoxifen in the membrane photoreactor

II.3.5.1 Batch tests and membrane characterization

The experiments of photodegradation of Tamoxifen (TAM) were performed in the same operative conditions used for the tests on Gemfibrozil. The aim was to evaluate the performance of the closed membrane photoreactor changing the type of drug.
In the preliminary tests, a Tamoxifen solubility in water of 0.9 mg L^{-1} (pH = 5.5) was determined. Therefore, in order to be able to analytically check its degradation, the solubility was increased by dissolving the drug in acidic solutions. Using a chloride aqueous solution at pH of about 3 a drug solubility of 8 mg L^{-1} was reached, while in an equimolar solution of citric acid the TAM solubility was 16 mg L^{-1} at pH of 4.
Moreover, photodegradation tests in the batch reactor were carried out with the purpose to determine the degradation behaviour of Chloride Tamoxifen and Citrate Tamoxifen (both at concentration of 8 mg L^{-1} in TAM) with UV light in absence (photolysis) and in presence (photocatalysis) of the catalyst at concentration of 0.1 g L^{-1} (Figure II.14).

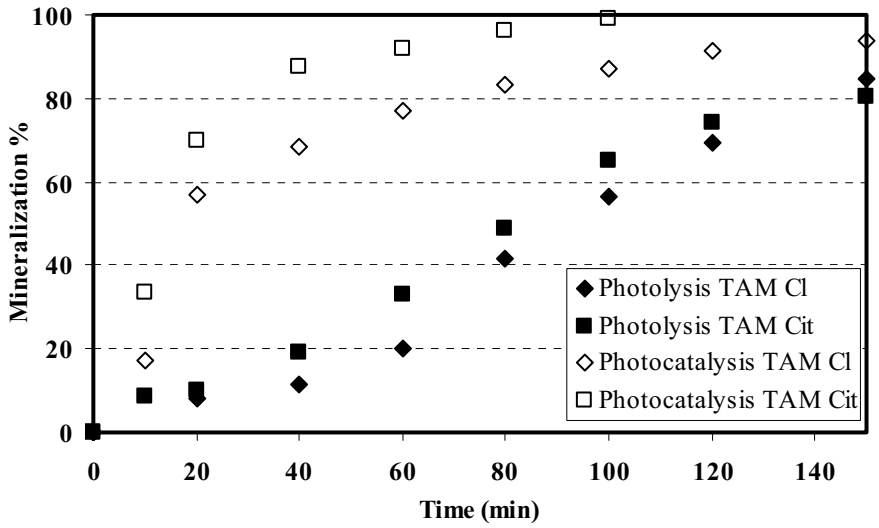

Figure II.14: Comparison between photolysis and photocatalysis on Chloride Tamoxifen and Citrate Tamoxifen solutions (suspended TiO_2 amount 0.1 g L^{-1}; C_{TAMin} = 8 mg L^{-1}; V = 700 mL; T = 30 °C; P_{O_2} = 0.5 bar).

Before carrying out the degradation experiments in the membrane photoreactor the permeability of the membrane was checked with ultrapure water and compared with that of Tamoxifen solutions and solutions of the drug containing the suspended catalyst 0.1 g L^{-1} (Table II.3).

The fluxes measured at the steady state in presence of the drug with and without the catalyst were quite the same (about 20 L h^{-1} m^{-2}) and lower than those observed with water (47.4 L h^{-1} m^{-2}) with constant values for all the test period of 75 min.

Table II.3: Fluxes measured in the PPMR with water, GEM solution and GEM solution with suspended TiO_2.

	Water	**TAM**	**TAM + TiO_2**
Flux (L $h^{-1}m^{-2}$)	47.4 ± 2.4	20.5 ± 1.1	18.9 ± 0.95

The lower flux was probably caused by adsorption of the TAM that generated a membrane fouling decreasing the flux of about an half compared to those measured with only ultrapure water. In presence of TAM and catalyst in suspension the flux remained unchanged. It was not possible determining the TAM rejection at steady state because the drug concentration decreased in the time reaching very low values.

II.3.5.2 TAM photodegradation in the closed PPMR

The photodegradation tests in the membrane reactor were performed using 700 mL of the Citrate Tamoxifen solution with 0.1 g L^{-1} of suspended TiO_2, at temperature of 30 °C and O_2 continuously bubbled at 0.5 bar. The pH was maintained at a constant value of about 4 by means of a diluted HCl solution. The membrane used was the NTR7410.

Figure II.15a shows the Tamoxifen concentrations in the retentate and permeate during a run. It can be noticed that the degradation of the drug occurred very quickly but it was observed its passage in the permeate with concentration values higher than the retentate. This means a negative rejection caused probably by an initial adsorption of the drug on the membrane surface and its following release in the permeate.

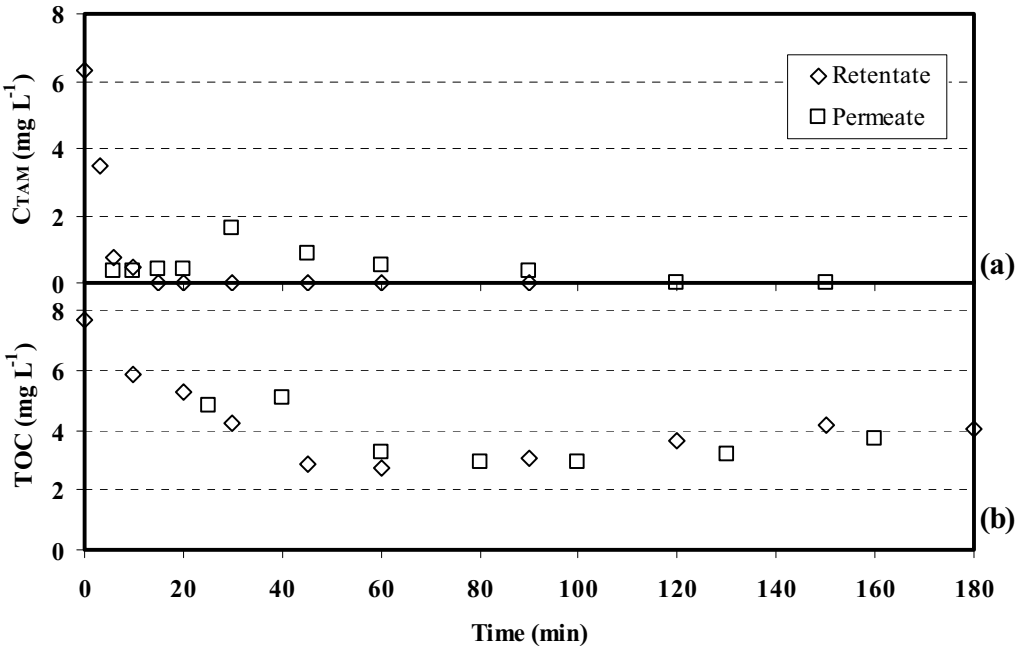

Figure II.15: Citrate Tamoxifen photodegradation test in the closed membrane photoreactor. Tamoxifen concentrations (a) and TOC values (b) vs. time in retentate and permeate.

By means of TOC analysis it was observed that the membrane was not able to hold the intermediate products being the concentration values of TOC in the permeate similar to those of retentate (Figure II.15b).

Comparing the data obtained in the batch and in the closed membrane photoreactors it can be observed that the photocatalytic systems allow a complete abatement of the drug in about 15 minutes and a mineralization higher than 60 % in about 60 minutes. Despite the data of TOC in Fig. 11b do not reach 100 % mineralization like that observed in the batch system, they show, however, that the membrane is not able to reject the Tamoxifen and its oxidation products.

These results are quite the same of that obtained in the degradation experiments with Gemfibrozil solutions. The photocatalytic process permits to obtain a fast degradation of the two drugs studied in this work and a complete mineralization in about 150 minutes, but the membrane employed in the membrane photoreactor showed a little rejection for one substrate (GEM) and its degradation products and no rejection for the other (TAM).

Therefore, further investigations are in progress to improve the membrane performance in terms of rejection towards both the drugs and their oxidation products and of membrane water flux.

II.3.6 Gemfibrozil degradation in the submerged membrane photoreactor

II.3.6.1 Characterization of the submerged membrane module

One of the major problems observed in the NF membrane photoreactor with the suspended catalyst is the membrane flux decline due to catalyst deposition and membrane fouling.

To solve this problem this research has been addressed towards the use of a different membrane module configuration, the submerged membrane system (see section I.3.3.2). Many strategies are described in literature to minimize membrane fouling and enhancing permeate flux (Mozia et al., 2007; Fu et al., 2006; Camera-Roda et al., 2007). One approach is the control of the hydrodynamic conditions near membrane surface to prevent particle deposition on the membrane. Gas sparging at the bottom of the membrane units is commonly used to achieve these favourable hydrodynamic conditions (Chan et al., 2007; Ghosh, 2006).

In particular, it was observed (Chin et al., 2007) that the gas sparging allows a mechanical agitation, that reduces the fouling of the membrane, as well as to keep the TiO_2 well suspended in the solution, acting also on the size of catalyst aggregates. Besides, it was demonstrated the possibility of using an intermittent permeation method in order to maintain a high flux (100 L h^{-1} m^{-2}) operating at low aeration rate, with low membrane fouling. However, one of the drawbacks observed in the above reported studies using ultrafiltration membranes was a non-adequate rejection of organic matter with low molecular weight. This problem can be reduced using a submerged nanofiltration membrane module (Choi et al., 2007).

In this part of the work a particular type of immersed membrane module has been studied. The module is locate separate from the irradiation source and some preliminary results are reported in the following.

The cell containing the pressurized flat sheet membrane of the photoreactor previously employed was substituted with the permeation system described in Figure

II.4 in which the membrane module was immersed in the aqueous media coming from the photoreactor and the permeate was withdrawn by means of a suction pump. Before starting the photodegradation experiments, the module was characterized with ultrapure water, setting the peristaltic pump to obtain different vacuum values (Figure II.16).

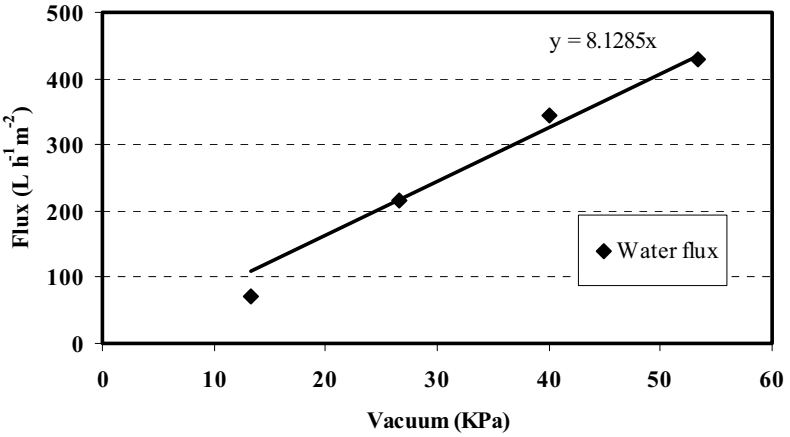

Figure II.16: Water fluxes vs. vacuum in the submerged membrane module.

High membrane permeabilities with fluxes in the range 71.6 – 429.6 L h^{-1} m^{-2} varying the vacuum from 13.3 to 53.3 kPa were obtained; a straight line passing from zero in the graph Flux vs. Vacuum was observed with a slope of 8.13 ± 0.01 L h^{-1} m^{-2} kPa^{-1}.

Although the highest flux was observed at a vacuum of 53.3 kPa, a vacuum of 13.3 kPa was chosen for the first set of experiments in order to minimize the trans-membrane pressure and to allow an optimal residence time of the substrate and their by-products in the reaction environment.

II.3.6.1 GEM photodegradation in the SPMR

The photodegradation tests in the SPMR were performed in the same conditions of the previous experiments carried out in the pressurized continuous membrane photoreactor.

A drug abatement of 100 % was reached in about 20 minutes in the retentate, while a complete passage of the Gemfibrozil was observed in the permeate. Furthermore, the

trend of TOC showed a passage of the intermediate products in the permeate during the run (Figure II.17) and a mineralization of 44.5 % in ca. 150 minutes.

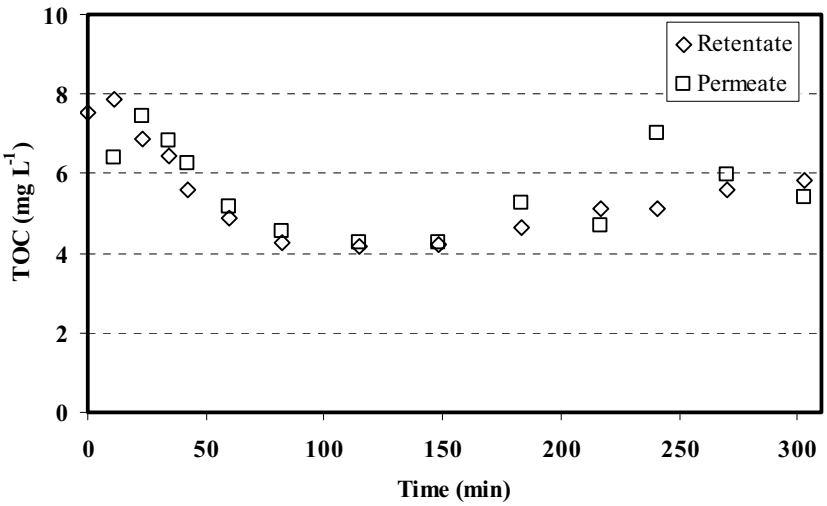

Figure II.17: TOC values versus the time in the degradation of GEM in the continuous submerged membrane photoreactor (continuous feed of GEM at concentration of 10 mg L^{-1}).

After 3 hours a little increase of concentration values was observed in the retentate and in the permeate both for the Gemfibrozil and the TOC, owing to the reaching of a steady-state with sinusoidal variation around the average value, caused also by the stepwise addition of the substrate simulating the continuous system.
The flux measured at the steady state was 65.1 L h^{-1} m^{-2} and it remained constant for all the run (about 6 h).

II.3.7 Comparison of the results

Comparing the data obtained in the two configurations of continuous membrane photoreactor (pressurized and de-pressurized membrane systems) it can be noticed that the presence of suspended catalyst allows a complete degradation of the drug in about 15 - 20 minutes and a partial mineralization of the organic intermediates with a TOC value at steady-state in the retentate of about 4.2 ± 0.7 mg L^{-1} for both the systems (Figure II.18).

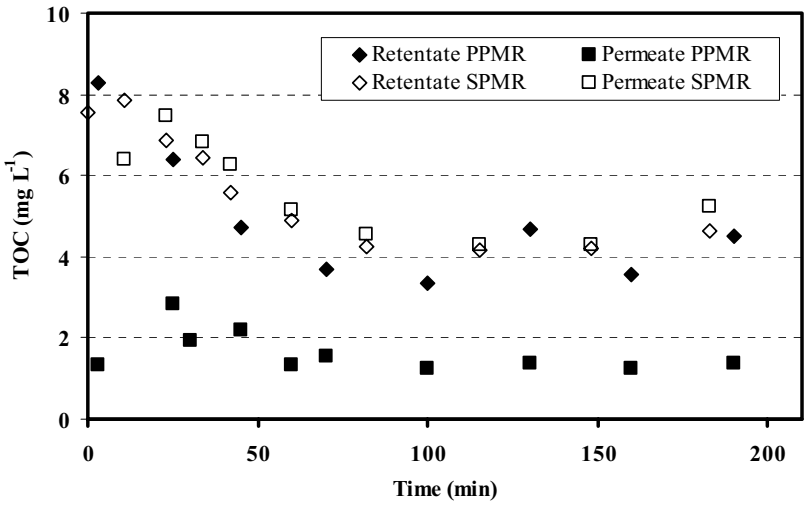

Figure II.18: Comparison of TOC concentrations between pressurized and submerged membrane photoreactors for GEM degradation.

The UF membranes used in the submerged system were not able to reject the drug and its degradation products compared to the NF membranes of the pressurized system that allowed a TOC rejection of (62 ± 5) % (Figure II.19).

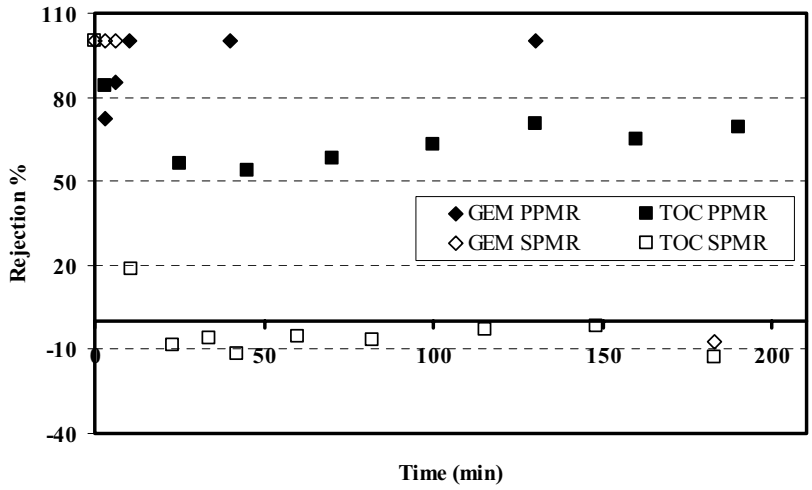

Figure II.19: Comparison rejection values between pressurized and submerged membrane photoreactors for GEM degradation.

The submerged membrane photoreactor, however, resulted more advantageous in terms of permeate flux, with values almost two times greater than those measured with the pressurized membranes.

II.4 SUMMARY REMARKS

The photodegradation of the drugs Gemfibrozil and Tamoxifen, selected as target molecules, resulted quickly and complete both in the batch tests without the membrane and in the membrane photoreactors, with a drug abatement of 99% in the first 20 minutes. The mineralization of the two drugs was higher than 90 % in about 120 minutes in the batch system.

Excessive disgregation of the catalyst and its passage in the permeate was avoided operating at 7 ± 3 pH values. High pump recirculation flow rate (46 L h^{-1}) reduced the deposition of the catalyst on the membrane surface and increased the drugs rejection. A simple washing of membranes with an enzymatic detergent was enough to restore the flux at acceptable values.

The membrane used in the PPMR system allowed to maintain the drug and the catalyst in the reaction environment, but it was not able to reject significantly the intermediate products which were also found in the permeate. The PPMR evidenced a good operating stability in the degradation of Gemfibrozil reaching a steady state in ca. 120 minutes, with a complete abatement of the drug, and values of mineralization (60 %) and permeate flux (38.6 L h^{-1} m^{-2}) that remained constant until the end of a run. A TOC rejection of about 62 % at steady state showed the need to identify a membrane with higher rejection to the intermediate products.

The new configuration of PMR, in which the submerged membrane module was located separately from the photoreactor and the oxygen was bubbled on the membrane surface, could be of interest to separate the photocatalytic zone from the separation zone with a reduction of the plant optimisation problems. The type of membrane used in the preliminary tests showed a steady-state flux of 65.1 L h^{-1} m^{-2} and a retention of only the catalyst in the reaction environment. Other types of membranes, more selective to substrates and intermediates, are under consideration.

Overall results show that PMRs can be of interest in the removal of organic pollutants from waters because they allow the recovery and reuse of the catalyst, permit to realize a continuous process and, if a suitable membrane is found, it is possible to retain the pollutant and its degradation products in the reaction environment.

SECTION III

PARTIAL OXIDATION REACTIONS IN PHOTOCATALYTIC MEMBRANE REACTORS: ONE-STEP SYNTHESIS AND SEPARATION OF PHENOL*

III.1 PHENOL

III.1.1 Phenol as important industrial compound

Phenol was isolated from coal tar in 1834 by the German chemist, Runge, who gave it the name karbolsäure (coal-oil acid or carbolic acid), though its composition was not known until 1841. The name carbolic acid can be misleading, as it does not contain the functional group normally associated with organic acids, even though it is slightly acidic (www.greener-industry.org).

Its market demand overcomes 7 million of tons per year and, actually, more than of 95% of its global manufacture is realized by the Cumene process, called also the Kellogg, Brown & Root (KBR) phenol process.

The production of 1-methylethylbenzene (cumene) can be used, therefore, as an indication of the levels of phenol production (Figure III.1).

---

* This part of work has been published as:

- Molinari R., Poerio T., Caruso A., Argurio P., Carnevale S.M., "Direct mild partial oxidation of benzene and methane in catalytic and photocatalytic membrane reactors", pp. 217-224. *DGMK Tagungsbericht 2008-3* - Ernst S., Jess A., Nees F., Peters U., Ricci M., Santacesaria E. - Hamburg, Germany: German Society for Petroleum and Coal Science and Technology, 2008. ISBN 978-3-936418-81-1.

And it has been submitted as:

- Molinari R., Caruso A., Poerio T., "One-step conversion of benzene to phenol in a hybrid photocatalytic membrane reactor", *submitted to Catalysis Today*.

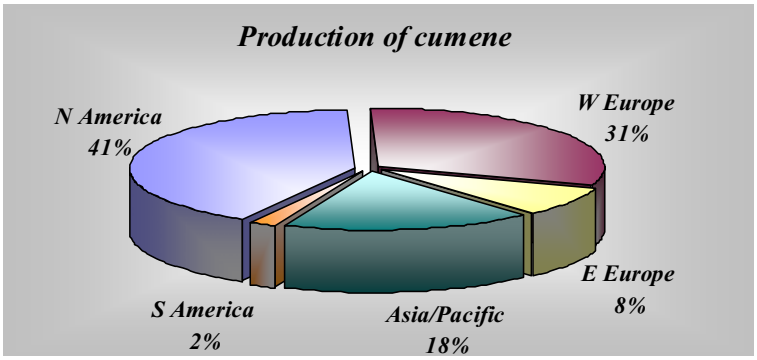

Production of cumene (millions of tonnes)	
N America	2.6
W Europe	2.0
E Europe	0.5
Asia/Pacific	1.2
S America	0.1

Figure III.1: Production of cumene as an indication of phenol production (adapted from www.greener-industry.org).

Phenol has been in production since the 1860s and actually it is used as substrate in the manufacture of a wide range of intermediates and products:

- Bisphenol A: for the production of epoxy resins;
- Caprolactam: used in the manufacture of nylon and polyamide plastics;
- Phenylamine (Aniline): antioxidant in rubber manufacture;
- Chloro-phenols: used in medical antiseptics and bactericides;
- Salicylic acid: in the production of aspirin and other pharmaceuticals.

In 1872, besides, it was found that phenol could be condensed with aldehydes (for example methanal) to make resinous compounds, which are still used to produce low cost thermosetting plastics such as melamine and bakelite.

III.1.2 Phenol production

III.1.2.1 Early production methods: sulphonation of benzene

Phenol was first manufactured commercially by distillation from coal tar, but the energy required and quantities produced meant this method could not be sustained.

Synthesis by the sulphonation of benzene was implemented by BASF in 1899 and continued until the 1960s.

The process involves several steps, but the overall reaction is:

$$\underset{\text{benzene}}{C_6H_6} + H_2SO_4 + 2NaOH \longrightarrow \underset{\text{phenol}}{C_6H_5OH} + Na_2SO_3 + 2H_2O$$

One of the main disadvantages is the poor atom economy of the reaction, a factor that has become increasingly important as the chemical industry seeks to develop more sustainable processes.

The atom economy of a reaction is found from:

$$\text{Atom Economy} = \frac{\text{Molecular Mass of Desired Product(s)}}{\text{Molecular Mass of All Reactants}} \text{ x } 100\%$$

If we assume a 100% yield, the atom economy works out to be 36.7% which means that considerably less than half the mass of reactants ends up in the required product. In practice the yield is more likely to be in the region of 88%, giving a figure of 32.3%, barely a third of the reactant mass.

Although sodium sulphite has uses in the wood pulp and paper industry, and in several other processes, the large amount of waste produced, the use of aggressive reagents and the low atom economy represent the reasons why the benzene sulphonation route is no longer used.

III.1.2.2 The cumene process

The main method used to manufacture phenol since the 1960s has been through the oxidation of 1-methylethylbenzene, commonly called cumene, which is made from benzene.

This process takes place in three stages:

1. Production of 1-methylethylbenzene (cumene)

Cumene is made from benzene and propene.

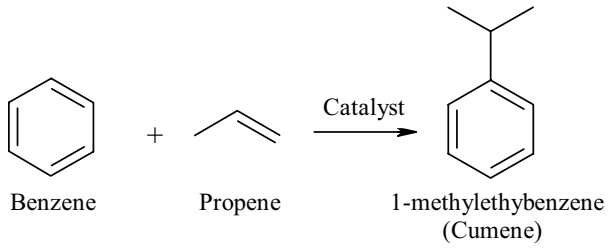

The Friedel-Crafts alkylation of benzene is catalysed by a catalytic Lewis acid and can be carried out in either the vapour or liquid phase.

In vapour phase reaction solid, pelletised phosphoric acid (H_3PO_4) is used as a catalyst, although it is very corrosive, it cannot easily be regenerated and disposal of waste from this process can be a problem. The Lewis acid aluminium chloride ($AlCl_3$) is used as the catalyst in the liquid phase. It has the advantage that the reaction will take place at 100°C and normal atmospheric pressure, but corrosive waste is produced, and the catalyst cannot easily be regenerated. Besides, in both cases the 1-methylethylbenzene (cumene) has to be separated from other products of the reaction, which will include the other addition product, propylbenzene.

Newer catalysts, in particular zeolite, are increasingly being used in this step with several advantages: the catalysts can be removed, regenerated and returned for re-use more or less indefinitely; they are relatively cheap; they work with lower quality feedstock, yet produce a higher quality product without hazardous waste or acidic emission; a higher proportion of 1 -methylethylbenzene, and little propylbezene are producted, with a reduction of energy used in purification.

2. Oxidation cumene to hydroperoxy-1-methylethylbenzene

The reaction is carried out at temperatures in the range 90 - 130ºC and pressures of 1-10 atmospheres. Careful control of acidity levels, temperature and pressure are vital as at higher temperatures, the hydroperoxide is unstable and can decompose violently.

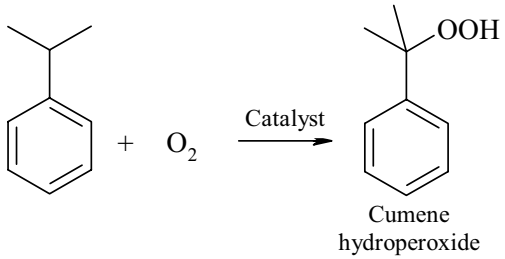

Cumene hydroperoxide

To help reduce the risk of this happening, only 25% of the cumene is allowed to react at any time in order to keep the concentration of the hydroperoxide within safe limits. Un-reacted cumene has to be separated out and recycled, increasing the costs.

This step also produces the major impurities of this process.

3. Decomposition of cumene hydroperoxide to phenol

The hydroperoxide is mixed with dilute sulphuric acid at 60 - 70ºC, to produce both phenol and propanone (acetone) as products. The decomposition of cumene hydroperoxide to phenol and acetone is often described as a cleavage reaction.

The products are extracted by distillation.

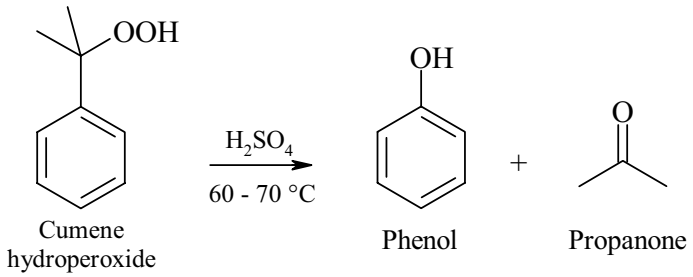

The overall process, from benzene to phenol and propanone, is:

$$C_6H_6 + C_3H_6 + O_2 \longrightarrow C_6H_5OH + CH_3COCH_3$$

If we assume that both phenol and propanone are desired products, and that the yield is 100%, this will clearly give an atom economy of 100% - all the atoms in the reactants appear in the products.

In practice the yield is more likely to be in the region of 90%, but even taking this into account, and assuming all the propanone is waste, still gives an atom economy of 55.7%, comparing favourably with the old sulphonation process at 36.7%.

The Mitsui company has developed the process to include recycling the propanone. It is converted to propene, a reactant in the first step, using two further steps. Though this may help address overproduction of propanone, a five step process using hydrogen is not an ideal solution.

Although there is a market for propanone as a solvent, its demand is rising at a lower rate than phenol, thus in the future propanone may become a waste product. The possibility of converting excess propanone to propene for re-use is being explored by some companies.

Besides, depending on the process conditions, up to 0.6 tonn of liquid wastes is generated per ton of phenol produced. The wastewater contains 2-3% phenol, 3-6%

acetone, up to 0.1% aromatic hydrocarbons (mainly cumene and α-methylstyrene) and 2-3% sodium salts (Kujawski et al., 2004).

This is one reason why alternative processes are being developed, combined with the fact that the cumene process is a three-step process with a potentially explosive intermediate.

III.1.2.3 Oxidation of methylbenzene (toluene)

One way to avoid the over-production of propanone associated with the cumene oxidation process, is to use a different reaction to produce phenol.

About 5% of phenol is produced using the oxidation of methylbenzene (toluene), a process sometimes called the Dow and California Research Process.

This is a two-step process:

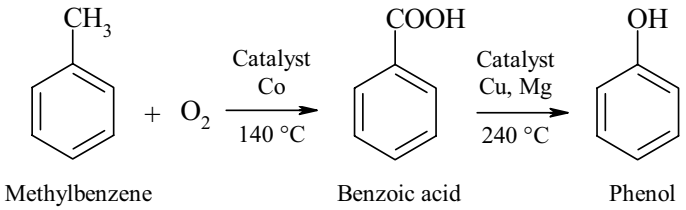

The advantage of the oxidation of methylbenzene is that it produces no propanone co-product and also very few impurities. It has a high theoretical atom economy, a high yield, and produces far less waste than the cumene oxidation process.

At present, however, the process is up to 3 to 4 times more energy intensive than the cumene oxidation process, and so it is not widely used.

The balanced equation for the process is:

$$C_6H_5CH_3 + 2O_2 \longrightarrow C_6H_5OH + CO_2 + H_2O$$

This process has an atom economy of 60.1% if phenol is the only useful product, which is a further improvement on the previous processes.

The fact that this process is not widely used reflects the fact that atom economy is, however, only one of many factors that must be taken into account.

III.1.3 One step preparation of phenol

The one-step hydroxylation of benzene via "green" process represents an attractive alternative pathway for the direct synthesis of phenol and many studies are performed with the aim to develop more efficient and environmentally benign processes.

Liptakova et al. (2004) studied the direct gas-phase oxidation of benzene to phenol with in situ produced nitrous oxide which was formed by the reaction of air and aqueous ammonium hydroxide over mixed calcium-copper-hydroxyapatite catalysts. In the first 3 h about 3% conversion of benzene and 97% phenol selectivity was achieved, but after this period the deactivation of the catalyst was pronounced.

The liquid-phase oxidation of benzene was carried out by Yamaguchi et al. (2005) in aqueous acetic acid solvent over V-substituted heteropolyacids (V-HPAs) using molecular O_2 and ascorbic acid as the oxidant and reducing reagent, respectively. Although phenol was exclusively obtained as the oxygenation product, the reuse of the V-HPA catalyst caused gradual deactivation for phenol formation.

In another study (Dong et al., 2005) the direct synthesis of phenol from benzene was obtained with high benzene conversion (30%) and phenol selectivity (90%) by using a microporous material $[Ca_{24}Al_{28}O_{64}]^{4+} \bullet 4O^-$ (C12A7-O2) as catalyst with oxygen and water.

Heteropolyacid (HPA) and $Pd(OAc)_2$, immobilized through chemical bonds onto the functional organic groups modified solid surfaces of hexagonal mesoporous silica (HMS) and polyimine (PIM) were used as heterogeneous catalysts for the oxidation of benzene to phenol by molecular oxygen (Liu Y. et al., 2006).

Gao et al. (2006) reported the highly selective direct hydroxylation of benzene to phenol with hydrogen peroxide on a clay-supported vanadium oxide catalyst, obtaining under mild reaction conditions high selectivity to phenol of 94% and 14% conversion of benzene.

Dimitrova et al. (2007) investigated the use of Vanadium grafted zeolites type Beta and ZSM-5 for direct oxidation of benzene to phenol and hydroxylation of phenol with hydrogen peroxide in acetonitrile media at 353 K.

III.1.3.1 Photocatalytic conversion of benzene to phenol

A direct synthesis of phenol from benzene has been tried also using photocatalytic reactions.

Several photocatalytic systems using TiO_2 as heterogeneous photocatalyst and polyoxometalate (POM) as homogeneous photocatalyst were studied by Park et al. (2005) investigating on the effects of various electron acceptors such as O_2, Fe^{3+}, H_2O_2, Ag^+, N_2O, surface-modified TiO_2 (platinization, fluorination, and silica loading). They observed that the phenol production yield and selectivity were enhanced with the addition of Fe^{3+}, H_2O_2, or Fe^{3+} + H_2O_2 or modifying the surface of the catalyst, but the highest yield observed in this study was obtained with the addition of POM to TiO_2 suspension.

Selective photo-oxidation of liquid benzene was studied, also, using: i) cation-exchanged zeolites dispersed in $C_6H_6/CH_3CN/H_2O$ mixture at room temperature by using molecular oxygen (Shimizu et al., 2004); ii) Mo complexes with Mo_1–Mo_4 nuclearities grafted on mesoporous silica FSM-16 (Zama et al., 2000) and iii) bis- and tris-(bipyridine) Ru complexes grafted on mesoporous FSM-16 (Fujishima et al., 2001) using hydrogen peroxide as an oxidant under the irradiation of UV-light.

In a photocatalytic system, the formed hydroxyl radical adds directly to benzene to produce a hydroxycyclohexadienyl (HCHD) radical which rapidly undergoes an H-atom abstraction by oxidants (O_2, Fe^{3+}, Cu^{2+}, etc.) leading to phenol.

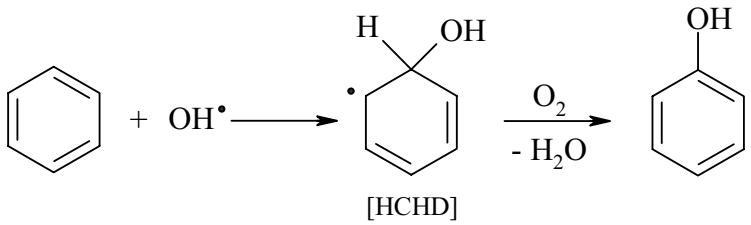

Despite the great potentialities of this photocatalytic reaction, one of the main problem, which limited its application, is the low selectivity of the process due to the higher reactivity of phenol towards the oxidation than benzene with the formation of oxidation by-products (Scheme III.1).

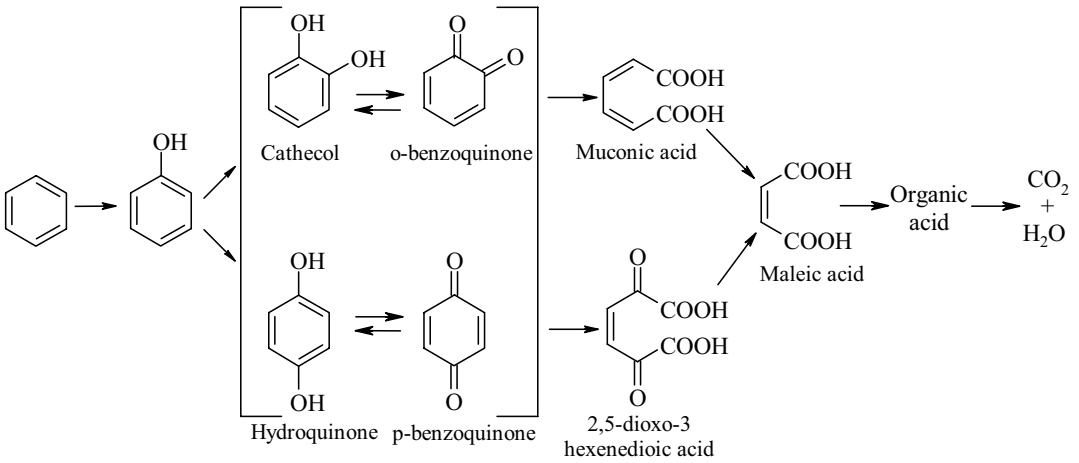

Scheme III.1: Route of the catalytic oxidation of phenol in aqueous phase (elaborated from Chen et al., 2002; Santos et al., 2002; Sobczynki et al., 2004).

The need to avoid these secondary products and to obtain the separation of phenol from the oxidant reaction environment remains one of the challenges in further photocatalytic engineering and reactor development.

To this purpose the use of a membrane system coupled with the photocatalytic process seems an useful solution since it allows the recovery and reuse of the photocatalyst and, if a suitable membrane is used, it is possible to obtain a selective separation of the products.

III.1.4 Photooxidation of benzene to phenol in a photocatalytic membrane contactor

III.1.4.1 Phenol separation

When a photocatalytic system is used as a synthetic pathway one of the major problems is the recovery of the catalyst and the separation of the product(s) from the reactive environment.

Some authors (Park et al., 2005) proposed a phenol recover from final mixture solution by simple distillation, since the boiling point of phenol is 60 °C lower than that of the others di-hydroxylated by-products. Nevertheless, this means the introduction of an additional step which does not allow to work in a continuous system.

Coupling the photocatalytic system with a membrane separation module can permit to solve this drawback. In particular, the use of a membrane allows simultaneously not only the recovery of the catalyst but also the separation of the product minimizing its secondary oxidation reactions that lead to undesirable by-products.
The recovery of phenol from aqueous solutions was studied using different membrane technique such as pervaporation (Kujawski et al., 2004), membrane contactors (Molinari et al., 2006b; Gonzales et al., 2003; Vospernik et al., 2003; Lazarova et al., 2004), supported liquid membranes (Park et al., 2000; Dastgir et al., 2005; Jaber et al., 2005; Venkateswaran et al., 2006).

III.1.4.2 Photocatalytic Membrane Contactors (PMC)

L-L membrane contactors can represent an useful technique to remove phenol from aqueous solutions. In a membrane contactor (see section I.3.3.3) the separation performance is determined by the distribution coefficient of a component in two phases and membrane acts only as an interface.
The liquid-liquid membrane contactor, in particular, is characterised by two liquid streams separated by a porous or nonporous membrane. In case of porous membrane the feed (or strip) phase can wet or not wet the membrane depending on their hydrophobic/hydrophilic interactions (Mulder, 1991).
Membrane contactors offer several advantages (Gabelman et al., 1999):

- The available surface area remains unchanged because the two fluid flows are independent and, therefore, the volume ratio between the two phases can be very high or very low.
- Emulsion formation does not occur, again because there is no fluid/fluid dispersion.
- They can accommodate fluids of identical density.
- Scale-up is more straightforward.
- Aseptic operation is possible, a feature which can be advantageous in processes such as fermentation
- During a synthetic route the product of interest can be continuously removed increasing conversion in equilibrium-limited chemical reactions.

- Interfacial area is known and is constant, which allows performance to be predicted more easily than with conventional dispersed phase contactors.
- Solvent loss is low, an attractive feature when using expensive solvents.

Gonzales et al. (2003) reported a study on the effects of temperature and hydrodynamics on the overall mass transfer coefficient of phenol, using a hydrophobic polypropylene hollow fibre membrane contactor and 1-decanol as stripping phase. Besides, in order to carry out the extraction and stripping processes simultaneously, a second membrane module was used obtaining the removal of more than 99% of the original phenol.

The application of membrane-based solvent extraction for the removal of phenol from solutions modelling wastewater from phenol production by cumene oxidation process was studied by Kujawski et al. (2004). The most efficient extractant, among the solvent investigated, was MTBE that allowed a phenol recovery of over 98 % in a single-stage extraction. However, a drawback in this study was the passage of MTBE in the aqueous solution. In fact, it dissolves relatively well in water (up to 5 %) and therefore should be regarded as a potential pollutant.

In a work on the recovery of phenol using a membrane contactor, reported by Molinari et al. (2006b), the liquid-phase catalytic benzene oxidation to phenol is studied by using a new biphasic system where a membrane is employed in order to avoid phase mixing during the oxidation reaction. The interesting result was the high value of selectivity to phenol in the organic phase (99.4 %) that reduced its further oxidation.

Several studies reported also the use of membrane contactors as separation technique in a photocatalytic system. For instance, the photocatalytic processes were coupled with: pervaporation for water detoxification (Camera-Roda et al., 2007), direct contact membrane distillation for degradation of organic pollutants in aqueous solution (Mozia et al., 2007), dialysis membrane for the depollution of turbid waters (Azrague et al., 2007). As it can be observed, these studies reported the use of hybrid systems for photodegradation processes, but the potentialities of these systems are greater than those described in literature. In fact, they can be an useful solution to separate the product of interest during a photosynthetic process and, in particular, if a suitable membrane and a proper strip phase is chosen, it is possible to obtain a

selective separation of the product(s) before that secondary reactions occur (Figure III.2). Despite the advantages of these integrated systems, to our knowledge, few studies are reported in literature on the use of a membrane contactor module coupled to photocatalytic synthetic pathway.

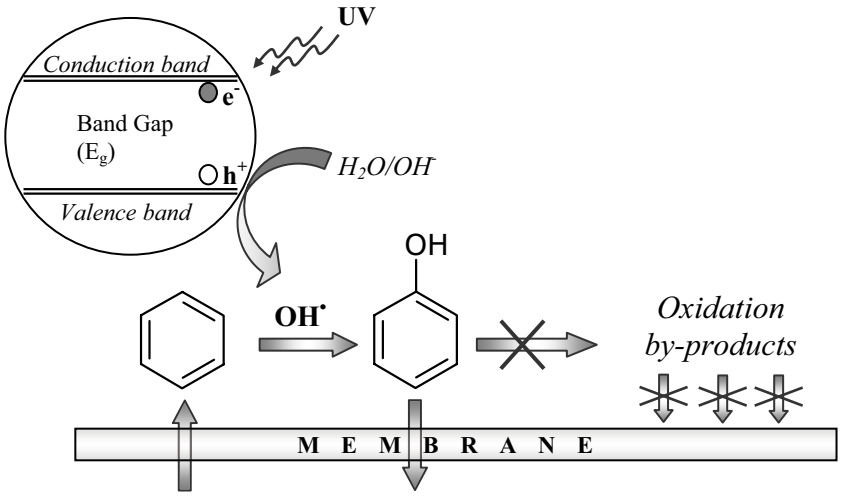

Figure III.2: Schematic representation of the photooxidation of benzene to phenol in a Photocatalytic Membrane Contactor.

III.1.5 The aim

Aim of this study was to demonstrate the possibility to use a membrane photoreactor for organic syntheses, developing a hybrid system in which the selective photocatalytic reaction and the separation of the product of interest occur in one step.
A **Photocatalytic Membrane Contactor** (PMC) for the one-step synthesis of phenol and its simultaneous separation was studied, using TiO_2 as catalyst, benzene as both reactant and extraction solvent and a polypropylene membrane to separate the organic phase from the aqueous reactive environment.
In order to develop a membrane photocatalytic system that allows both high yields and good selectivity of the process, limiting the formation of undesirable by-products, and an efficient separation of phenol with a complete rejection to the catalyst, some parameters were investigated.

Particular attention was addressed to some aspects related to the photocatalytic reaction (catalyst concentration, initial amount of substrate, pH) and to the membrane module (breakthrough pressure, extraction efficiency) which affect the synthesis and separation of phenol and oxidation by-products.

The obtained results were then used to run the PMC in the photooxidation of benzene to phenol and its extraction from the reactive environment. Some preliminary results on the use of dissolved ions (Fe^{3+}, Cu^{2+} and V^{3+}) to enhance the photocatalytic efficiency and the extraction of phenol are also reported.

III.2 EXPERIMENTAL

III.2.1 Materials and reagents

TiO_2, Degussa P25 type (specific surface area = 44 m^2 g^{-1}, crystallographic phase ca. 80 % anatase and 20 % rutile, band gap 3.2 eV) was used as photocatalyst.

TiO_2 X500 (100% anatase) and TiO_2 C380 (100% anatase) from TitanPE technology (Shanghai) were also tested as photocatalysts.

Benzene (C_6H_6, MW 78.11 g mol^{-1}, purity 99.8%) from Carlo Erba Reagenti was used both as substrate and as organic phase. Phenol (C_6H_5OH, MW 94.11 g mol^{-1}, purity 99.99%), benzoquinone ($C_6H_4O_2$, MW 154.2 g mol^{-1}, purity 99.9%), biphenyl ($C_{12}H_{10}$, MW 154.21 g mol^{-1}, purity 99.99%), hydroquinone ($C_6H_6O_2$, MW 110.11 g mol^{-1}, purity 99%), resorcinol ($C_6H_6O_2$, MW 110.11 g mol^{-1}, purity 98%), catechol ($C_6H_6O_2$, MW 110.11 g mol^{-1}, purity 99.5%) from Sigma–Aldrich were used for analytical calibrations.

Iron(III) chloride hexahydrate ($FeCl_3 \cdot 6H_2O$, MW 270.3 g mol^{-1}) from Fluka, copper(II) chloride dihydrate ($CuCl_2 \cdot 2H_2O$, MW 170.48 g mol^{-1}) and Vanadium(III) chloride (VCl_3, MW 157.30 g mol^{-1}) from Aldrich were used in the photocatalytic tests with dissolved ions.

Hydrophobic polypropylene porous membrane (Accurel, manufactured by Membrana, thickness 142 μm; pore size 0.2 μm; porosity 70%) was used in the membrane reactor.

Sodium hydroxide (NaOH, MW 40.00 g mol^{-1}, purity 98 %) from Sigma, hydrochloric acid 37 % w/w (HCl, MW 36.46 g mol^{-1}) from Riedel-de Haen and sulphuric acid 96% (H_2SO_4, MW 98.078 g mol^{-1}) were used to correct the pH of aqueous phases.

III.2.2 Methods

The identification of the oxidation products was performed analysing the solutions by Gas Chromatograph Mass Spectrometer (GC-MS QP2010S) from Shimadzu.

Phenol and oxidation by-products concentrations in the aqueous and organic phases were measured by high performance liquid chromatography (HPLC, Agilent 1100 Series instrument) using a GEMINI C18 (250 * 4.60 mm) column by UV readings at 254 nm. The mobile phase consisted of an acetonitrile / water / acetic acid solution 50 / 49 / 1 v/v fed to a flow-rate of 1.0 mL min^{-1}. The column pressure was 110 bar and the injection volume was 20 μL.

Phenol mineralization was evaluated by Dissolved Organic Carbon (DOC) measurements, performed by using a TOC-VCSN from Shimadzu.

All the aqueous samples were filtered by means of a low-adsorbing hydrophilic polypropilene membrane (Pall Corporation, mean pore size 0.2 μm) before carrying out the analyses.

Ultrapure water used throughout the work was obtained from Milli-Q equipment by Millipore.

A pH meter (WTW Inolab Terminal Level 3) with a glass pH-electrode SenTix 81 (WTW), was used for pH measurements.

The UV light intensity was measured by a UVX Digital Radiometer (from UVP).

Contact angle measurements were performed by Contact Angle Meter 200 (KSV Instrument LTD, Helsinki, Finland).

III.2.3 Apparatus

The preliminary tests and the batch photooxidation experiments were carried out in the system described in Figure III.3a, excluding the membrane zone.

This part of the system set-up is constituted by a batch reactor (1) equipped with Pyrex glass jacket surrounding it which allows to maintain the system at a temperature of 25 °C.

On the top of the reactor is placed a 500 W medium pressure Hg lamp (Helios Italquartz) emitting a light intensity in the UV-Vis range (maximum centred at λ = 366 nm with the emission profile between 240 and 440 nm) equal to 6.0 mW cm^{-2} (2). The reactive solution, magnetically stirred (3), was constituted by 500 mL of ultrapure water with the suspended catalyst and the substrate to oxidize.

When the membrane module was used the photocatalytic experiments were performed in whole system reported in Figure III.3.

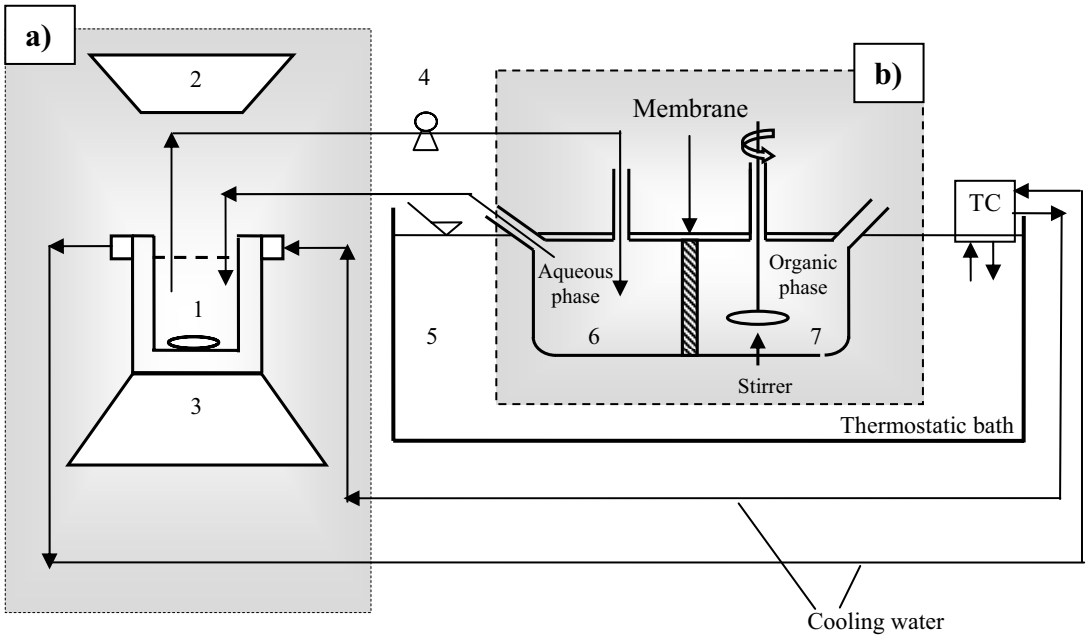

Figure III.3: System set-up: photocatalytic reactor (a) coupled with the membrane contactor (b).

It was realized by coupling the membrane contactor module (b) to the batch photocatalytic reactor by means of a peristaltic pump (4) that withdraws the solution from the photocatalytic zone to the separation zone. The retentate comes back in the photoreactor by gravity.

The permeation module, immersed in a thermostatic bath (5), is constituted by two compartment cells (each one with a volume of 130 mL) separated by a flat sheet polypropylene membrane with an exposed membrane surface area of 28.3 cm^2. The first compartment (6) contains the aqueous reactive phase coming from the photoreactor while the second one (7) an organic strip solution constituted by benzene and mechanically stirred by a motor.

Samples were periodically withdrawn from the two phases and analysed.

III.2.4 Parameter investigated

III.2.4.1 Photosynthesis and separation in a PMC

In a PMC the phenol concentration in the organic phase is the result of three different reactions involving phenol:

$$\text{Benzene} \xrightarrow{k_1} \text{Phenol}_{(a)} \qquad (1)$$

$$\text{Phenol}_{(a)} \xrightarrow{k_2} \text{Oxidation by - products} \qquad (2)$$

$$\text{Phenol}_{(a)} \underset{k_{-3}}{\overset{k_3}{\rightleftharpoons}} \text{Phenol}_{(o)} \qquad (3)$$

The rate of phenol production (r_1) depends on reactive parameters, such as pH, light intensity and catalyst concentration. This operative conditions influence also the rate of phenol oxidation (r_2). Both the reactions can be described by the Langmuir-Hinshelwood (L-H) kinetic model (Section I.4.3).
For the reaction (3), at the equilibrium condition:

$$r_3 = r_{-3} = k_3 C_{aqPh} = k_{-3} C_{orgPh}$$

with the equilibrium constant:

$$K_{eq} = \frac{C_{orgPh}}{C_{aqPh}} = \frac{r_{-3}/k_{-3}}{r_3/k_3} = K_D$$

which corresponds to the distribution coefficient K_D.

III.2.4.2 Photocatalytic parameters

The efficiency of the photocatalytic reactions was studied in terms of productivity, yield and rate of phenol production.
The productivity (P) is defined as the amount of obtained product (g) at the time t on the amount of catalyst used (g).

$$P = \frac{g_{phenol}}{g_{catalyst} * h}$$

The molar Yield (Y) is defined as the moles of obtained product on the initial moles of substrate:

$$Y = \frac{n_{phenol}}{n^{in}_{benzene}} * 100$$

The rate of phenol production is reported as variation of phenol concentration in the time:

$$r_{phenol} = dC/dt = mg\ L^{-1}min^{-1}$$

Since some of the oxidation by-products remained unknown, it was not possible to estimate the selectivity of the process.

III.2.4.3 Parameters related to the separation performance

When a liquid-liquid system is used for the separation of a substrate (A) an important parameter, which gives an indication of the substance solubility in the two phases, is the partition or distribution coefficient K_D. It can be defined by the equilibrium concentration ratio of the component A in the organic and aqueous phases:

$$K_D = \frac{[A]_{org}}{[A]_{aq}}$$

This parameter should be considered in the choice of the membrane characteristics. In fact, the lowest membrane mass transfer resistance in a membrane contactor is obtained if the pores are filled with the fluid in which the solute is most soluble. This suggests the use of a hydrophilic or hydrophobic membrane for a low or high K_D solute, respectively. That is, a low K_D solute is more soluble in a polar solvent than in a non-polar one, and the polar solvent will wet the pores of a hydrophilic membrane; the situation is analogous for a high K_D solute and a hydrophobic membrane (Gabelman et al., 1999).

Another important parameter is the degree of extraction *E* defined as:

$$E = \frac{(n_A)_{org}}{(n_A)^i_{aq}}$$

where $(n_A)^i_{aq} = (n_A)_{aq} + (n_A)_{org}$ are the initial moles of S in the aqueous phase and $(n_A)_{org}$ are the moles at equilibrium.

If V_{aq} and V_{org} are the aqueous and organic phase volumes, then:

$$E = \frac{(n_A)_{org}}{(n_A)_{org} + (n_A)_{aq}} = \frac{[A]_{org} V_{org}}{[A]_{org} V_{org} + [A]_{aq} V_{aq}} = \frac{\frac{[A]_{org}}{[A]_{aq}}}{\frac{[A]_{org}}{[A]_{aq}} + \frac{V_{aq}}{V_{org}}}$$

When $V_{aq} = V_{org}$

$$E = \frac{K_D}{(K_D + 1)}$$

In this work, since the continuous PMC system did not reach the equilibrium condition, the distribution of the compounds between the two phases is reported at the time t as distribution ratio $R_D = [A]_{org}/[A]_{aq}$ and the extraction efficiency is reported for this time in terms of extraction quotient percentage $Q_E\% = (n_{org}/n_{tot}) * 100$.

The transport of a substrate in a membrane contactor can be described by the Fick's law in which the flux *J* is given by the following equation:

$$J_A = \frac{dC}{dt} = \frac{D_A}{l}(C_{A,o} - C_{A,a})$$

where $C_{A,o}$ and $C_{A,a}$ are the concentration of the component A in the organic and aqueous phases, respectively, l is the thickness of the membrane and D_A is the diffusion coefficient of the component A, illustrated by the Stokes-Einstein equation which shows that D_A is inversely proportional to the viscosity of the organic phase (η):

$$D = \frac{kT}{6\pi\eta}$$

In this study, the reported flux ($J_{org\ Ph}$) was calculated as variation of mmol of phenol in the organic phase per unit of area and time: $J_{org\ Ph}$ = mmol h^{-1} m^{-2}.

III.3 RESULTS AND DISCUSSION

III.3.1 Determination of optimal operative conditions

III.3.1.1 Photolysis tests and "dark" reactions

By means of photolysis tests and "dark" reactions, on benzene solutions in absence of the catalyst or UV light respectively, it was demonstrated that the oxidation reaction proceeded via photocatalyzed mechanism because no oxidation products were measured during these experiments.

Besides, one important drawback observed in the open batch reactor was the maintaining of an useful concentration of benzene in solution because of its tendency to rapidly vaporize. Thus, it was established to work in presence of an excess of substrate that permitted to maintain its concentration in the reactive ambient until the end of a run.

III.3.1.2 Choice of the photocatalyst

The photocatalytic conversion of benzene to phenol was initially studied testing different types of titanium dioxide. In particular three photocatalysts were used: Degussa P25 (80 % anatase and 20 % rutile) and X500 and C380 (constituted by only anatase). These catalysts were tested at concentration of 0.1 g L^{-1} and pH 3.1 in the batch reactor.

Comparing the results obtained in terms of productivity after 360 minutes (Figure III.4) it can be observed that the Degussa P25 type was the best catalyst, with a productivity two times greater than those obtained with the other photocatalysts.

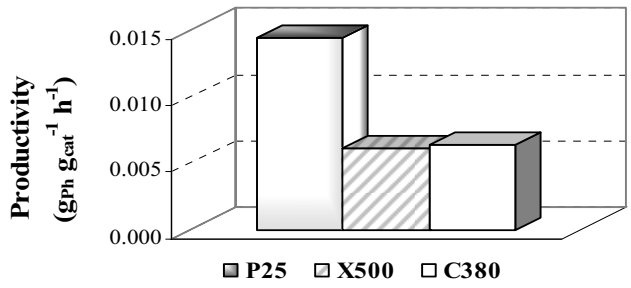

Figure III.4: Phenol productivity with different photocatalysts after 6 hours.

This behaviour could be explained by considering the different energy structure of anatase and rutile crystals which results in a different photoreactivity (see Section I.1.2.2).

Therefore, TiO_2 Degussa P25 was selected as photocatalyst to employ in all tests.

III.3.1.3 Phenol photodegradation

As previously described (Section I.1.1.2), the pH plays an important role on the adsorption of the substrate onto the catalyst surface, where it can be oxidized by the hydroxyl radicals. As reported by Bekkouche et al. (2004) in a study of adsorption of phenol on TiO_2, at alkaline value the catalyst surface is negatively charged and phenol is at the state of phenolat. In these conditions a phenomenon of repulsion can be hypothesized that could determine a low adsorption of the substrate and, therefore, a decrease in its degradation rate.

This aspect was investigated by photocatalytic degradation tests on phenol solutions at initial concentration of 10 mg L^{-1} and different pH values with suspended catalyst at 0.1 g L^{-1} (Figure III.5).

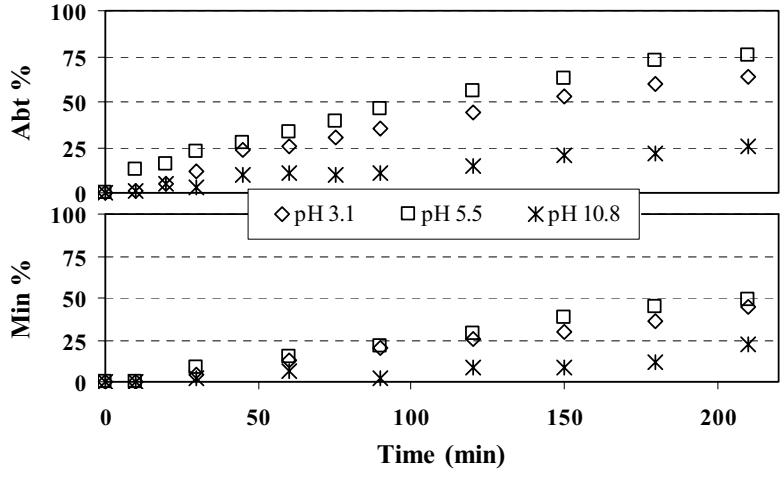

Figure III.5: Phenol abatement and mineralization at different pH values.

The obtained results confirmed the previous supposition: the alkaline pH determines a decrease of the abatement and mineralization of phenol with a degradation rate which results three times lower than acidic pH (0.012 ± 0.001 vs 0.035 ± 0.002 mg L^{-1} min^{-1}).

III.3.2 Photocatalytic oxidation in the batch reactor

To investigate the influence of pH, catalyst concentration, presence of O_2 and light intensity on the conversion of benzene to phenol in the photocatalytic system some photooxidation experiments in the batch reactor were performed. The tests were carried out in the reactor of Figure III.3a (without the membrane) adding to 500 mL of ultrapure water the catalyst and benzene and varying one parameter for each run. The obtained results, summarized in Table III.1, will be discussed in the following paragraphs.

Table III.1: Comparison of the results obtained in the batch experiments.

Operative parameter	$\mathbf{r_{phenol\ (100)}}$ **(mg L^{-1} min^{-1})**	$\mathbf{C_{phenol\ (240)}}$ **(mg L^{-1})**
Initial substrate amount (mL)		
1 mL	0.102	10.9
5 mL	0.126	15.46
10 mL	0.126	17.09
TiO_2 concentration (g L^{-1})		
0.01	0.060	9.23
0.1	0.126	15.46
0.5	0.139	17.79
1	0.185	21.39
pH		
11	0.128	20.23
5.5	0.126	15.46
3.1	0.094	14.45
3.1 (H_2SO_4)	0.122	18.65
O_2 bubbled	0.121	15.32

III.3.2.1 Role of the initial substrate amount

To understand as the initial amount of benzene influenced its water solubility and the rate of phenol production, photooxidation tests using three different initial volumes of benzene, 1 mL (which corresponded to the amount equal to its solubility in water, 1.77 g L^{-1}), 5 mL and 10 mL were carried out.

The obtained results (Table III.1) showed an oxidation kinetics quite the same in the first 100 minutes ($r_{phenol\ (100)}$), but it rapidly decreased when 1 mL of substrate was used (Figure III.6).

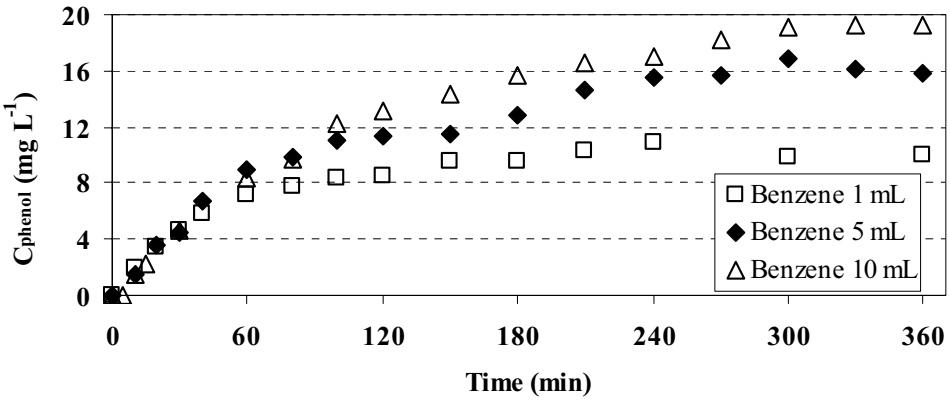

Figure III.6: Phenol concentrations versus the time using increasing initial substrate amount (pH = 5.5, TiO_2 = 0.1 g L^{-1}, I = 6.0 mW cm^{-2}, T = 25 °C).

This finding can be explained considering the concentration of benzene in solution which resulted of about 350 ± 50 mg L^{-1} with 5 mL and 10 mL vs 40 ± 10 mg L^{-1} with 1 mL after 3 h. The phenol production, therefore, did not depend on the undissolved substrate but from the little solubilised amount, evidencing the need to realize a system that provides continuously benzene in order to maintain a constant concentration in the aqueous ambient.

III.3.2.2 Influence of the catalyst concentration

Several studies showed that the photocatalytic reaction rate depends on the catalyst concentration, though it was observed that above a certain value the reaction rate becomes independent on the catalyst mass. Indeed, for high amounts of catalyst, aggregation of particles, increase of opacity and light scattering decrease the photocatalytic efficiency. Therefore, an optimal catalyst concentration value is necessary for controlling the performance of the system.

A set of experiments was carried out to investigate the effect of suspended catalyst on phenol production using TiO_2 in a concentration range of 0.01-1 g L^{-1}.

For high catalyst amount a rapid degradation of phenol was observed (Figure III.7) indicating a higher reactivity of the system.

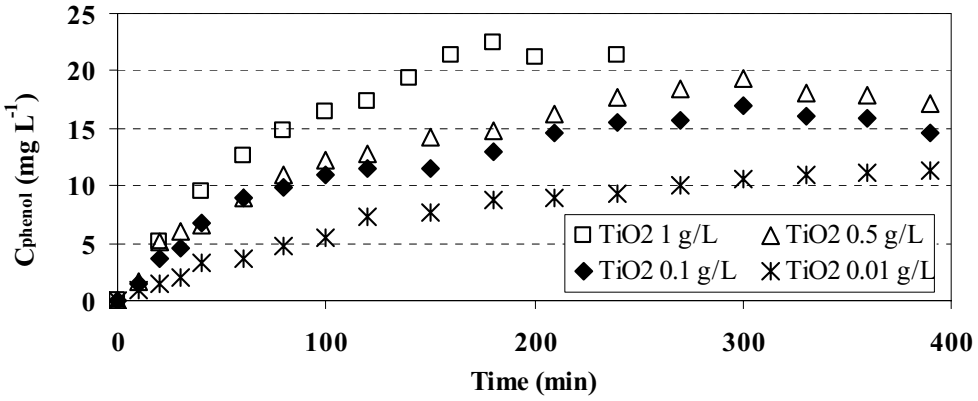

Figure III.7: Phenol concentrations versus the time at different catalyst amount (pH = 5.5, I = 6.0 mW cm^{-2}, T = 25 °C).

Besides, observing the rate values (see Table III.1) it can be noticed that the reaction kinetics increased with increasing TiO_2 concentration but no significant variation was achieved changing the concentration from 0.1 g L^{-1} to 1 g L^{-1}. For this reason an optimal catalyst concentration of 0.1 g L^{-1} was established.

III.3.2.3 Effect of the pH

As previously discussed, the pH is another important parameter which influences the photocatalytic process leading to the formation of different reaction products because of the acid-base character of TiO_2.

This effect was studied by adding to the aqueous suspension of TiO_2 and benzene at initial pH 5.5, a diluted solution of HCl or NaOH (Figure III.8).

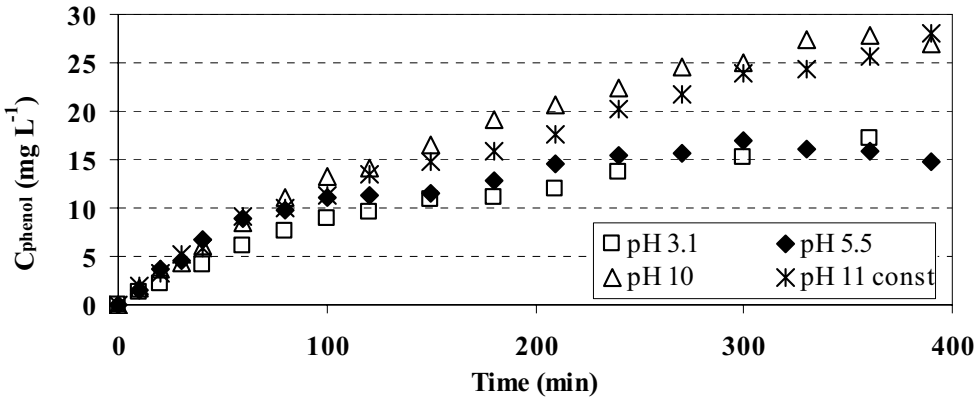

Figure III.8: Phenol concentrations versus the time at different pH values.

Although the obtained results showed a similar initial oxidation rate, a significant increase of phenol concentration at alkaline pH was observed after the second hour, reaching a productivity at 360 minutes almost two times greater than the acidic pH. This evidence can be explained by considering a lower phenol adsorption on the catalyst surface with a consequent decrease of its photodegradation.

Moreover, using sulphuric acid to reduce the pH, it was observed that the oxidation was also influenced by the type of anions in solution. In particular, the sulphate ion increased initial rate and productivity but it reduced the selectivity of the process (Table III.1), leading to the formation of several oxidation by-products that were revealed as intermediate peaks on the HPLC chromatograms.

III.3.2.4 Other parameters: bubbling oxygen and light intensity

To decrease the system reactivity and to limit the following undesirable oxidation reactions of phenol, the effect of light intensity was tested. The results obtained reducing the light intensity to 3.8 mW cm^{-2} showed a lower oxidation kinetics (with an initial rate of 0.07 mg $L^{-1}min^{-1}$) and a decrease of the oxidation by-products proportionally to the decrease in phenol concentration.

In a photocatalytic system, molecular oxygen acts as electrons acceptor avoiding the charge recombination that leads to a reduction of the photocatalytic efficiency. Besides, its reduction leads to superoxide ions which give other reactive radicals involved in the oxidation reactions (according to the mechanism described in Section

I.1.1.2). To verify if in our system the oxygen guaranteed from the air contacting the surface represents the limiting reagent in the oxidation reactions, a set of experiments was performed in the same conditions previously described (pH = 5.5, TiO_2 = 0.1 g L^{-1}, C_6H_6 = 5 mL, I = 6.0 mW cm^{-2}) and bubbling oxygen at 0.2 bar during the run.
The trends of phenol concentration with and without added oxygen showed a similar kinetics, with an initial rate of phenol production of 0.121 vs 0.126 mg L^{-1} min^{-1}, respectively. Although the oxygen from the air did not represent the limiting reagent, a more rapid decrease of benzene concentration in the reactive environment was observed when the oxygen was bubbled, probably due to a stripping effect.

III.3.3 System characterization

III.3.3.1 Extraction tests

Since in a membrane contactor the separation is determined by the distribution coefficient of the component in two phases, the choice of the organic extractant represents an important step in the optimisation of the system.
Among the various organic extractants reported in literature (Gonzales et al., 2003; Kujawski et al., 2004), 1-decanol was initially studied for its high distribution coefficient and low solubility in water.

Table III.2: Organic extractants for phenol separation from aqueous solutions (elaborated from (a) Gonzales et al., 2003 and (b) Kujawski et al., 2004).

Solvent	Distribution coefficient	Solubility in water (mg L^{-1})
[(a)] *Methyl-iso-butyl ketone*	83.2	17000 (25°C)
[(a)] *1-Decanol*	25.4	37 (25°C)
[(a)] *Toluene*	1.7	526 (25°C)
[(b)] *Methyl-ter-butyl ether*	57.4	42000 (20°C)
[(b)] *Cumene*	1.6	insoluble

As reported by Gonzales et al. (2003), when L-L extraction tests are carried out with decanol in a volume ratio (Vaq : Vor) = 1:1, this solvent allows to obtain an extraction percentage of 96,21% (calculated by reported results).

Although the high degree of extraction, when decanol was in contact with only ultrapure water, it was observed a quick increase of the TOC trend in the aqueous solution reaching a value of 28.36 mg L^{-1} (in about 2 h) which correspond almost to its solubility in water (37.38 mg L^{-1}).

This means that when decanol is used as organic phase in a PMC, it represents a potential pollutant in the reactive ambient, competing with the substrate for the oxidation reaction and leading to undesirable by-products.

On this basis and considering that one of the requirements observed in the batch tests was the need to provide a constant concentration of the substrate, benzene was tested as organic extractant.

A first set of experiments was carrier out in order to verify the optimal pH value for the aqueous solution. L-L extractions were carried out mixing aqueous solutions of phenol at three different pH values with equal volumes of benzene and thermostatted at 25 °C until phase separation.

As expected, the obtained results (Figure III.9) showed that the pH plays an important role in the separation due to the acidic character of phenol. At alkaline pH, in fact, phenol is in the anionic form which results less soluble in the organic solvent, negligible differences were observed, instead, in a pH range of 3-6.

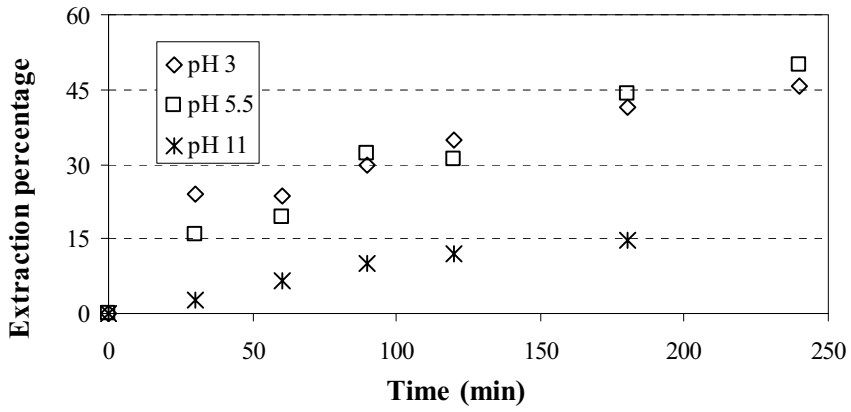

Figure III.9: Extraction percentage of phenol in L-L extraction tests between aqueous and benzene phases at different pH.

The distribution coefficient was calculated using different volume ratios of aqueous and organic phases (with a constant initial concentration of phenol in the aqueous phase).

The phenol concentration in the organic phase was plotted as function of phenol concentration in the aqueous phase measured at equilibrium after each single extraction.

The obtained equilibrium isotherm (at 25 °C) was a straight line passing from zero (Figure III.10) with the slope corresponding to the distribution coefficient of phenol between the two phases. Its value was $K_D = 2.082$ with a $R^2 = 0.998$ showing a good correlation.

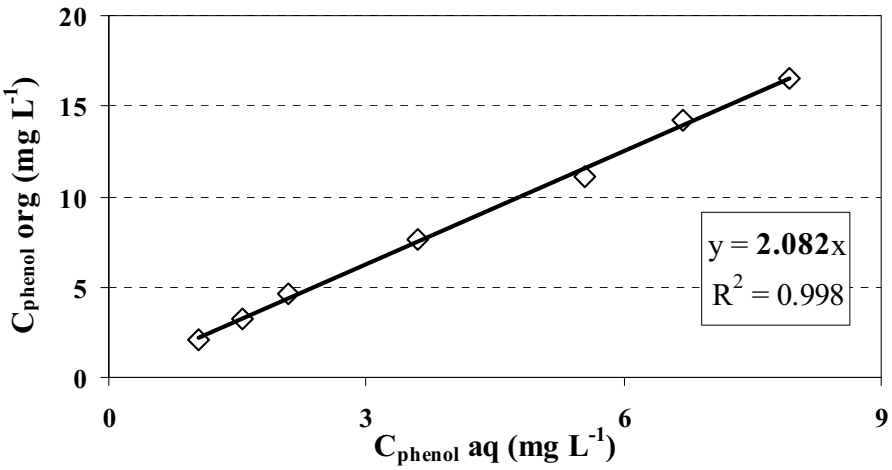

Figure III.10: Phenol extraction isotherm at 25 °C between aqueous and benzene phases.

Despite the lesser extraction percentage (68.04 %) and the lower distribution coefficient measured at acidic pH for the aqueous/benzene system, the high benzene solubility in water (1.77 g L^{-1} at 20 °C) can be exploited for assuring a constant restocking of the substrate to the reactive environment, avoiding, also, the presence of other organic solvents.

III.3.3.2 Hydrodynamic conditions on the membrane surface

In membrane contactor systems the pores of the porous membrane used are filled with the fluid that wets the membrane. Nonpolar fluids will wet hydrophobic membranes, while polar fluids will wet hydrophilic ones.

In this study the permeation module was constituted by two compartments containing an aqueous solution and benzene phase, respectively, separated by a flat sheet hydrophobic polypropylene membrane with a pore size of 0.2 μm. Therefore, benzene filled the pores of the polypropylene membrane by capillary forces (wetting fluid). To avoid its complete passage into the aqueous reactive ambient (non wetting fluid), the pressure of the aqueous phase on the membrane surface must be maintained slightly higher (Figure III.11). Furthermore, to maintain the benzene in the membrane pores, the pressure of the aqueous phase must be kept below a critical value known as wetting or breakthrough pressure (ΔP_b) (Gabelman et al., 1999).

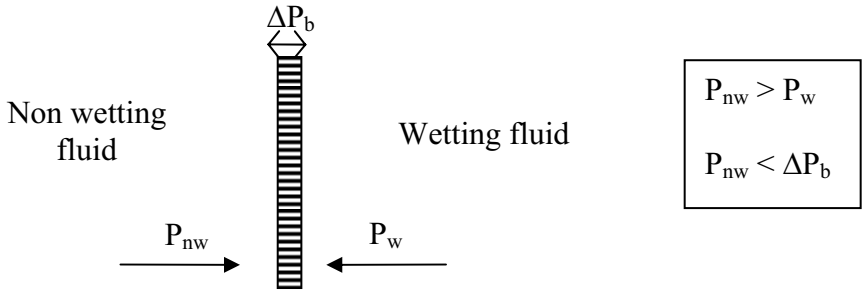

Figure III.11: Schematisation of the hydrodynamic condition on the membrane surface in a membrane contactor.

The breakthrough pressure is given by Laplace equation:

$$\Delta P_b = (2\gamma\cos\theta)/r$$

where γ is the interfacial tension between the two liquids, θ the contact angle between the membrane and the wetting fluid and r is the pore radius of the membrane.

The contact angle θ is the angle formed between the wetting fluid and the membrane. It is specific for any given system and it increases with increasing polarity difference

between the membrane material and the fluid. In particular, less energy is needed for an higher contact angle to remove the wetting fluid from a pore, and, therefore, a lower breakthrough pressure.

About the effect of interfacial tension γ, when it increases, more energy to bring the two fluids together is required, hence more pressure is needed to displace one fluid from the pores using the other one.

The role of the pore radius r is related to the ratio of the pore surface to its volume. Decreasing the pore radius the solid/fluid interaction increases, resulting in a higher breakthrough pressure (Gabelman et al., 1999).

Measuring the contact angle (Figure III.12).between benzene and the polypropylene membrane (10.292 at time zero) and knowing the interfacial tension benzene/water (35.0 mJ m^{-2}) (www.galenotech.org/chimfis6.htm) and the membrane pore radius (0.1 μm) the calculated breakthrough pressure was 688.8 kPa.

Figure III.12: Drop of benzene on the surface of the polypropylene membrane.

Since the pressure of the aqueous phase on the membrane surface measured for our system was of 0.61 -0.40kPa (the liquid (hydrostatic) pressure on the membrane surface can be expressed as: $P = \rho gh$), the requested condition resulted broadly satisfied.

III.3.3.3 Transport experiments

To verify the efficiency of the realized system in terms of flux and extraction degree of phenol, preliminary transport tests were carried out.

The obtained results, reported in Figure III.13, showed that the equilibrium condition (K_D of about 2.0) was reached after 360 minutes, with a phenol extraction percentage (E %) of 24 ± 2 % and a constant benzene concentration in the aqueous phase of about 200 mg L^{-1}.

The flux of phenol ($J_{org\ Ph}$) in the organic phase, measured in the first 180 minutes, was 1.7 mmol $h^{-1}m^{-2}$.

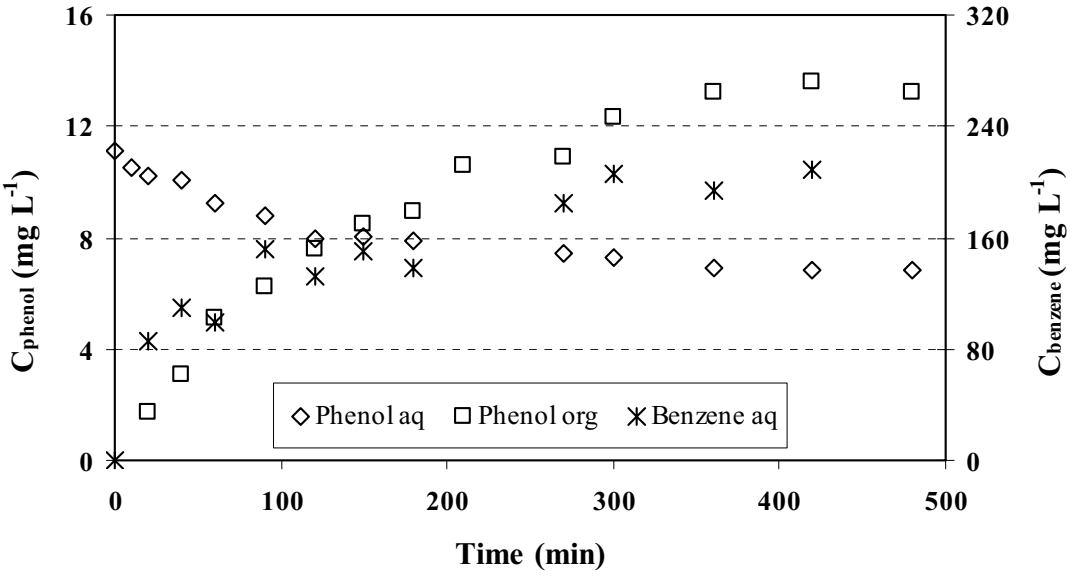

Figure III.13: Concentrations of phenol in aqueous and organic phases and benzene concentration in the aqueous phase during the transport tests.

These data confirm the possibility to use a membrane contactor for the separation of phenol from the aqueous phase, assuring, also, a constant restock of the substrate in the reactive ambient.

III.3.4 Photooxidation tests in the PMC

On the basis of the obtained results the operative conditions used during the photooxidation tests in the PMC were:

- 700 mL of aqueous phase at acidic pH with suspended TiO_2 at concentration of 0.1 g L^{-1} and 5 mL of benzene (to guaranteed a high initial substrate concentration);
- 130 mL of organic phase constituted by only benzene;
- a pressure difference on the membrane surface water side of 0.20-0.40 kPa, a constant temperature of the whole system at 25°C and a constant restocking of the substrate guaranteed from the solubility of benzene in water.

The reaction tests were carried out for 8 h, following the phenol concentration and their intermediate products in the two phases.

In these conditions, the influence of pH, catalyst concentration and light intensity on the overall process (synthesis and separation) was studied, considering, also, the effects of these parameters on the intermediate products.

III.3.4.1 PMC performance at different pH

Since it was observed that the pH influences not only the photocatalytic reaction but also the extraction performance in the system, a first set of experiments using acidic aqueous solution (pH 3.1 and 5.5) was performed.

Although it was previously reported an increase of phenol production at pH of 10-11, in this work the alkaline environment was not used due to the lower phenol extraction obtained in these conditions.

The first results obtained at a pH value 5.5, which corresponds to that of the TiO_2 solution without further variations, showed a phenol production of 11.2 ± 0.2 mg after 8 hours with a constant benzene concentration in the aqueous phase of 280 ± 20 mg L^{-1}. With respect to the difference between the initial and final benzene volume (consumed benzene in the system), the yields of the process was 0.1 %, with a productivity of 0.014 g_{Ph} g_{cat}^{-1} h^{-1}. As can be observed in Figure III.14, the organic phase allowed the separation of phenol with a flux that reached a constant value of 1.06 mmol h^{-1} m^{-2} after the first 2 hours. However, during the run it was observed an increase of the distribution ratio R_D which reached a value of 1.37 at the end of the

test, with a $Q_{E\ Ph}$ % of 20.25 %. This means that in this time (8 hours) an equilibrium condition was not achieve in the extraction system.

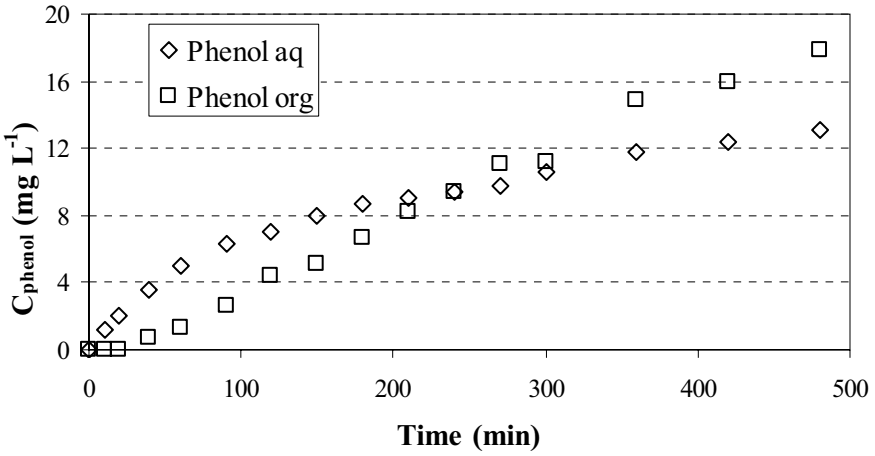

Figure III.14: Phenol concentration in the aqueous and organic phases vs. time for a test in the PMC at pH 5.5.

Performing the experiments at a more acidic pH (about 3.1) the obtained results showed a trend of phenol concentrations in the aqueous and organic phases (Figure III.15) similar to those observed at pH 5.5.

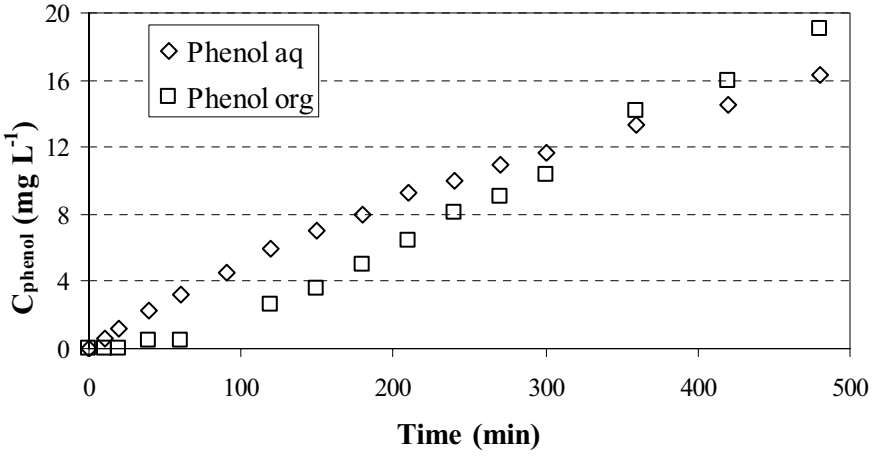

Figure III.15: Phenol concentration in the aqueous and organic phases vs. time for a test in the PMC at pH 3.1.

The amount of phenol produced at the end of the tests was 13.3 ± 0.6 mg, with a flux in the organic phase of 1.27 mmol h^{-1} m^{-2} and a $Q_{E\ Ph}$ % of 17.86 % (after 8 hours).

III.3.4.2 Intermediate products

Although negligible differences on the phenol extraction performance of the system were observed, an important different behaviour towards some intermediates was revealed (Figure III.16)

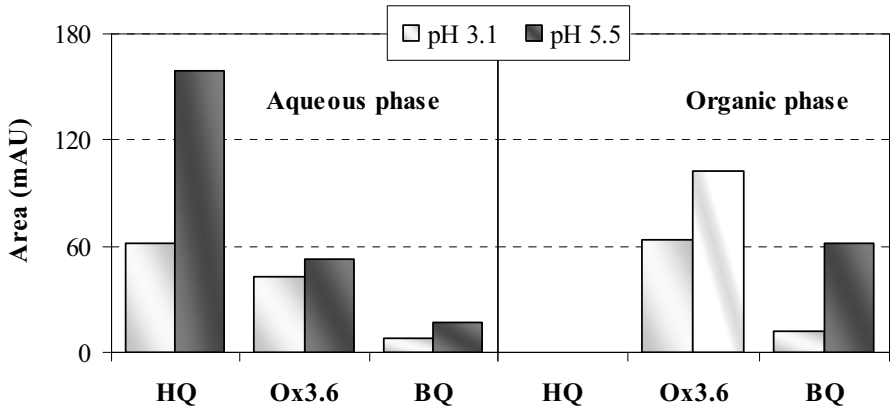

Figure III.16: Area of the intermediates in the aqueous and organic phases at pH 3.1 and 5.5.

Three main oxidation by-products were detected as HPLC peaks at retention times of 3.0, 3.6 and 3.9 minutes. By GC-MS measurements on the aqueous and organic phases, hydroquinone (HQ) and p-benzoquinone (BQ) were identified in traces as the intermediates at retention times of 3.0 and 3.9, respectively. The other oxidation by-products reported in literature, such as cathecol, o-benzoquinone, biphenyl, resorcinol, were not found in this system.

The peak at 3.6 minutes (Ox3.6) was identified as 2,4-hexadienil-1,6-diol, a product which can be hypothesized deriving from the following oxidation reactions that led to the opening of the cyclic structure, though, this intermediate is actually under study.

However, since the identification of all oxidation by-products were achievable only after pre-concentration of the solutions, it is possible to affirm that their concentrations in the aqueous and organic phases during the reactions were in traces, and therefore indicative considerations on their extraction were done using the HPLC areas.

As can be observed in Figure III.16, the system permitted to maintain completely the HQ in the aqueous phase, but it was not able to reject the other by-products, which passed in the organic phase due to their greater solubility in benzene.
The most acidic pH, however, allowed to obtain a lower formation and extraction of these intermediates. This finding was particularly evident for BQ and HQ and can be explained considering the equilibrium position of the reaction of conversion of HQ to BQ which is switched to the left in acidic conditions.

III.3.4.3 Effects of catalyst concentration and light intensity

In the batch tests an increase of phenol concentration increasing the catalyst concentration was observed (see Table III.1). However, at a value of 1 g L^{-1}, the high reactivity of the system led, also, to a quick degradation of phenol. The use of an extractive system coupled to the photocatalytic synthesis can allow to solve the problem of the secondary reaction, minimizing the phenol degradation.
Therefore, the performance of the PMC was also studied using a catalyst concentration of 1 g L^{-1} and pH 3.1. The results obtained in these tests showed an increase in the reaction kinetics (Figure III.17), with a flux of 1.70 mmol h^{-1} m^{-2}.

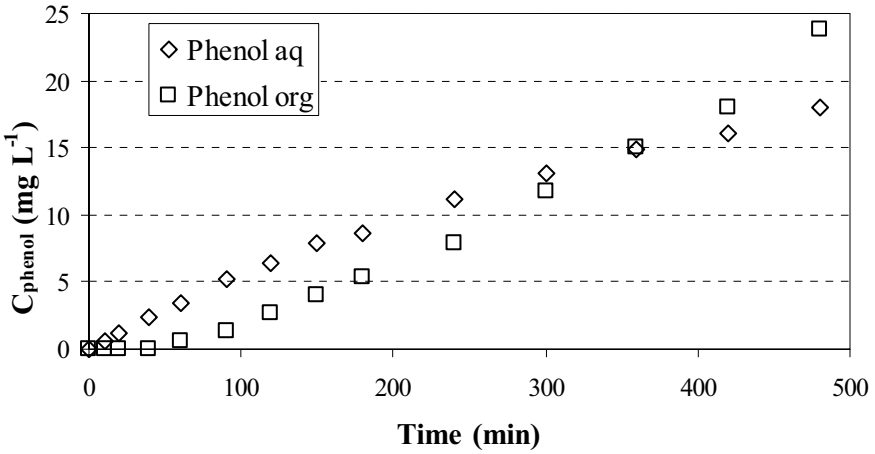

Figure III.17: Phenol concentration in the aqueous and organic phases vs. time for a test in the PMC with a TiO_2 concentration of 1.0 g L^{-1}.

Nevertheless, the lower system productivity obtained after 480 minutes (0.002 g_{Ph} g_{cat}^{-1} h^{-1}) with respect to that measured with a TiO_2 concentration of 0.1 g L^{-1} (0.017 g_{Ph} g_{cat}^{-1} h^{-1}), led to consider this last catalyst concentration the best operative condition.

To decrease the system reactivity and to enhance the separation of phenol before its successive oxidation, a test using a lower light intensity was also performed.

As expected, a lower irradiation intensity (4.7 mW cm^{-2}) led to a decrease in phenol production with a $J_{org\ Ph}$ of 0.85 mmol $h^{-1}m^{-2}$ and a productivity of 0.012 g_{Ph} g_{cat}^{-1} h^{-1} after 8 hours (Table III.3).

Table III.3: Obtained results for a test in the PMC with a light intensity of 4.7 mW cm^{-2}.

Phenol aq (mg L^{-1})	10.8
Phenol org (mg L^{-1})	13.3
$Q_{E\ Ph}$ %	18.66
Productivity (g_{Ph} g_{cat}^{-1} h^{-1})	0.012
$J_{org\ Ph}$ (mmol h^{-1} m^{-2})	0.85

However, the $Q_{E\ Ph}$ % of 18.66 % obtained in this test, demonstrated that the extraction kinetics is independent on the phenol amount in the aqueous phase.

III.3.4.4 Comparison of the results

Figure III.18 and Table III.4 report a comparison between the photooxidation tests performed in the PMC.

The achieved results show that:

- The realized system allowed to obtain the one-step photooxidation of benzene to phenol, although the yields of the process resulted very low;
- The use of benzene as organic phase permitted to separate phenol and to guarantee a constant restocking of the substrate in the reactive environment;
- No significant variation in terms of productivity and separation performance of the system were observed changing some of the parameters influencing the overall process;

- Some oxidation by-products, like benzoquinone, hydroquinone and other oxidized molecules, were revealed during the tests. Their production and extraction can be minimized lowering the pH;
- The enhanced system reactivity, by increasing the catalyst concentration, caused a little increase of phenol flux in the organic phase. However, the productivity of the system decreased of one order of magnitude leading to a system economically disadvantageous;
- In this system the rate of phenol extraction was not enough to avoid its following oxidation in the reactive environment.

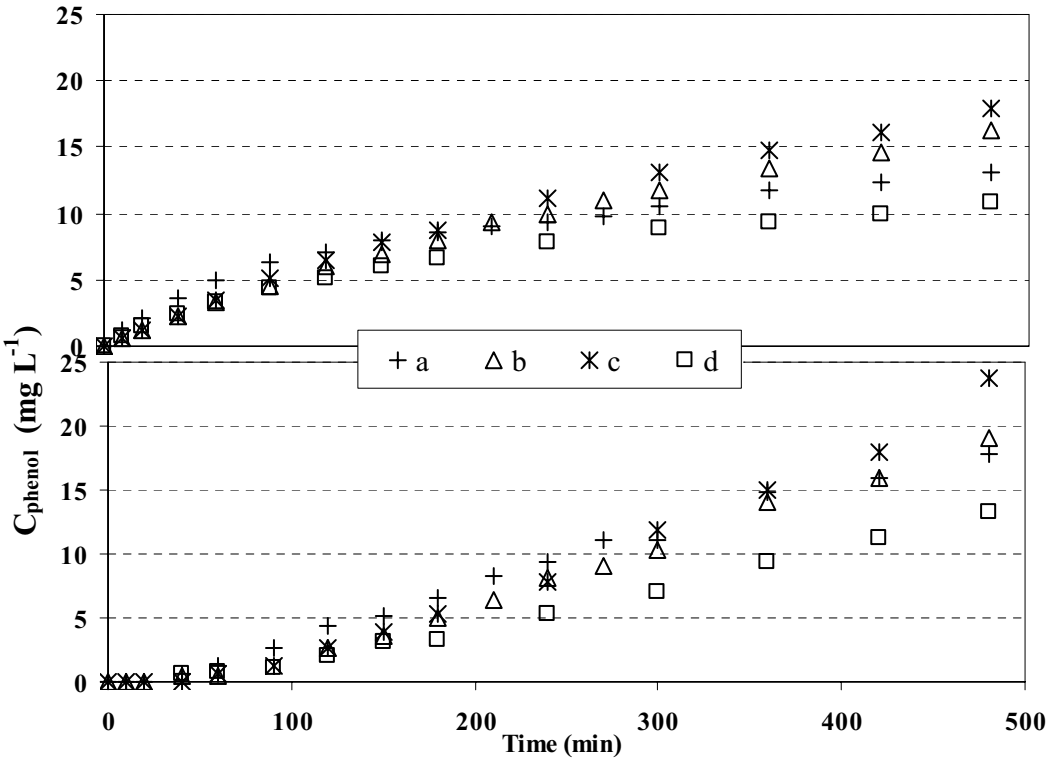

Figure III.18: Comparison of the obtained results in the tests performed in the PMC at different operative conditions: (a) TiO_2 0.1 = g L^{-1}, pH = 5.5, I = 6.0 mW cm^{-2}; (b) TiO_2 0.1 = g L^{-1}, pH = 3.1, I = 6.0 mW cm^{-2}; (c) TiO_2 1.0 = g L^{-1}, pH = 3.1, I = 6.0 mW cm^{-2}; (d) TiO_2 0.1 = g L^{-1}, pH = 5.5, I = 4.7 mW cm^{-2}).

Table III.4: Productivity, flux and extraction percentage values in the tests performed in the PMC at different operative conditions.

	TiO_2 0.1 pH 5.5 - I 6.0	**TiO_2 0.1 pH 3.1 - I 6.0**	**TiO_2 1.0 pH 3.1 - I 6.0**	**TiO_2 0.1 pH 5.5 - I 4.7**
Productivity ($g_{Ph}\ g_{cat}^{-1}\ h^{-1}$)	0.014	0.017	0.002	0.012
$J_{org\ Ph}$ ($mmol\ h^{-1}\ m^{-2}$)	1.06	1.27	1.70	0.85
$Q_{E\ Ph}\%$	20.25%	17.86%	19.71%	17.30%
$Q_{E\ HQ}\%$	0.00%	0.00%	0.00%	0.00%
$Q_{E\ Ox3.6}\%$	26.60	21.71%	23.39%	26.61%
$Q_{E\ BQ}\%$	40.84	21.68%	33.17%	44.08%

Considering the obtained data, in order to increase the selectivity of the photocatalytic reaction and the separation performance of the membrane contactor, the effect of dissolved metal ions was also studied.

III.3.5 Effects of dissolved ions on the PMC performance

As reported by several studies (Brezova et al., 1995; Sykora et al., 1997; Konstantinou et al., 2004) (see Section I.), dissolved metal ions influence the photocatalytic reactions because, when they are used in their higher oxidation state, they act as photoelectron acceptors preventing the charge-carrier recombination:

$$M^{n+} + e^- \rightarrow M^{(n-1)+}$$

Moreover, the reduced species can react with H_2O_2, generated in the photocatalytic system, to give additional $^{\bullet}OH$ by photo-Fenton reaction:

$$M^{(n-1)+} + H_2O_2 \rightarrow M^{n+} + {}^{\bullet}OH + OH^-$$

In this condition the metal ion is regenerated in its higher oxidation state.

In particular, since the photoexcitation of TiO_2 semiconductor particles results in the formation of electron (e^-) in the conduction band with a band edge potential of -0.1 V vs. NHE, the standard reduction potential of metal ions must be higher than this value.

On these basis, the effects of dissolved Fe^{3+} ($E^0_{(Fe^{3+}/Fe^{2+})}$ = + 0.77 V), Cu^{2+} ($E^0_{(Cu^{2+}/Cu^{+})}$ = + 0.167 V) and V^{3+} ($E^0_{(V^{3+}/V^{2+})}$ = - 0.20 V) (Table III.5) on the efficiency and separation performance of the PMC were investigated.

Table III.5: Standard reduction potential for the redox systems of the studied metal ions.

$M^{n+} + e^- \leftrightarrows M^{(n-1)+}$	E^0 (V)
$Fe^{3+} + e^- \leftrightarrows Fe^{2+}$	+ 0.77
$Cu^{2+} + e^- \leftrightarrows Cu^{+}$	+ 0.167
$V^{3+} + e^- \leftrightarrows V^{2+}$	- 0.20

All the tests were performed dissolving $FeCl_3$, $CuCl_2$ or VCl_3 at concentration 1 mM in the aqueous phase (pH 3.1) with TiO_2 concentration of 0.1 g L^{-1}.

Comparing the achieved results with those obtained with only TiO_2 (Figure III.19) it can be observed a positive influence in presence of ferric ion but inhibition effects with dissolved Cu^{2+} and V^{3+}.

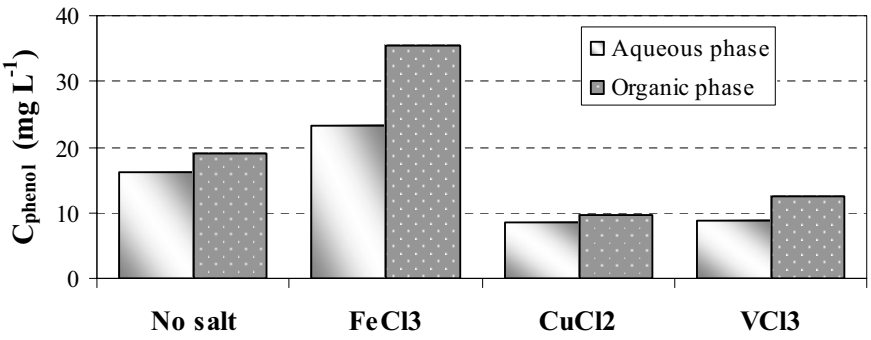

Figure III.19: Comparison of phenol concentrations in PMC with dissolved ions.

As demonstrated by Brezova et al. (1995), the decrease of photocatalyst activity with cupric ions can be explained supposing its reduction into the unreactive form Cu^0 and its deposition on the TiO_2 surface.

Regarding the separation performance, an increase of the phenol extraction percentage with Fe^{3+} and V^{3+} was obtained, while no influence was observed in presence of Cu^{2+} (Table III.6). This aspect was probably due to an enhanced ionic strength of the aqueous phase with $FeCl_3$ and VCl_3 which affects positively the phenol extraction in the organic phase.

Table III.6: Results obtained in the photooxidation experiments in the PMC in presence of dissolved metal ions.

	No salt	**$FeCl_3$**	**$CuCl_2$**	**VCl_3**
mg produced	13.86	20.94	7.31	7.74
mg extracted	2.48	4.62	1.26	1.63
R_D	1.17	1.52	1.12	1.44
Q_E%	17.86	22.06	17.19	21.12
Productivity ($g_{Ph}\ g_{cat}^{-1}\ h^{-1}$)	0.0173	0.0262	0.0091	0.0097
$J_{org\ Ph}$ ($mmol\ h^{-1}\ m^{-2}$)	1.27	2.12	0.64	0.85

Observing the area of the oxidation by-products, it can be noticed that the general trend was an increase in their production with the dissolved ions. Nevertheless, although the lower productivity obtained with vanadium cation, a positive effect in terms of selectivity was observed with the formation of the only intermediates at retention time of 3.6 minutes. This aspect will be studied in the future.

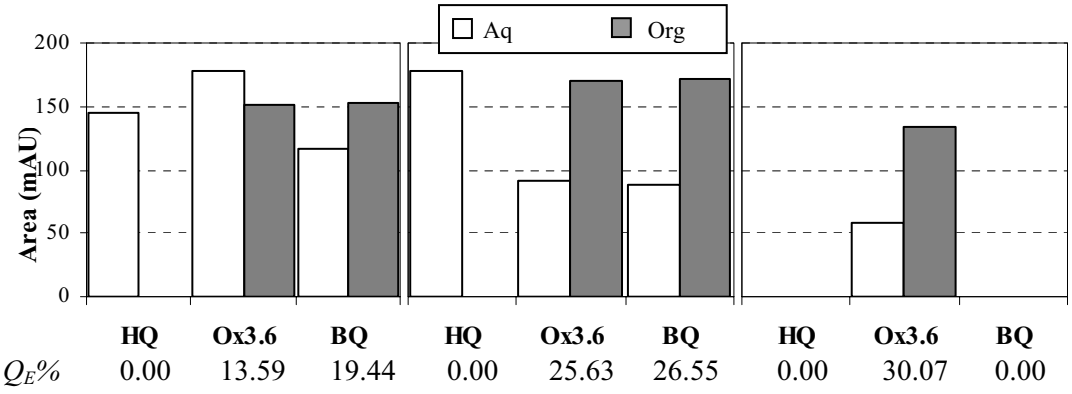

Figure III.20: Comparison of by-product areas and Q_E% in PMC with dissolved ions.

III.4 SUMMARY REMARKS

The photocatalytic tests in the batch reactor showed that increasing the catalyst concentration the reaction kinetics increases although with a C_{TiO_2} of 1.0 g L^{-1} a quick degradation of phenol was observed. Alkaline pH allowed to obtain a higher phenol concentration (20.2 vs 15.0 ± 0.5 mg L^{-1} in acidic conditions) due to a lower phenol adsorption on the catalyst surface which reduced its degradation. An initial excess of benzene was necessary to guarantee enough amount of substrate for the reaction, while no influence on the reaction rate was observed bubbling oxygen in the reactive environment.

L-L extraction tests and mass transport experiments showed that use of benzene as organic phase in the role of solvent (other than substrate) allowed the separation of phenol from the aqueous ambient with a K_D which reached a value of 2.1, providing also a constant restocking of substrate (about 200 mg L^{-1}) in the aqueous phase.

The realized PMC allowed to obtain the phenol production and its separation, although the formation of intermediate oxidation by-products, like benzoquinone, hydroquinone and other oxidized molecules was observed.

The reduction of pH to 3.1 did not influence significantly the system productivity with $J_{org\ Ph}$ of 1.27 mmol $h^{-1}m^{-2}$ with respect to 1.06 mmol $h^{-1}m^{-2}$ at pH 5.5. Nevertheless, the most acidic condition permitted to control the selectivity towards the intermediates, allowing to obtain a lower formation and extraction of these oxidation by-products.

Despite the enhancement of system reactivity by increasing the catalyst concentration, a little increase of the phenol flux in the organic phase was observed. However, the productivity of the system decreased of one order of magnitude leading to a less interesting operating condition.

Use of dissolved metal ions, like Fe^{3+}, Cu^{2+} and V^{3+}, to improve the system productivity showed an increase in the phenol production only using iron(III) ion, whereas an inhibiting influence with the other two cations was observed. Regards the separation performance of the system, the enhanced ionic strength of the aqueous phase, with $FeCl_3$ and VCl_3 allowed to reach a R_D of 1.52 and 1.54, respectively, in comparison to a value of 1.17 obtained without salts.

CONCLUSIONS

This study demonstrated the possibility to integrate photocatalytic reactions with membrane processes to obtain a very interesting "green" technology in water purification and organic synthesis.

Photocatalytic Membrane Reactors represent a very promising method that combines the advantages of the classical photoreactors, with the catalyst in suspension, and that of membrane processes, separating simultaneously the product(s) of interest and recovering the catalyst.

Different configuration of PMRs are optimized for total and partial oxidation reactions of organic compounds in water, using suspended TiO_2 as photocatalyst.

The total oxidation of pharmaceuticals (Gemfibrozil and Tamoxifen) were performed in a photocatalytic reactor coupled with two membrane modules: Pressurized and Submerged Photocatalytic Membrane Reactors.

The obtained results showed a quickly and complete abatement (99%) of the target molecules in about 20 minutes and a mineralization higher than 90 % in about 120 minutes in the batch system. The complete abatement of Gemfibrozil, a mineralization of 60 %, the constant permeate fluxes and the retention of the suspended catalyst, showed a good operating stability of both the continuous systems studied. However, a TOC rejection of about 62 % in the pressurized photoreactor and the no TOC rejection obtained in the de-pressurized system, underlined the necessity to identify membranes with higher rejection to the intermediate products. The higher permeate fluxes measured in the SPMR with respect to those observed in the PPMR (65.1 L h^{-1} m^{-2} vs. 38.6 L h^{-1} m^{-2}) showed the first system more interesting for application purposes.

The partial oxidation of benzene to phenol was studied in a Photocatalytic Membrane Contactor. The one-step synthesis and separation of phenol was realized by coupling to a photocatalytic reactor a membrane contactor module in which benzene was used both as substrate and organic extractant.

The achieved data demonstrated a negligible difference on the phenol flux in the organic phase (1.16 ± 0.11 mmol $h^{-1}m^{-2}$) changing the pH in acidic range.

Nevertheless, a better control of formation and extraction of oxidation by-products at pH of 3.1 was obtained. The influence of dissolved ions (Fe^{3+}, Cu^{2+} and V^{3+}) on the efficiency of the system was also investigated. The results showed an increase in the system productivity and separation performance in presence of iron(III) ion with a phenol flux in the organic phase almost two times greater than those measured without salts.

To summarize this PhD study a general conclusion can be made: the two application areas of the studied Photocatalytic Membrane Reactors show the importance to optimize some fundamental parameters to apply these systems both as purification technique and synthetic pathway. They, in perspective, can be very interesting when direct solar light as energy source is used.

REFERENCES

- Aarthi T., G. Madras, *Catal. Commun.* **2008**, *9*, 630.
- Abu Tariq M., M. Faisal, M. Muneer, D. Bahnemann, *J. Mol. Catal. A: Chem.* **2007**, *265*, 231.
- Addamo M., V. Augugliaro, E. Garcia-Lopez, V. Loddo, G. Marcì, L. Palmisano, *Catal. Today* **2005**, *107-108*, 612.
- Ahn W.-Y., S.A. Sheeley, T. Rajh, D.M. Cropek, *Appl. Catal., B* **2007**, *74*, 103.
- Almquist C.B., P. Biswas, *Appl. Catal., A* **2001**, *214*, 259.
- Amat A.M., A. Arques, F. Galindo, M.A. Miranda, L. Santos-Juanes, R.F. Vercher, R. Vicente, *Appl. Catal., B* **2007**, *73*, 220.
- Anastas P., J. Warner, *Green Chemistry: Theory and Practice*, Oxford University Press: New York, **1998**.
- Anpo M., *Pure Appl. Chem.* **2000**, *72*, 1265.
- Arana J., A. Pena Alonso, J.M. Dona Rodriguez, J.A. Herrera Melian, O. Gonzales Diaz, J. Perez Pena, *Appl. Catal., B* **2008**, *78*, 355.
- Augugliaro V., E. Garcia-Lopez, V. Loddo, S. Malato-Rodriguez, I. Maldonado, G. Marcì, R. Molinari, L. Palmisano, *Sol. Energy* **2005**, *79*, 402.
- Augugliaro V., M. Litter, L. Palmisano, J. Soria, *J. Photochem. Photobiol., C* **2006**, *7*, 127.
- Augugliaro V., S. Coluccia, V. Loddo, L. Marchese, G. Martra, L. Palmisano, M. Pantaleone, M. Schiavello, *Studies in Surface Science and Catalysis*, 663-672, 3rd Word Congress on Oxidation Catalysis, R.K. Grasselli, S.T. Oyama, A.M. Gaffney and J.E. Lyons (Eds.), Elsevier Science Publishers B.V., Amsterdam., The Netherlands, **1997a**.
- Augugliaro V., S. Coluccia, V. Loddo, L. Marchese, G. Martra, L. Palmisano, M. Schiavello, *Appl. Catal., B* **1999**, *20*, 15.
- Augugliaro V., V. Loddo, G. Marcì, L. Palmisano, M.J. López-Muñoz, *J. Catal.* **1997b**, *166*, 272.
- Azrague K., P. Aimar, F. Benoit-Marquié, M.T. Maurette, *Appl. Catal., B* **2007**, *72*, 197.

- Baran W., A. Makowski, W. Wardas, *Dyes Pigm.* **2008**, *76*, 226.
- Bekkouche S., M. Bouhelassa, N. Hadj Salah, F.Z. Meghlaoui, *Desalination* **2004**, *166*, 355.
- Bendz D., N.A. Paxeus, T.R. Ginn, F.J. Loge, *J. Hazard. Mater*. **2005**, *122*, 195.
- Bhatkhande D.S., S.P. Kamble, S.B. Sawant, V.G. Pangarkar, *Chem. Eng. J.* **2004**, *102*, 283.
- Bi J., L. Wu, Z. Li, X. Wang, X. Fu, *Mater. Lett.* **2008**, *62*, 155.
- Biard P.-F., A. Bouzaza, D. Wolbert, *Appl. Catal., B* **2007**, *74*, 187.
- Bonchio M., M. Carraro, M. Gardan, G. Scorrano, E. Drioli, E. Fontananova, *Top. Catal.* **2006**, *40*, 1-4, 133.
- Brezova V., A. Blazkova, E. Borosova, M. Ceppan, R. Fiala, *J. Mol. Catal. A: Chem.* **1995**, *98*, 109.
- Brezova V., A. Blazkova, I. Surina, B. J. Havlinova, *J. Photochem. Photobiol., A* **1997**, *107*, 233.
- Brosillon S., H. Djelal, N. Merienne, A. Amrane, *Desalination* **2008b**, *222*, 331.
- Brosillon S., L. Lhomme, C. Vallet, A. Bouzaza, D. Wolbert, *Appl. Catal., B* **2008a**, *78*, 232.
- Cai R., Y. Kubota, T. Shuin, H. Sakai, K. Hashimoto, A. Fujishima, *Cancer Research* **1992**, *52*, 2346.
- Camera-Roda G., F. Santarelli, *J. Sol. Energ. –T. ASME* **2007**, *129*, 68.
- Canonica S., L. Meunier, U. von Gunten, *Water Res.* **2008**, *42*, 121.
- Cappelletti G., C.L. Bianchi, S. Ardizzone, *Appl. Catal., B* **2008**, *78*, 193.
- Caronna T., C. Gambarotti, L. Palmisano, C. Punta, F. Recupero, *J. Photochem. Photobiol., A* **2005**, *171*, 237.
- Chan C.C.V., P.R. Bérubé, E.R. Hall, *J. Membr. Sci.* **2007**, *297*, 104.
- Chen C., Z. Wang, S. Ruan, B. Zou, M. Zhao, F. Wu, *Dyes Pigm.* **2008**, *77*, 204.
- Chen C.-C., *J. Mol. Catal. A: Chem.* **2007**, *264*, 82.
- Chen D., A.K. Ray, *Chem. Eng. Sci.* **2001**, *56*, 1561.
- Chen F., T. Hua Wua, X. Ping Zhou, *Catal. Commun.* **2008**, *9*, 1698.
- Chen J., L. Eberlein, C.H. Langford, *J. Photochem. Photobiol., A* **2002**, *48*, 183.
- Chen Y., E. Stathatos, D.D. Dionysiou, *Surf. Coat. Technol.* **2008**, *202*, 1944.
- Chin S.S., T.M. Lim, K. Chiang, A.G. Fane, *Chem. Eng. J.* **2007**, *130*, 53.

- Choi J.H., K. Fukushi, K. Yamamoto, *Sep. Purif. Technol.* **2007**, *52*, 470.
- Choi W., *Catal. Surv. Asia* **2006**, *10*, 16.
- Choo K.-H., D.-I. Chang, K.-W. Park, M.-H. Kim, *J. Hazard. Mater.* **2008**, *152*, 183.
- Colmenares J.C., M.A. Aramendìa, A. Marinas, J.M. MArinas, F.J. Urbano, *Appl. Catal., A* **2006**, *306*, 120.
- Comeau F., C. Surette, G.L. Brun, R. Losier, *Sci. Tot. Environ.* **2008**, *396*, 132.
- Comoretto L., S. Chiron, *Sci. Total Environ.* **2005**, *349*, 201.
- Coronado J.M., J. Soria, J.C. Conesa, R. Bellod, C. Adàn, H. Yamaoka, V. Loddo, V. Augugliaro, *Top. Catal.* **2005**, *35*, 3–4, 279.
- Dastgir M.G., L.G. Peeva, A.G. Livingston, *Chem. Eng. Sci.* **2005**, *60*, 7034.
- De Heredia J.B., J. Torregrosa, J.R. Dominguez, J.A. Peres, *J. Hazard. Mater.* **2001**, *83*, 255.
- Demeestere K., J. Dewulf, B. De Witte, A. Beeldens, H. Van Langenhove, *Build. Environ.* **2008**, *43*, 406.
- Dey G.R., A.D. Belapurkar, K. Kishore, *J. Photochem. Photobiol., A* **2004**, *163*, 503.
- Di Paola A., Cufalo G., Addamo M., M. Bellardita, R. Campostrini, M. Ischia, R. Ceccato, L. Palmisano, *Colloids Surf., A* **2008**, *317*, 366.
- Dijkstra M.F.J., H. Buwalda, A.F. de Jong, A. Michorius, J.G.M. Wilkelman, A.A.C.M. Beenackers, *Chem. Eng. Sci.* **2001**, *56*, 547.
- Dimitrova R., M. Spassova, *Catal. Commun.* **2007**, *8*, 693.
- Doll T.E., F.H. Frimmel, *Water Res.* **2004**, *38*, 955.
- Dong T., J. Li, F. Huang, L. Wang, J. Tu, Y. Torimoto, M. Sadakata, Q. Li, *Chem. Commun.* **2005**, 2724.
- Du P., J.A. Moulijin, G. Mul, *J. Catal.* **2006**, *238*, 342.
- Du P., J.T. Carneiro, J.A. Moulijn, G. Mul, *Appl. Catal., A* **2008**, *334*, 119.
- Egerton T.A., J.A. Mattinson, *J. Photochem. Photobiol., A* **2008**, *194*, 283.
- Emeline A.V., V. Ryabchuk, N. Serpone, *J. Photochem. Photobiol., A* **2000**, *133*, 89.
- Eriksson E., N. Christensen, J.E. Schmidt, A. Ledin, *Desalination* **2008**, *226*, 371.

- Fernandez P., J. Blanco, C. Sichel, S. Malato, *Catal. Today* **2005**, *101*, 345.
- Franken T., *Membr. Technol.* **1998**, *97*, 7.
- Fu J., M. Ji, Z. Wang, L. Jin, D. An, *J. Hazard. Mater. B* **2006**, *131*, 238.
- Fujishima A., K. Honda, *Nature* **1972**, *238*, 37.
- Fujishima A., T.N. Rao, D.A. Tryk, *J. Photochem. Photobiol., C* **2000**, *1*, 1.
- Fujishima K., A. Fukuoka, A. Yamagishi, S. Inagaki, Y. Fukushima, M. Ichikawa, *J. Mol. Catal. A: Chem.* **2001** *166*, 211.
- Gabelman A., S.-T. Hwang, *J. Membr. Sci.* **1999**, *159*, 61.
- Gao X., J. Xu, *Appl. Clay Sci.* **2006**, *33*, 1.
- Ge L., *J. Mol. Catal. A: Chem.* **2008**, *282*, 62.
- Ghosh R., *J. Membrane Sci.* **2006**, *274*, 73.
- Gòmez M.J., M.J. Martìnez Bueno, S. Lacorte, A.R. Fernàndez-Alba, A. Aguera, *Chemosphere* **2007**, *66*, 993.
- Gondal M.A., A. Hameed, Z.H. Yamani, A. Arfaj, *Chem. Phys. Lett.* **2004**, *392*, 372.
- Gonzales M.A., S.G. Howell, S.K. Sikdar, *J. Catal.* **1999**, *183*, 159.
- Gonzalez-Munoz M.J., S. Luque, J.R. Alvarez, J. Coca, *J. Membr. Sci.* **2003**, *213*, 181.
- Gora A., B. Toepfer, V. Puddu, G. Li Puma, *Appl. Catal., B* **2006**, *65*, 1.
- Guettaı N., H.A. Amar, *Desalination* **2005**, *185*, 439.
- Guillard C., T.-H. Bui, C. Felix, V. Moules, B. Lina, P. Lejeune, *C.R. Chimie* **2008**, *11*, 107.
- Gurunathan K., *J. Mol. Catal. A: Chem.* **2000**, *156*, 59.
- Heberer T., *Toxicol. Lett.* **2002**, *131*, 5.
- Hernández-Alonso M.D., J.M. Coronado, A.J. Maira, J. Soria, V. Loddo, V. Augugliaro, *Appl. Catal., B* **2002**, *39*, 257.
- Herrmann J.-M., C. Duchamp, M. Karkmaz, B. Thu Hoai, H. Lachheb, E. Puzenat, C. Guillard, *J. Hazard. Mater.* **2007**, *146*, 624.
- Herrmann J.-M., *Top. Catal.* **2005**, *34*, 49.
- Higashida S., A. Harada, R. Kawakatsu, N. Fujiwara, M. Matsumura, *Chem. Commun.* **2006**, 2804.

- Hoffmann M.R., S.T. Martin, W. Choi, D.W. Bahnemannt, *Chem. Rev.* **1995**, *95*, 69.
- Huang G., Y. Zhu, *Mat. Sci. Eng. B* **2007**, *139*, 201.
- Huang J., X. Wang, Y. Hou, X. Chen, L. Wu, X. Wang, X. Fu, *Microporous Mesoporous Mater.* **2008**, *110*, 543.
- Huang X., M. Leal, Q. Li, Water Res. **2008**, 42, 1142.
- Huang X., Y. Meng, P. Liang, Y. Qian, *Sep. Purif. Technol.* **2007**, *55*, 165.
- Imoberdorf G.E., H.A. Irazoqui, O.M. Alfano, A.E. Cassano, *Chem. Eng. Sci.* **2007**, *62*, 793.
- Ito S., K.R. Thampi, P. Comte, P. Liska, M. Gratzel, *Chem. Commun.* **2005**, 268.
- Jaber A.M.Y., A.A. Ali, G.O. Yahaya, *J. Membr. Sci.* **2005**, *250*, 85.
- Jana A.K., *J. Photochem. Photobiol., A* **2000**, *132*, 1.
- Jang J.S., S.H. Choi, N. Shin, C. Yu, J.S. Lee, *J. Solid State Chem.* **2007**, *180*, 1110.
- Jitputti J., Y. Suzuki, S. Yoshikawa, *Catal. Commun.* **2008**, *9*, 1265.
- Kansal S.K., M. Singh, D. Sud, *J. Hazard. Mater.* **2007**, *141*, 581.
- Kansal S.K., M. Singh, D. Sud, *J. Hazard. Mater.* **2008**, *153*, 412.
- Kanthasamy R., S.C. Larsen, *Micropor. Mesopor. Mat.* **2007**, *100*, 340.
- Karunakaran C., R. Dhanalakshmi, *Sol. Energy Mater. Sol. Cells* **2008**, *92*, 588.
- Karunakaran C., S. Senthilvelan, *Electrochem. Commun.* **2006**, *8*, 95.
- Kavita, K., C. Rubina, L.S. Rameshwar, *Ind. Eng. Chem. Res*. **2004**, *43*, 7683.
- Kim B., D. Kim, D. Cho, S. Cho, *Chemosphere* **2003**, *52*, 277.
- Kim S.D., J. Cho, I.S. Kim, B.J. Vanderford, S.A. Snyder, *Water Res.* **2007**, *41*, 1013.
- Kobasa I.M., G.P. Tarasenko, *Theor. Chem. Acc.* **2002**, *38*, 4, 255.
- Kolpin D.W., M. Skopec, M.T. Meyer, E.T. Furlong and S.D. Zaugg, *Sci. Total Environ.* **2004**, *328*, 119.
- Konstantinou I.K., T.A. Albanis, *Appl. Catal., B* **2004**, *49*, 1.
- Ku Y., W.H. Lee, W.Y. Wang, *J. Mol. Catal. A: Chem.* **2004**, *212*, 191.
- Kudo A., *Catal. Surv. Asia* **2003**, *7*, 1, 31.
- Kudo A., M. Sekizawa, *Chem. Commun.* **2000**, 1371.

- Kujawski W., A. Warszawski, W. Ratajczak, T. Porebski, W. Capala, I. Ostrowska, *Desalination* **2004**, *163*, 287.
- Kuo W.S., Y.H. Chiang, L.S. Lai, *Dyes Pigm.* **2008**, *76*, 82.
- Lacey C., G. Mcmahon, J. Bones, L. Barron, A. Morrissey, J.M. Tobin, *Talanta* **2008**, *75*, 1089.
- Lair A., C. Ferronato, J.-M. Chovelon, J.-M. Herrmann, *J. Photochem. Photobiol., A* **2008**, *193*, 193.
- Lazarova Z., S. Boyadzhieva, *Chem. Eng. J.* **2004**, *100*, 129.
- Le-Clech P., E.-K. Lee, V. Chen, *Water Res.* **2006**, *40*, 323.
- Lee S.-A., K.-H. Choo, C.-H. Lee, H.-I. Lee, T. Hyeon, W. Choi, H.-H. Kwon, *Ind. Eng. Chem. Res.* **2001**, *40*, 1712.
- Lhomme L., S. Brosillon, D. Wolbert, *J. Photochem. Photobiol.,* A **2007**, *188*, 34.
- Li Puma G., B. Toepfer, A. Gora, *Catal. Today* **2007**, *124*, 124.
- Li S., Z. Ma, J. Zhang, J. Liu, *Catal. Commun.* **2008**, *9*, 1482.
- Li X., S. Ouyang, N. Kikugawa, J. Ye, *Appl. Catal., A* **2008**, *334*, 51.
- Lin X., F. Huang, W. Wang, Z. Shan, J. Shi, *Dyes Pigm.* **2008**, *78*, 39.
- Ling Q., J. Sun, Q. Zhou, *Appl. Surf. Sci.* **2008**, *254*, 3236.
- Liptàkova B., M. Bàhidsky, M. Hronec, *Appl. Catal., A* **2004**, *263*, 33.
- Liu X., Y. Li, X. Wang, *Mater. Lett.* **2006**, *60*, 1943.
- Liu Y., K. Murata, M. Inaba, *J. Mol. Catal. A: Chem.* **2006**, *256*, 247.
- Liu Y., L. Deng, Y. Chen, F. Wu, N. Deng, *J. Hazard. Mater. B* **2007**, *139*, 399.
- Lou X., J. Han, W. Chu, X. Wang, Q. Cheng, *Mat. Sci. Eng. B* **2007**, *137*, 268.
- Malato S., J. Blanco, A. Vidal, D. Alarcon, M.I. Maldonado, J. Caceres, W. Gernjak, *Sol. Energy* **2003**, *75*, 329.
- Maldotti A., L. Andreotti, A. Molinari, S. Tollari, A. Penoni, S. Cenini, *J. Photochem. Photobiol., A* **2000**, 133, 129.
- Maldotti A., R. Amadelli, I. Vitali, L. Borgatti, A. Molinari, *J. Mol. Catal. A: Chem.* **2003**, *204*, 703.
- Maldotti A., R. Amadelli, L. Samiolo, A. Molinari, A. Penoni, S. Tollari, S. Cenini, *Chem. Commun.* **2005**, 1749.

- Marais E., R. Klein, E. Antunes, T. Nyokong, *J. Mol. Catal. A: Chem.* **2007**, *261*, 36.
- Marcì G., M. Addamo, V. Augugliaro, S. Coluccia, E. García-López, V. Loddo, G. Martra, L. Palmisano, M. Schiavello, *J. Photochem. Photobiol., A* **2003**, *160*, 105.
- Marinkovic S., N. Hoffmann, *Chem. Commun.* **2001**, 1576.
- Mascolo G., R. Comparelli, M.L. Curri, G. Lovecchio, A. Lopez, A. Agostiano, *J. Hazard. Mater.* **2007**, *142*, 130.
- Mizukoshi Y., Y. Makise, T. Shuto, J. Hu, A. Tominaga, S. Shironita, S. Tanabe, *Ultrason. Sonochem.* **2007**, *14*, 387.
- Mohamed O.S., A.E.-A.M. Gaber, A.A. Abdel-Wahab, *J. Photochem. Photobiol., A* **2002**, *148*, 205.
- Molinari A., G. Varani, E. Polo, S. Vaccari, A. Maldotti, *J. Mol. Catal. A: Chem.* **2007**, *262*, 156.
- Molinari R., A. Caruso, P. Argurio, T. Poerio, *J. Membr. Sci.* **2008**, *319*, 54.
- Molinari R., C. Grande, E. Drioli, L. Palmisano, M. Schiavello, *Catal. Today* **2001**, *67*, 273.
- Molinari R., F. Pirillo, M. Falco, V. Loddo, L. Palmisano, *Chem. Eng. Process.* **2004**, *43*, 1103.
- Molinari R., F. Pirillo, V. Loddo, L. Palmisano, *Catal. Today* **2006a**, *118*, 205.
- Molinari R., L. Palmisano, E. Drioli, M. Schiavello, *J. Membrane Sci.* **2002**, *206*, 399.
- Molinari R., M. Mungari, E. Drioli, A. Di Paola, V. Loddo, L. Palmisano, M. Schiavello, *Catal. Today* **2000**, *55*, 71.
- Molinari R., T. Poerio, P. Argurio, *Catal. Today* **2006b**, *118*, 52.
- Mozia S., A.W. Morawski, *Catal. Today* **2006**, *118*, 181.
- Mozia S., M. Tomaszewska, A.W. Morawski, *Catal. Today* **2007**, *129*, 3.
- Mulder M., *Basic Principles of Membrane Technology*, second ed., Kluwer Academic Publishers, Dordrecht, **1991**.
- Ni M., M.K.H. Leung, D.Y.C. Leung, K. Sumathy, *Renew. Sust. Energ. Rev.* **2007**, *11*, 401.
- Nikolaou A., S. Meric, D. Fatta, *Anal. Bioanal. Chem.* **2007**, *387*, 1225.

- Noguchi H., A. Nakajima, T. Watanabe, K. Hashimoto, *Environ. Sci. Technol.* **2003**, *37*, 153.
- Ohtani B., B. Pal, I. Shigeru, *Catal. Surv. Asia* **2003**, *7*, 165.
- Ökte A.N., M.S. Resat, Y. Inel, *J. Photochem. Photobiol., A* **2000**, *134*, 59.
- Ollis D. F., *Top. Catal.* **2005**, *35*, 217.
- Ollis D.F., *C. R. Acad. Sci. Paris, Serie IIc, Chimie: Chemistry* **2000**, *3*, 405.
- Ortiz-Gomez A., B. Serrano-Rosales, H. De Lasa, *Chem. Eng. Sci.* **2008**, *63*, 520.
- Palmisano G., M. Addamo, V. Augugliaro, T. Caronna, A. Di Paola, E. Garcia Lopez, V. Loddo, G. Marcì, L. Palmisano, M. Schiavello, *Catal. Today* **2007b**, *122*, 118.
- Palmisano G., S. Yurdakal, V. Augugliaro, V. Loddo, L. Palmisano, *Adv. Synth. Catal.* **2007c**, *349*, 964.
- Palmisano G., V. Augugliaro, M. Pagliaro, L. Palmisano, *Chem. Commun.* **2007a**, 3425.
- Papadam T., N.P. Xekoukoulotakis, I. Poulios, D. Mantzavinos, *J. Photochem. Photobiol., A* **2007**, *186*, 308.
- Park H, W. Choi, *Catal. Today* **2005**, *101*, 291.
- Park S.-W., K.-W. Kim, I.-J. Sohn, C.F. Kaseger, *Sep. Purif. Technol.* **2000**, *19*, 43.
- Parra S., V. Sarria, S. Malato, P. Péringer, C. Pulgarin, *Appl. Catal., B* **2000**, *27*, 153.
- Peng F., L. Cai, H. Yu, H. Wang, J. Yang, *J. Solid State Chem.* **2008**, *181*, 130.
- Pillai U.R., E. Sahle–Demessie, *J. Catal.* **2002**, *211*, 434.
- Poliakoff M., P. Licence, *Nature* **2007**, *450*, 810.
- Pulgarin C., M. Invernizzi, S. Parra, V. Sarria, R. Polania, P. Péringer, *Catal. Today* **1999**, *54*, 341.
- Qourzal S., N. Barka, M. Tamimi, A. Assabbane, Y. Ait-Ichou, *Appl. Catal., A* **2008**, *334*, 386.
- Ranjit K.T., R. Krishnamoorthy, T.K. Varadarajan, B. Viswanathan, *J. Photochem. Photobiol., A* **1995**, *86*, 185.
- Rengaraj S., X.Z. Li, *Chemosphere* **2007**, *66*, 930.
- Rideh L., A. Wehrer, D. Ronze, A. Zoulalian, *Catal. Today* **1999**, *48*, 357.

- Rincon A.G., C. Pulgarin, *Appl. Catal., B* **2003**, *44*, 263.
- Rivas L., I.R. Bellobono, F. Ascari, *Chemosphere* **1998**, *37*, 6, 1033.
- Robert D., *Catal. Today* **2007**, *122*, 20.
- Robert D., S. Malato, *Sci. Total Environ.* **2002**, *291*, 85.
- Robertson P.K.J., *J. Cleaner Prod.* **1996**, *4*, 203.
- Sakkas V.A., I.M. Arabatzis, I.K. Konstantinou, A.D. Dimou, T.A. Albanis, P. Falaras, *Appl. Catal., B* **2004**, *49*, 195.
- Santos A., P Yustos, A. Quintanilla, S. Rodriguez, F. Garcia-Ochoa, *Appl. Catal., B* **2002**, *39*, 97.
- Sarria V., P. Péringer, J. Càceres, J. Blanco, S. Malato, C. Pulgarin, *Energy* **2004**, *29*, 853.
- Sasirekha N., S.J. Sardhar Basha, K. Shanthi, *Appl. Catal., B* **2006**, *62*, 169.
- Satuf M.L., R.J. Brandi, A.E. Cassano, O.M. Alfano, *Catal. Today* **2007**, *129*, 110.
- Schindler W., H. Kisch, *J. Photochem. Photobiol., A* **1997**, *103*, 257.
- Schoumacker K., C. Geantet, M. Lacroix, E. Puzenat, C. Guillard, J.-M. Hermann, *J. Photochem. Photobiol., A* **2002**, *152*, 147.
- Serpone, N. *J. Photochem. Photobiol., A* **1997**, *104*, 1.
- Sharma V.K., B.V.N. Chenay, *J. Appl. Electrochem.* **2005**, *35*, 775.
- Shimizu K., H. Akahane, T. Kodama, Y. Kitayama, *Appl. Catal., A* **2004**, *269*, 75.
- Shon H.K., S. Phuntsho, S. Vigneswaran, *Desalination* **2008**, *225*, 235.
- Sing Tan S., L. Zou, E. Hu, *Sci. Technol. Adv. Mat.* **2007**, *8*, 89.
- Singh H.K., M. Saquib, M.M. Haque, M. Muneer, *J. Hazard. Mater.* **2007**, *142*, 425.
- Sirkar K.K., P.V. Shanbhag, A.S. Kovvali, *Ind. Eng. Chem. Res.* **1999**, *38*, 3715.
- Sleiman M., P. Conchon, C. Ferronato, J.M. Chovelon, *Appl. Catal., B* **2007**, *71*, 279.
- Sobana N., M. Muruganandam, M. Swaminathan, *Catal. Commun.* **2008**, *9*, 262.
- Sobana N., M. Swaminathan, *Sol. Energ. Mat. Sol. C.* **2007**, *91*, 727.
- Sobczynski A., L. Duczmal, W. Zmudzinski, *J. Mol. Catal. A: Chem.* **2004**, *213*, 225.

- Sohrabi M.R., M. Ghavami, *J. Hazard. Mater.* **2008**, *153*, 1235.
- Sopajaree K., S.A. Qasim, S. Basak, K. Rajeshwar, *J. Appl. Electrochem.* **1999a**, *29*, 533.
- Sopajaree K., S.A. Qasim, S. Basak, K. Rajeshwar, *J. Appl. Electrochem.* **1999b**, *29*, 1111.
- Su W., J. Chen, L. Wu, X. Wang, X. Wang, X. Fu, *Appl. Catal., B* **2008**, *77*, 264.
- Subba Rao K.V., B. Srinivas, A.R. Prasad, M. Subrahmanyam, *Chem. Commun.* **2000**, 1533.
- Sun H., Y. Bai, W. Jin, N. Xu, *Sol. Energy Mater. Sol. Cells* **2008**, *92*, 76.
- Sun L., H. Lu, J. Zhou, *Dyes Pigm.* **2008**, *76*, 604.
- Sykora J., M. Pado, M. Tatarko, M. Izakovic, *J. Photochem. Photobiol., A* **1997**, *110*, 167.
- Takei G., T. Kitamori, H.-B. Kim, *Catal. Commun.* **2005**, *6*, 357.
- Tan S.S., L. Zou, E. Hu, *Catal. Today* **2008**, *131*, 125.
- Tan S.S., L. Zou, E. Hu, *Sci. Technol. Adv. Mat.* **2007**, *8*, 89.
- Tang C., V. Chen, *Water Res.* **2004**, *38*, 2775.
- Tang J., J. Ye, *Chem. Phys. Lett.* **2005**, *410*, 104.
- Taylor C.E., *Top. Catal.* **2005**, *32*, 179.
- Topalov A., D. Molnar-Gabor, M. Kosanic, B. Abramovic, *Water Res.* **2000**, *34*, 5, 1473.
- Torres R.A., J.I. Nieto, E. Combet, C. Petrier, C. Pulgarin, *Appl. Catal., B* **2008**, *80*, 168.
- Troupis A., A. Hiskia, E. Papaconstantinou, *Appl. Catal., B* **2004**, *52*, 41.
- Troupis A., E. Gkika, T. Triantis, A. Hiskia, E. Papacostantinou, *J. Photochem. Photobiol.,, A* **2007**, *188*, 272.
- Tsuru T., T. Kan-no, T. Yoshioka, M. Asaeda, *Catal. Today* **2003**, *82*, 41.
- Venkateswaran P., K. Palanivelu, *J. Hazard. Mater.* **2006**, *131*, 146.
- Vospernik M., A. Pintar, G. Bercic, J. Levec, *Catal. Today* **2003**, *79–80*, 169.
- Waldner G., A. Bruger, N.S. Gaikwad, M. Neumann-Spallart, *Chemosphere* **2007**, *67*, 779.
- Wang C.-T., *J. Non-Cryst. Solids* **2007**, *353*, 1126.
- Wang K.-H., H.-H. Tsai, Y.-H. Hsieh, *Appl. Catal., B* **1998**, *17*, 313.

- Wang L., N. Wang, L. Zhu, H. Yu, H. Tang, *J. Hazard. Mater.* **2008**, *152*, 93.
- Wang X., S.O. Pehkonen, A. K. Ray, *Electrochim. Acta* **2004**, *49*, 1435.
- Wang Y.H., X.Q. Liu, G.Y. Meng, *Mater. Res. Bull.* **2008**, *43*, 1480.
- Wong M.-S., S.-W. Hsu, K.K. Rao, C.P. Kumar, *J. Mol. Catal. A: Chem.* **2008**, *279*, 20.
- Wu C.-H., G.-P. Chang-Chien, W.-S. Lee, *J. Hazard. Mater. B* **2005**, *120*, 257.
- Wu G., T. Chen, W. Su, G. Zhou, X. Zong, Z. Lei, C. Li, *Int. J. Hydrogen Energy* **2008**, *33*,1243.
- Wu L., J. Bi, Z. Li, X. Wang, X. Fu, *Catal. Today* **2008**, *131*, 15.
- Xia H., H. Zhuang, T. Zhang, D. Xiao, *Mater. Lett.* **2008**, *62*, 1126.
- Xiao G., X. Wang, D. Li, X. Fu, *J. Photochem. Photobiol., A* **2008**, *193*, 213.
- Xu H., H. Wang, H. Yan, *J. Hazard. Mater.* **2007**, *144*, 82.
- Xu J., Y. Ao, D. Fu, C. Yuan, *Appl. Surf. Sci.* **2008**, *254*, 3033.
- Xu Y., C.H. Langford, *J. Photochem. Photobiol., A* **2000**, *133*, 67.
- Yahaya A.H., M.A. Gondal, A. Hameed, *Chem. Phys. Lett.* **2004**, *400*, 206.
- Yamaguchi S., S. Sumimoto, Y. Ichihashi, S. Nishiyama, S. Tsuruya, *Ind. Eng. Chem. Res.* **2005**, *44*, 1.
- Yamazoe S., T. Okumura, T. Tanaka, *Catal. Today* **2007**, *120*, 220.
- Yan T., J. Long, Y. Chen, X. Wang, D. Li, X. Fu, *C. R. Chimie* **2008**, *11*, 101.
- Yang X., L. Xu, X. Yu, Y. Guo, *Catal. Commun.* **2008**, *9*, 1224.
- Yurdakal S., V. Loddo, V. Augugliaro, H. Berber, G. Palmisano, L. Palmisano, *Catal. Today* **2007**, *129*, 9.
- Zama K., A. Fukuoka, Y. Sasaki, S. Inagaki, Y. Fukushima, M. Ichikawa, *Catal. Lett.* **2000**, *66*, 251.
- Zang Y., R. Farnood, *Appl. Catal., B* **2008**, *79*, 334.
- Zertal A., D. Molnar-Gabor, M.A. Malouki, T. Sehili, P. Boule, *Appl. Catal., B* **2004**, *49*, 83.
- Zhang T., L. You, Y. Zhang, *Dyes Pigm.* **2006**, *68*, 95.
- Zhang T., T. Oyama, S. Horikoshi, H. Hidaka, J. Zhao, N. Serpone, *Sol. Energy Mater. Sol. Cells* **2002**, *73*, 287.
- Zhang X., L. Lei, *J. Hazard. Mater.* **2008**, *153*, 827.
- Zhang Y., J.L. Zhou, B. Ning, *Water Res.* **2007**, *41*, 19.

- Zmudziński W., A. Sobczyńska, A. Sobczyński, *React. Kinet. Catal. Lett.* **2007**, *90*, 293.
- Zwiener C., F.H. Frimmel, *Sci. Total Environ.* **2003**, *309*, 201.

Consulted web-site:

- www.epa.gov/greenchemistry
- www.galenotech.org/chimfis6.htm
- www.greener-industry.org
- www.lenntech.com/membrane-technology.htm

APPENDIX

A1: SCIENTIFIC ACTIVITY IN THE THREE DOCTORATE YEARS

- "5th European Meeting on Solar Chemistry and Photocatalysis: Environmental Applications – SPEA 5", Mondello (PA), 4-8 Ottobre 2008.
- "XXVII Congresso Nazionale di Chimica Industriale – Energia, materiali e prodotti da tecnologie e processi eco-sostenibili", Genova, 30 Giugno - 3 Luglio 2008.
- "5th Chemical Engineering Conference for Collaborative Research in Eastern Mediterranean Countries – EMCC5", Cetraro (CS), 24-29 Maggio 2008.
- "Convegno Congiunto delle Sezioni Calabria e Sicilia - Società Chimica Italiana", Messina, 3-4 Dicembre 2007.
- "IX Scuola Nazionale per Dottorandi della Divisione di Chimica Inorganica – Chimica dei Materiali Inorganici", Arcavacata di Rende (CS), 26-30 Novembre 2006.
- "NATO-ASI International School on New Organic Chemistry Reactions and Methodologies for Green Production", Lecce - Otranto, 29 Ottobre – 10 Novembre 2006.
- "Euromembrane 2006", Taormina, 24-28 Settembre 2006.
- "Convegno Congiunto delle Sezioni Calabria e Sicilia - Società Chimica Italiana", Catania, 5-6 Dicembre 2005.

- Vincitrice del finanziamento di progetti di ricerca "Giovani Ricercatori" – Università della Calabria – Arcavacata di Rende (CS) – Dal 11/02/2008 al 11/02/2009.

A2: PUBLICATIONS ON JOURNALS AND CONFERENCE PROCEEDINGS

Articles

- Molinari R., Caruso A., Poerio T., "One-step conversion of benzene to phenol in a hybrid photocatalytic membrane reactor", *submitted to Catalysis Today.*
- Molinari R., Caruso A., Argurio P., Poerio T., "Degradation of the drugs Gemfibrozil and Tamoxifen in pressurized and de-pressurized membrane photoreactors using suspended polycrystalline TiO_2 as catalyst", *Journal of Membrane Science*, 2008, Vol. 319, pp. 54-63.
- Molinari R., Caruso A., Argurio P., Poerio T., "Diclofenac transport through stagnant sandwich and supported liquid membrane systems", *Industrial & Engineering Chemistry Research*, 2006, Vol.45, pp. 9115-9121.
- Molinari R., Argurio P., Poerio T., Caruso A., "Stagnant sandwich and supported liquid membrane systems for removal of pharmaceuticals in water", *Desalination*, 2006, Vol. 199, pp. 529-531.

Chapters in Books

- Molinari R., Caruso A., Palmisano L., "Photocatalytic membrane reactors in the conversion or degradation of organic compounds", in *Membrane operations. Innovative Separation and Transformations*, E. Drioli, L. Giorno (Ed.s), Wiley-VCH (textbook processing).
- Molinari R., Caruso A., Palmisano L., "Photocatalytic processes in membrane reactors", in *Comprehensive Membranes Science and Engineering*, E. Drioli (Ed.), Elsevier Publisher (textbook processing).
- Molinari R., Poerio T., Caruso A., Argurio P., Carnevale S.M., "Direct mild partial oxidation of benzene and methane in catalytic and photocatalytic membrane reactors", pp. 217-224. *DGMK Tagungsbericht 2008-3* - Ernst S., Jess A., Nees F., Peters U., Ricci M., Santacesaria E. - Hamburg, Germany: German Society for Petroleum and Coal Science and Technology, 2008. ISSN 1433-9013. ISBN 978-3-936418-81-1.

Conference Proceedings

Oral presentations

- Molinari R., Caruso A., Argurio P., Poerio T., "Pressurized and De-pressurized Membrane Photoreactors for Removal of Pharmaceuticals from Waters". Atti del convegno "International Congress on Membranes and Membrane Processes – ICOM 2008", Honolulu, Hawaii, 12-18 Luglio 2008.
- Molinari R., Caruso A., Poerio T., Argurio P., "Preliminary study on the "green" oxidation of benzene to phenol in a photocatalytic membrane reactor" - Atti del convegno "XXVII Congresso Nazionale di Chimica Industriale – Energia, materiali e prodotti da tecnologie e processi eco-sostenibili", Genova, 30 Giugno - 3 Luglio 2008, pp. ECG-C09.
- Molinari R., Caruso A., Argurio P., Poerio T., "Photocatalytic membrane reactors in the degradation of Gemfibrozil" - Atti del convegno "Convegno Congiunto delle Sezioni Calabria e Sicilia-Società Chimica Italiana", Messina, 3-4 Dicembre 2007, pp C13.
- Molinari R., Caruso A., Argurio P., Poerio T., "Rimozione di Farmaci da Acque mediante Membrane Liquide nelle configurazioni Sandwich e Supportate" - Atti del convegno "Convegno Congiunto delle Sezioni Calabria e Sicilia - Società Chimica Italiana", Catania, 5-6 Dicembre 2005, pp C27.

Posters

- Caruso A., Poerio T., Molinari R., "One-step synthesis of phenol in photocatalytic membrane contactor". Atti del convegno "5th European Meeting on Solar Chemistry and Photocatalysis: Environmental Applications – SPEA 5", Mondello (PA), 4-8 Ottobre 2008, PP4.5.
- Molinari R., Caruso A., Argurio P., Poerio T., "Photodegradation of pharmaceuticals in water using suspended TiO_2 in membrane reactors". Atti del convegno "VI Convegno Nazionale AICIng 2008", Ischia (NA), 25-27 Settembre 2008, pp. 105-106.
- Molinari R., Caruso A., Argurio P., Poerio T., "Photocatalytic membrane reactors (PMRs) for the removal of drugs from waters using polycrystalline TiO_2" - Atti del convegno "5th Chemical Engineering Conference for Collaborative Research

in Eastern Mediterranean Countries – EMCC5", Cetraro (CS), 24-29 Maggio 2008, pp. 363-366.

- Molinari R., Caruso A., Argurio P., Poerio T., "Membrane Photocatalytic Systems for drugs degradation" - Atti del convegno "IX Scuola Nazionale per Dottorandi della Divisione di Chimica Inorganica – Chimica dei Materiali Inorganici", Arcavacata di Rende (CS), 26-30 Novembre 2006, pp. P1.
- Molinari R., Argurio P., Poerio T., Caruso A., "Removal of pharmaceuticals from water by using Stagnant Sandwich and Supported Liquid Membrane Systems" - Atti del convegno "Proceedings of First Mediterranean Congress Chemical Engineering for Environment", Venezia, 4-6 Ottobre 2006, pag. 292.

A3: TEACHING ACTIVITY

- Esercitatrice di uno dei corsi di Chimica, primo anno dei Corsi di Laurea in Ingegneria, A.A. 08/09 – Università della Calabria.
- Docenza nei corsi di potenziamento A.A. 08/09 svolti nell'ambito del progetto POR CALABRIA 2000/2006, MISURA 3.7 AZIONE 3.7.a - Università della Calabria.
- Animazione nei corsi di potenziamento A.A. 08/09 svolti nell'ambito del progetto POR CALABRIA 2000/2006, MISURA 3.7 AZIONE 3.7.a – Università della Calabria.
- Esercitatrice di uno dei corsi di Chimica, primo anno dei Corsi di Laurea in Ingegneria, A.A. 07/08 – Università della Calabria.
- Esercitatrice di uno dei corsi di Chimica, primo anno dei Corsi di Laurea in Ingegneria, A.A. 06/07 – Università della Calabria.
- Esercitatrice di uno dei corsi di Chimica, primo anno dei Corsi di Laurea in Ingegneria, A.A. 05/06 – Università della Calabria.

ACKNOWLEDGMENTS

First of all, I would like to express my gratitude to my supervisor, Professor Raffaele Molinari, for giving me the opportunity to work with him and to develop my passion for research. His experience, attention to detail, hard work and wisdom guided me in these years, and, thanks to his support and suggestions, I have improved the quality of the way in which I do research.

I am really grateful to a great friend and researcher, Dr. Teresa Poerio. Her energies, passion and positive view donated me a deep curiosity and interest in things, an open mind to observe and analyse my work and determinacy in my actions. Dear WonderTerry I hope we will still have the opportunity to work together in the future.

I wish to thank also Ing. Pietro Argurio and Dr. Stella Carnevale for supporting me in these years.

I am thankful to all the people that I have met in the Laboratory of "Fondamenti Chimici delle Tecnologie", in particular Massimo, Gianni, Angelo and all fellows and students who made my PhD experience enjoyable under a human as well as a scientific point of view and with whom I shared nice moments.

Many thanks also to Daniela who has always been helpful, friendly and full of useful suggestions, and to all the other members of the Department of Chemicals and Materials Engineering with whom I feel at home.

I would also like to thank my friends, Frà, Antonella, Maryco, Ga&Seve, Nadia&Antonio, Anto&Ale, Isa, Ale, Naty, Ely, Lety, Kià&Vini. All these people, each one in his/her way, gave me support, serenity and the strength to reach this important achievement.

A special special thanks goes to my personal "Prrrof. Pai" for always being ready to spend hours talking and sharing ideas on our works, lifes and on my role of "first lady". I don't know anything about my future, but I hope that you will be close to me while I discover it.

Finally, the most important thanks is to my parents, Franco and Enza, and my "soricè" Ilaria, to whom this thesis is dedicated. They always provide me energy, teachings and trust which really helped me all over in these years, without their support and "patience" this experience would not be possible.